

# RCA Lancaster

Color TV, Conversion, and Power Tubes



## Electron Tubes: A Constant Challenge

When the history of our time is analyzed in future centuries, I feel certain that communications will be singled out as the key factor in making possible the "one world" concept—the basis for man's best hopes for the future. RCA's business is communications, and the people of our Lancaster plant have been a strong link in the development of modern systems through which men exchange ideas and convey information.

Lancaster contributed to the success of the rapidly growing television industry by establishing the first automatic high-volume production facilities for black-and-white picture tubes immediately following World War II.

This was a major milestone in industrial progress. Later, during 1954 to 1961, Lancaster built the first automatic high-volume production facilities to produce shadow-mask color picture tubes. The worldwide industry was skeptical about the practicality of the shadow-mask precision tolerances and complexity. Lancaster effort proved to be so successful that the entire industry has adopted the design and followed RCA's pioneering leadership. Color television was one of the major growth industries of the 1960's. To the engineer goes the credit for the indispensable design of the tube and the tube processing equipment.



**H. R. Seelen**  
Division Vice President and  
General Manager  
Television Picture Tube Div.  
Electronic Components



And yet all that has gone before is only a forerunner of communications systems still waiting to be developed. Some systems will incorporate computers; some will, perhaps, have solid-state display panels; but without doubt, whatever their nature, the engineers at Lancaster can be expected to play a key development role.

The Lancaster operation is an ultra-modern industrial and engineering complex producing a wide variety of electron tubes for a myriad of exciting and important applications in many fields of modern technology; for example, new medical diagnostic techniques; night vision employing light from the stars as the only source of illumination; power amplification for linear accelerators used to probe the secrets of the atom; surveillance satellite cameras used to better identify the natural resources of the world, just to name a few.

The advent of solid-state devices and technologies which was reputed to sound the death knell of tubes has, in fact, accelerated the growth of the industrial tube business. Combining the older tube technologies with new solid-state knowledge has advanced the fields in which electronics participate and we at Lancaster look forward to many new advances in the tube art.

At Lancaster, the engineer can pursue his professional career in an amazing number of fields ranging from mechanical design to new optical techniques. The Lancaster Plant is unique in the range of professional skills demanded by the products designed and manufactured here. No where is the engineering challenge so varied or the opportunity for professional recognition so great. The engineer is limited only by his own ambition and aspirations.



**C. H. Lane**  
Division Vice President and  
General Manager  
Industrial Tube Division  
Electronic Components



### Our Cover

The three tubes superimposed above the engineering scene on our cover are but a small sample of the myriad tube types designed and produced by the RCA Lancaster facility. Yet, these three tubes—a color TV tube, an L-band module, and an image orthicon—set the theme for this issue by representing the three principal areas of engineering competence at Lancaster: color, power, and conversion tubes. The engineers working at the image isocon test set are E. M. Musselman (seated) and O. Choi, both of RCA Lancaster. Photo credit: Tom Cook, RCA Laboratories.

## Contents

Papers		
Milestones in color-picture-tube development	H. R. Seelen	2
Development of cathodoluminescent phosphors	A. L. Smith	5
Gases and getters in color picture tubes	Dr. J. C. Turnbull, Dr. J. J. Moscony, A. Month, J. R. Hale	10
Colorimetry and contrast performance of color picture tubes	G. M. Ehemann, W. G. Rudy	14
Autotest—automatic production-test and process-control system for color picture tubes	W. E. Bahls, F. C. Fryburg, A. C. Grover, J. F. Stewart, N. A. Teixeira, E. D. Wyant	18
Vidicon photoconductors	J. F. Heagy	22
The image isocon—an improved image orthicon	E. M. Musselman, R. L. VanAsselt	24
Ceramic-metal tetrodes for distributed amplifier service	C. E. Doner, W. R. Weyant	29
Klystron for the Stanford two-mile linear accelerator	A. C. Grimm, F. G. Hammersand	32
Environmental engineering laboratory	J. M. Forman, J. B. Grosh	36
Design of a 915-MHz power triode for microwave cooking	W. P. Bennett, D. R. Carter, I. E. Martin, F. W. Peterson, J. D. Stabley, D. R. Trout	38
RCA Lancaster—25 years of engineering excellence		43
The heat pipe, an unusual thermal device	R. A. Freggens, R. C. Turner	44
Ruggedization of camera tubes for space applications	J. G. Ziedonis	48
The Coaxitron	J. A. Eshleman, B. B. Adams	52
Noble-gas-ion lasers	R. J. Buzzard, J. A. Powell, J. T. Mark, H. E. Medsger	56
Design of cermolox tubes for single-sideband	A. Bazarian	60
A sterilizable and ruggedized vidicon	Dr. S. A. Ochs, F. D. Marschka	64
Broadband, high-gain, L-band, power amplifier module	R. L. Bailey, J. R. Jasinski	68

# Milestones in color-picture-tube development

H. R. Seelen

Frequently a company, however heterogeneous its output, becomes identified in the mind of the public with a single, best-known product. The RCA Lancaster plant's life-span has encompassed many developments of high interest to scientists, engineers, the military services, and ordinary laymen. But of all the Lancaster products, the public is most aware of television picture tubes, and, in particular, color tubes. The 19 years during which Lancaster engineers have been engaged in developing and producing color tubes has been an eventful period.



**Harry R. Seelen**  
Division Vice President and General Manager  
Television Picture Tube Division  
Electronic Components

received the BS in Physics from Providence College, and in June, 1968, Mr. Seelen received an Honorary Doctor of Business Administration degree from it. Mr. Seelen was appointed Division Vice President and General Manager, Television Picture Tube Division, of Electronic Components on August 20, 1965. Previously, he had been General Manager of the division since July 20, 1965. Mr. Seelen joined RCA in 1930 as a tube design engineer at the Harrison, New Jersey, plant. Subsequently he became Manager of the Tube Development Shop. In 1942, he organized and set up the Engineering organization and laboratories at the new Lancaster plant. In 1943, with the transfer of all non-receiving tube engineering to Lancaster, he assumed charge of Engineering Services. Seven years later, he was appointed Manager of all Laboratory Engineering at Lancaster. In 1954, Mr. Seelen became Manager of the Color Kinescope Operations Department and later returned to Harrison as Manager, Kinescope Operations. In 1963, he was appointed Manager, Television Picture Tube Operations Department of the RCA Television Picture Tube Division, until his promotion to General Manager of the division. He is a Fellow of the IEEE and a Registered Professional Engineer in the State of New Jersey. He is a member of the Association for the Advancement of Arts and Sciences, as well as Sigma Pi Sigma, honorary engineering fraternity. In 1955, he received the RCA Victor Award of Merit, the company's highest tribute.

Final manuscript received October 10, 1968.

FROM THE BEGINNING, effort has been applied principally to the shadow-mask type, which appeared most suitable for development of the several forms of color tubes investigated by the RCA Laboratories. We are often asked, today, why RCA has adhered steadfastly over the years to this tube. The answer has good technical and commercial foundations: no other type has shown so desirable a combination of good performance characteristics and mass-production suitability, brought about by a long series of engineering developments. Admittedly, the three-beam shadow-mask system is less efficient than other systems as regards light output, and it has convergence complexities. But its advantages are dominant: high contrast and resolution, capabilities for uniform color fields and high color saturation (which is built into the tube), fine dot-screen structure, and moderate circuit requirements, considering both complexity and stability.

Pioneering work in color TV had been done by RCA prior to World War II, but the major advances in the commercial program occurred after 1945. An important milestone was passed in 1949 when field tests began and the first demonstrations of the RCA compatible system were held for the Federal Communications Commission. For this early work, the receivers used a separate picture tube for producing each of the three primary colors, and the three pictures were combined optically.

The next big step, then, was to provide a single, directly viewed tri-color tube. Of prime importance at this time was the fabrication of a group of such tubes

to aid continued development of the RCA color TV system as a whole, and to permit additional demonstrations of the system at various stages beginning in the Spring of 1950. Ultimately, the system developed by RCA served as the "backbone" of the National Television Systems Committee recommendations, which were finally adopted by the F.C.C. late in 1953. RCA thus became the major contributor to formulation of the present national standards for color TV transmission.

## Early color tubes

In addition to furnishing tubes for the RCA color program, it was, of course, an important part of Lancaster's assignment to develop the color-tube design, with a view to eventual mass production. The approach followed during this early period beginning in 1949 was to explore the potentials of the flat-screen, flat-mask system. Because accurate positioning of mask apertures with respect to the phosphor-screen dots (*register*) is extremely important, great emphasis was placed on mounting arrangements for the thin, rather flexible, metal mask. In this connection it was felt that tensioning the mask in a frame would provide greatest accuracy and stability of aperture position. As a correlative advantage, a flat screen opened up various possibilities for high-speed phosphor application: initially, silk-screening; later, letter-press or offset methods. These approaches to fabrication of mask assembly and screen required that all mask-aperture arrays be similar, and all phosphor-dot arrays be alike, within the narrow tolerances permitted by the shadow-mask system's geometry. In other words, there was a need for

“interchangeability”; any mask should “fit” any screen. Another advantage of using the flat mask-screen assembly was the feasibility of adjusting relative positions of these parts for best register, as a final step before insertion into the bulbs. Many acceptable tubes of the flat mask-screen type were made. The 15GP22 was put in production in 1953, and a larger 19-inch tube of the same type was developed.

### Curved screen tubes

Meanwhile, various curved-screen, curved-mask proposals had been considered. It was fully realized that a phosphor screen on the face of the bulb would be desirable because of better appearance, a larger picture in the same size bulb, and several other factors; but it was also realized that interchangeability might be difficult to attain if curved masks and screens were used. Furthermore, an interchangeable system seemed more suitable for mass production; non-interchangeability would require that each mask be mated to a particular screen, through all of the many processing steps. In addition, a problem would arise if the curved mask did not remain sufficiently stable through the heat treatments to which a vacuum tube must be subjected during fabrication.

In the fall of 1953, another tube manufacturer announced and demonstrated a tube of the curved-mask, curved-screen type. Although this tube evidenced register problems, it gave some indication that a curved mask might be reasonably stable through tube processing. RCA decided to investigate this type more thoroughly.

Earlier work had been done in the RCA Laboratories on a photographic method for depositing phosphor dots, a method well suited for screen application to a curved surface. With this background, the Lancaster program for design and construction of curved-screen color tubes was initiated late in 1953.

Among the first of these tubes were both round and rectangular samples. The round tubes used 19-inch-diameter bulbs that had a final closure of welded metal flanges presealed to the face-panel and the funnel. For the all-glass rectangular tubes, standard 21-inch, 90-

degree bulbs were cut near the panel seal, and, after screen deposition and mask mounting, were resealed with a low-temperature glass frit.

These first tests were so encouraging that, within the next few months, an intensive developmental effort was being placed on curved-mask tubes. A 21-inch size was selected because of the popularity of this size in black-and-white picture tubes; a round shape was chosen for reasons of stability of bulb and mask assembly, and a metal envelope was used for flexibility in design. From this development evolved the 21AXP22, which went into production in the fall of 1954. This tube incorporated many changes in addition to the curvature of mask and screen. It not only provided a larger screen (260 square inches instead of 88-1/2-square-inch size of the 15GP22) but did so at a slightly decreased overall length by widening the deflection angle from 45 to 70 degrees.

Photographic application of the three phosphors to the curved face plate involved development of processing techniques for production use, as well as design and development of a special equipment called a “lighthouse”. The purpose of this equipment is to provide exposure of the photosensitive phosphor layers in arrays of “dots” properly located so that they are bombarded by the respective electron beams when the tube is completed and in operation. An innovation, called a “radial correction lens”, was made in the lighthouse to provide a correction by optical simulation of the electron paths. This compensation is needed because of the manner in which the deflection field acts on an electron beam, effectively changing its “source” position with increasing deflection angle.

The photographic method of phosphor deposition required development of a mask-frame assembly which could be removed from its normal position within the front end of the tube or “top-cap” and accurately replaced several times. Stability of the curved mask itself was ensured by mounting on a rigid frame; repeated, precise positioning of the mask-frame assembly in the top-cap was attained by special leaf-springs attached to the frame which engaged studs on the cap wall.

In addition, a new triple-beam gun structure, which had originally been developed for the flat-screen tubes, was introduced in the 21AXP22. This gun included magnetic pole pieces for convergence control of individual beams. In this assembly, the three guns were tilted slightly toward the axis to provide static convergence at the screen center; dynamic fields, in synchronism with the scanning frequencies, could then be applied to the pole pieces to provide the change in convergence angle needed as the beams were deflected. This development permitted accurate convergence to be obtained even at the much wider deflection angle.

### The glass tube

During and following this period, both round and rectangular glass bulbs were investigated to determine whether glass was potentially desirable for either technical or commercial reasons, and to assess the problems connected with a rectangular shape. Some of the early glass bulbs using metal flanges have already been mentioned. A major improvement relating to glass bulbs occurred with the introduction of a special frit glass developed by Corning Glass Works which devitrifies, during sealing of the “top-cap” to the funnel, at a temperature low enough not to harm the phosphor or internal parts.

This development was followed by the introduction, in 1957, of the first color tube in an all-glass bulb, designated type 21CYP22. For screening this tube, a “degroupping correction lens” was introduced. This lens has an asymmetric contour superimposed on the radial correction contour to compensate for beam degroupping incidental to dynamic convergence. This latter innovation permitted enlargement of the mask apertures at the center, and increased transmission by about 40%. It also permitted a graduated tapering of the aperture walls which effectively increased transmission about 20%.

As mask material, cold rolled steel was substituted for the expensive copper-nickel alloy previously used. The aperture walls were tapered in such a way that only “knife edges” could be struck by the beams. This modification reduced electron scattering and consequently improved contrast.

The glass bulb proved advantageous in several ways. Its insulating properties simplified tube mounting problems for the receiver designer. Its mechanical stability and uniformity of face contour provided very significant improvement in register. Moreover, an improved referencing system for the lighthouse and for the frit-sealing operation also contributed to consistently good results. The mask-mounting method originally developed for the 21AXP22 was well adapted to provide the accuracy needed for this system. All of these features which provided stability and accuracy contributed significantly to improved uniformity of both color fields and white, and to greater ease of setup in the receiver. These improvements were the keys to initial commercial success in the fabrication of shadow-mask tubes.

In late 1960, another major improvement was introduced in the tube type 21FBP22. New green and red (sulfide) phosphors, having higher efficiencies and shorter persistence, supplanted those formerly used. The advantages included an important enhancement in picture brightness (about 50%), freedom from "smear" in rapid-action scenes, and better balance between the currents required from the three guns to produce white. Thus, the all-sulfide phosphor screen permitted driving to higher white-light output without serious red halo. The improvement in current balance also simplified receiver setup, particularly the adjustment of video drive for black-and-white picture reproduction. In addition, a protective window of 61% transmission filter glass was laminated to the tube face with a clear resin to improve contrast and color saturation.

### Today's tubes

The last few years have seen the development of the first RCA 90-degree rectangular tube, the 25AP22, and the proliferation of its brothers and smaller cousins. The rectangular bulb shape, and particularly the higher deflection angle, have introduced additional problems requiring a higher degree of engineering sophistication for satisfactory solutions. Use of the rectangular bulb has required solution to problems of bulb stability and alignment, as well as development of completely

new approaches to design and mounting of the mask assembly. Frame weight, replaceability, and thermal stability were among the factors which had to be reconsidered. A simple, inexpensive, lightweight assembly permitting good beam-to-screen register control has been developed for the entire tube family. The control of register and contrast has established a standard which has been or is now being emulated by our competitors.

Important advances have also been made in the art and science of lighthouse lens design, aided by use of a computer. We have been able to deposit phosphor dots to a higher degree of precision than heretofore thought possible. The increase in radial misregister brought about by the increase in deflection angle and the greater nonuniformity caused by factors of panel deformation and panel obliquity have required greater control. Also, higher beam degrouping factors brought about by the increase in deflection angle and the greater nonuniformity of these factors as a result of yoke characteristics also required higher degrees of control. Optimum designs of mask and lens contours have been developed for such control. We have indeed come a long way from the initial simple radial lens on a path of progress which has been vital to the success of wide-angle tubes.

Another innovation was the introduction of smaller neck size to permit use of smaller-diameter yokes. This change increased the efficiency of scanning needed for the larger deflection angle, and also reduced beam separation, thus minimizing misconvergence. Development of the small gun to fit the small neck required further improvements in beam formation and focus to maintain the quality performance of the larger gun used in the round tubes. Low-wattage heaters were developed to reduce thermal problems in the stem area. As a result, movement of parts because of thermal expansion has been reduced and convergence drift has been minimized. Einzel-lens guns have also been developed in the small size which permit fixed focus and thus simplify circuitry in portable receivers.

The development of high-efficiency red-emitting phosphors has been extremely important. The red sulfide phosphor was succeeded by yttrium vanadate in 1964

and by yttrium oxysulfide 2 years later. The yttrium-oxysulfide red-phosphor efficiency has made the "Unity Current Ratio" mode of operation a reality in the color picture tube. No longer must brightness be limited by red-gun "blooming". Now all guns may be uniformly driven to their resolution capability to provide maximum gun-screen efficiency and thus a brighter picture. Because of this permitted increase in current to the screen, the mask-frame thermal-compensating system called "Perma-Chrome" has become a necessity. Brightness has been gained without sacrificing resolution, purity, or white uniformity.

The success of these tube developments has literally echoed around the world. Our licensees in Japan and Western Europe have been tooling up to make similar tubes, and RCA itself has started up new tube plants in Scranton, Pa., Midland, Ontario, and Skelmersdale, England; in addition, our RCA plant in Puerto Rico is supplying gun assemblies.

### Color picture devices in the future

We continue optimistic about the potential of the shadow-mask tube for further development, and we expect to exploit ideas not yet fully explored. People frequently ask, "Is the shadow-mask tube likely to be supplanted by some new device in the near future?" Any new device would have to show at least as good performance, and it would probably require novelty (such as a large, thin panel to be hung on the wall), but far more important than any physical qualities would be the potential for cost reduction. A replacement for the shadow-mask tube which would meet such criteria is not presently within our field of view; we feel, therefore, that advanced versions of the shadow-mask tube will be serving us for a number of years to come.

Gen. David Sarnoff's words at the first tri-color tube demonstration on March 29, 1950, still ring true:

"Measured in comparison with every major development in radio and television over the past 50 years, this color tube will take its place in the annals of television as a revolutionary and epoch-making invention. When historians at the close of the 20th century evaluate the most important scientific developments, I will predict that this tube will be among the great inventions of the second half of this century."

# Development of cathodoluminescent phosphors

Dr. A. L. Smith

Phosphors are solid materials that have the ability to convert one or more forms of energy into visible or near-visible radiation; luminescence is the generic term for the phenomenon of this conversion. There are a number of excellent books and review articles covering the theoretical aspects of luminescence and the various phosphor systems that have been studied.<sup>1-10</sup> Some of these treat cathodoluminescence in detail,<sup>1,2,3,10</sup> and one is written with practical commercial development problems as its main theme.<sup>9</sup> None of them, however, deals specifically with the problems associated with the commercial development of cathodoluminescent materials, the subject of this article.

PHOSPHORS have been commercially important for a much longer period of time than other electronically active solids.<sup>11</sup> However, despite the long history associated with them and the very extensive literature on the subject of luminescence, their theoretical basis is not nearly as well understood as that of the more recently developed semiconductors, such as transistors. Things have not changed much since an introductory paper presented in 1954 stated that the manufacture of phosphors is largely an experimental science, if not a craft.<sup>12</sup> Research, development, and technology of phosphors is today still a combination of art, intuition, and fundamental knowledge.

RCA's present interest in luminescence is centered primarily on cathodoluminescent phosphors, i.e., those materials that have the ability to transform the energy of an electron beam into visible or ultraviolet radiation, because this energy transformation is the basis of RCA's extensive cathode-ray-tube business. Color-television tubes provide by far the greatest dollar volume in the tube market; for this reason, phosphor research and development done by the Materials Group at Lancaster is slanted heavily toward support of this item.

A large number of compounds are known to be luminescent, but the specific requirement that they be economically useful in a cathode-ray device immediately imposes a series of

design parameters which narrows the field of investigation to a surprisingly few chemical systems. These stringent design requirements also make the invention of a new commercial phosphor extremely difficult, for not only must the proposed material have exceptional luminescent properties, but it must also possess the combination of chemical and physical properties which will make it suitable as a screen material for cathode-ray tubes. Although characteristics of a phosphor can be varied within moderate limits, there is usually an interaction between the variables so that as one is improved, another is degraded. The result is that any phosphor represents a compromise in which the variable considered most important in a given application is optimized.

## Design requirements

The design requirements of commercial cathodoluminescent phosphors can be divided into two broad categories; those dealing with luminescent characteristics and those dealing with physical-chemical properties. The first considers phosphors simply as energy converters and sets their operational requirements in a particular device. The second category views phosphors as tube components which must remain stable during the manufacturing process.

## Luminescent characteristics

A phosphor must convert the energy of an electron beam into emitted radiation efficiently. This requirement



Dr. A. L. Smith, Ldr.  
Phosphor Development  
Chemical and Physical Laboratory  
Television Picture Tube Division  
Electronic Components  
Lancaster, Pa.

received the BS in chemistry from Fordham University in 1941 and the MS and PhD from the Polytechnic Institute of Brooklyn in 1943 and 1946 respectively. He joined the Chemical and Physical Laboratory at the RCA Lancaster plant in 1945. The major part of his career has been in the capacity of Engineering Leader of the Phosphor Development Group. He is the author of a number of papers on phosphors and has been granted fourteen patents related to phosphors and color tube screens. Memberships include the American Chemical Society, Phi Lambda Upsilon, Sigma Xi and the Electrochemical Society. He has held various positions in the ECS, being Chairman of the Electronics Division in 1953 and a presidential candidate in 1955.

may seem obvious, but there are many phosphors that are efficiently excited by ultraviolet radiation but not by an electron beam and therefore are useless in cathode-ray tubes. On the other hand, there are literally thousands of chemical combinations that luminesce under electron bombardment but have an efficiency of conversion of electron-beam energy into light that is too low to make them commercially useful. The most efficient and practical cathodoluminescent phosphors have been estimated to convert, at best, only 20% of beam power into radiant energy<sup>12</sup>. Sometimes the tube designer is willing to accept less than optimum conversion efficiency if some other characteristic, such as a unique decay property, is his major concern. Under any circumstance, however, conversion efficiency always has a high priority among the requirements. Unfortunately, there is little theoretical knowledge to guide the optimization of this parameter because the mechanism by which beam energy is dissipated in a crystal and transformed by a luminescent center into visible emission is but superficially understood. The closing of this knowledge gap is, today, the greatest challenge in the field of phosphor development. An advance in information in this area could revolutionize cathodoluminescence.

Another luminescent characteristic required of a phosphor is that it emit in some predetermined portion of the spectrum. Cathode-ray tubes are used in a wide variety of applications, and the phosphors used in them must emit in an area of the spectrum suitable to a specific application.

Although most tubes manufactured are used in the black-and-white or color television entertainment area, there are

a number of industrial applications in which screens are coupled to a particular photographic film type or photosensitive surface. In these uses, the output of the phosphor is tailored to match, as closely as possible, the response characteristics of the system. Because the phosphors developed by RCA are used principally for color television, the major interest is in rather narrow regions of the spectrum comprising the three primaries used in color tv: red, blue, and green. Colorimetry of the phosphors is of paramount importance because the gamut of hues obtainable in a color picture is defined by the coordinates of the three primaries<sup>14-16</sup>.

In addition to efficient energy conversion and emission, the persistence (the phosphorescence or decay rate) of a phosphor must be of the proper magnitude. The requirements in this category vary widely. In tubes designed for industrial or military applications, the range may be from 10<sup>-8</sup> second (or less) to several seconds duration, depending on end use. A medium-short persistence is desirable for entertainment tube types because the decay must be fast enough to insure that there is no smearing of the image in rapid action, yet slow enough so that flicker does not become objectionable. In multiple-phosphor screens, such as those used in color television tubes, the persistence of the three phosphors must be reasonably matched or color trailing (image blur) becomes noticeable.

It is desirable that the light output of each phosphor in a multi-color screen vary linearly with power, and each with the same slope, so that high and low brightness areas of a picture will be properly shaded. Because the total output of the screen is dependent on beam power (the product of beam voltage and beam current) it is important that the voltage and current characteristic of each of the phosphors be stable. As the voltage of the tube is usually fixed, the variation in output characteristics of the phosphor with variable current becomes the major concern. In some systems, such as sulfides, the light output of the phosphor does not always increase with current in the linear manner desired, but begins to drop off at some intermediate operating current. This phenomenon

is known as current saturation, or "droop-on-drive".

Another equally undesirable characteristic is known as color shift, a change of hue of emission with increased current. The higher the current, the more pronounced is the color shift. Color shift manifests itself in the appearance of a new, spurious emission band (usually at lower wavelengths) superimposed on the desired emission band. The phenomenon frequently occurs simultaneously with current saturation of the main band. Both main-band saturation and color shift are detrimental to color picture tube quality because they noticeably distort the hue in the highlights of the picture.

#### Physical-chemical characteristics

Commercially, phosphors are applied to a tube faceplate to form a screen by a variety of application techniques. Settling, slurring, and dusting are the methods commonly employed. The method used dictates the average particle size and distribution of the phosphors to be used. Ideally, the phosphor chemist should develop preparation processes that are flexible enough to produce the variety of particle sizes required for the different application techniques. This condition is frequently difficult to achieve, however, because the high temperatures required to develop optimum luminescent characteristics simultaneously causes crystal growth. The phosphor developmental engineer must therefore make suitable compromises to obtain the brightest material that can be applied in a reasonable manner.

A phosphor must also be chemically compatible with the application media. Most application methods involve aqueous systems which are pH sensitive. The phosphor must, therefore, be stable in water to the extent that it does not decompose to form basic or acidic constituents. Such constituents would alter the properties of the slurry formulation and its application characteristics. Of course, the phosphor should be inert so that its intrinsic luminescent properties are preserved. If the phosphor is not inert, it will suffer severe loss of efficiency during tube processing.

The surface properties of a phosphor must fit the screening techniques so



Phosphor slurry being dispensed.

that the phosphor can be well dispersed in the medium, yet bond well to the glass substrate. A variety of "coatings," which might be thought of as a "cement", is designed to facilitate bonding in the particular application technique used. Colloidal silica, silicates, and phosphates are the most frequently used chemical coatings, presumably because they form surfaces which bond well to glass, the most common substrate to which phosphors are applied. The laws governing surface properties are at present not completely understood.

Because phosphors are used in a vacuum, they must not decompose or evaporate during processing or under electron bombardment. Organic luminescent materials cannot be used because of their instability under these conditions. Their decomposition products could then poison the electron-emitting cathode or raise the gas pressures that would destroy the usefulness of the tube. Even when a material has a vapor pressure low enough to withstand a vacuum, the energy of the electron beam itself can cause crystal changes that destroy the luminescence of the materials. Halide phosphors, particularly the fluorides, have notoriously poor tube life because the chemical reducing power of the beam causes permanent crystal damage and ultimately destroys screen efficiency.

A phosphor must be able to maintain its important physical properties during tube processing; i.e., it must demonstrate chemical, thermal, and vacuum stability. During outgassing, a tube is subjected to temperatures of about 400 to 450°C. At these temperatures, the organic binders used in screen deposition are decomposed and yield a combination of gaseous reaction products, including CO, CO<sub>2</sub>, and H<sub>2</sub>O. Although the phosphor may be unaffected by these individual gases at room temperature and atmospheric pressure, the combination of gases and elevated temperature could prove disastrous.

### Phosphor cost

One of the more important commercial considerations not yet mentioned is phosphor cost. It must be possible to manufacture a phosphor in a reproducible manner at a reasonable cost;

a rather high unit cost can be tolerated provided some outstanding characteristic can be obtained. The red phosphor now used in RCA's color tubes is a case in point. It costs substantially more per tube than any previous phosphor but its outstanding efficiency makes the added cost worthwhile in tube and set performance.

### Group organization and responsibilities

The RCA engineering group devoted to the achievement of the phosphor characteristics described above, the Materials Group, is located in Lancaster, Pa. Its activities range from Applied Research through Development and into Pilot Plant production. When necessary, factory assistance is given and close liaison exists between Laboratory and Factory Engineering personnel.

### Laboratory engineering

Laboratory Engineering has the ability to follow an idea from its basic conception through factory production and, in addition, makes its staff available to Marketing and Sales as field engineers. Laboratory Engineering then is involved in the whole gamut of the business enterprise. The general philosophy of the Laboratory Engineering group is to concentrate on phosphor technology and to leave testing and analyses to other groups more knowledgeable in those areas. Laboratory Engineering does, however, draw heavily on these supporting specialists and the well-instrumented laboratories available to them.

### Analytical group

The Analytical Group performs a wide variety of services. Of particular note are the spectrographic and X-ray diffraction work which is relied upon heavily in purity and compositional studies of phosphors. Particle size analysis is another function of considerable importance. Because some work involves the interaction of many variables, the aid of a statistician is enlisted occasionally in setting and interpreting statistically designed experiments.

### Colorimetry group

The Colorimetry Group is essential to the phosphor development operation, for it is they who make the necessary



Microscopic screen inspection.

efficiency, persistence, and color-coordinate measurements.

### Applied research

The worker in the phosphor field is often accused of alchemy because he sometimes uses rather unorthodox methods to achieve rather unusual results. His background should be in either inorganic or physical chemistry and, ideally, should include a very broad spectrum of experience; a surprising number of disciplines are necessary in the successful development of a commercial phosphor. (A sense of humor has also been known to help.)

The role of Applied Research in phosphor development is twofold. First, its efforts are directed toward the achievement of a basic understanding of those processes which are used in synthesizing the blue and green-emitting sulfide phosphors. Second, it carries on a search for new phosphor systems and new ways of using older systems. The approach to each type of research is quite different.

Efforts in the first area might be called purely scientific in that the approach, at least, can be well organized according to basic principles. Because the blue and green-emitters are sulfides precipitated from aqueous solutions, such fundamental properties as the kinetics of the precipitation and the role of the precipitating conditions on the final characteristics of the phos-



Inserting the shadow mask after phosphor application.

phor are being studied. The influence of the flux and flux systems, including phase diagram studies, and diffusion as it affects particle growth, are also under investigation. Much of the work in this first area is conducted along classical lines where chemical theory is well developed and mathematical models exist. All theory and models must of course be interpreted with a view toward fulfilling present needs. Note that the researcher must be conversant with a wide variety of chemical knowledge, for he deals with solution chemistry as well as with high-temperature and solid-state chemistry. His life is orderly though complex. He seeks new knowledge, but more or less within the framework of existing procedure.

The second area of research, that of new systems, is quite different. Here, intuition and art are as important as fundamental knowledge. There is no guiding theory and much of the work is empirical. The chemist's work in this area is frustrating in large part because thousands of samples may be prepared before one of even moderate promise is found. Many of the chemical systems have been worked and reworked, not only within RCA, but in a large number of laboratories throughout the world. Statistically, the chances of finding a completely new phosphor are exceedingly low. The researcher must not only consider a compound as such, but he must be concerned about the way that compound is synthesized, for often success or failure is due to some unique preparatory scheme which imparts just the right amount of crystalline irregularity necessary for an efficient phosphor. Consideration must also be given to the "antique" compounds,

known to be luminescent, but never tested under modern cathode-ray conditions.

#### Development

The job of the chemist who develops phosphors is reasonably straightforward; he develops new phosphors and their manufacturing processes to a fine degree. His interaction with other groups is much more varied than the research man and includes an occasional assignment as a technical field representative with Sales and Marketing. (RCA enjoys a very substantial share of the market for zinc and zinc-cadmium sulfide phosphors used in cathode-ray tubes throughout the industry.) His knowledge must be very broad in the field of inorganic physical chemistry because he tackles problems as diverse as ultra-purification of materials, high-temperature syntheses, control of crystal growth, and surface properties of materials. It is generally he who must attempt to satisfy all the criteria listed in the earlier part of this article, or at least determine the optimum compromise.

#### Pilot plant

The Pilot Plant has proven to be an invaluable aid in the phosphor development operation in that it performs a variety of functions including scale-up of developmental procedures, rough cost analyses, manufacture of phosphors used in small quantities in either lab or factory, and investigations leading to new or improved processes. The equipment used in the Pilot Plant more closely approximates factory size than does the lab equipment, therefore, such items as firing time and

temperature are developed best in this plant. The engineering in the Pilot Plant is then true chemical engineering as distinguished from the pure chemistry of the other groups. Pilot Plant personnel must have a knowledge of production-type equipment and its capabilities, a talent for process simplification, and a healthy respect for costs. It is up to them to render a phosphor process practical from the viewpoint of production. Frequently, the Pilot Plant has been the initial production unit for a new material and has sold its product to the tube factory. In the early stages of phosphor development, reasonable cost estimates can be made, scrap potentials discovered and corrected, and process reproducibility assessed. Interaction with other groups is, of course, greatest with the development engineers and factory personnel, but some liaison with Applied Research is also necessary. Vendor relationships through Purchasing are also important, not only in equipment areas, but in materials as well. Prior to acquisition of the Pilot Plant, the Phosphor Factory itself had to do its own scale-up and process development. This procedure was undesirable and led to much delay because tests had to be squeezed into existing production schedules.

#### Technical progress

Table I is a modified, up-dated version of previously published data<sup>11,18</sup>. The listings within each color are chronological in time of commercial color-television usage and show how the improvement in phosphors has contributed to the advances in color tube performance.

Table I—Commercially used phosphors

Types of emitters	Phosphor notation	Powder colorimetric data <sup>1</sup>		
		x	y	Y (Lumens/W)
<b>Blue</b>				
Calcium Magnesium Silicate: Titanium	CaO: MgO: 2SiO <sub>2</sub> : Ti	0.169	0.134	8.7
Zinc Sulfide: Silver: Chloride <sup>2</sup>	ZnS: Ag: Cl	0.146	0.052	7.5
Zinc Sulfide: Silver: Chloride <sup>2</sup>	ZnS: Ag: Cl	0.150	0.059	9.1
<b>Green</b>				
Zinc Silicate: Manganese	2ZnO: SiO <sub>2</sub> : Mn	0.218	0.712	31.1
Zinc Cadmium Sulfide: Silver: Chloride <sup>3</sup>	(ZnCd)S: Ag: Cl	0.242	0.529	56.0
Zinc Cadmium Sulfide: Silver: Chloride <sup>3</sup>	(ZnCd)S: Ag: Cl	0.303	0.587	70.3
<b>Red</b>				
Cadmium Borate: Manganese	2CdO: B <sub>2</sub> O <sub>3</sub> : Mn	0.630	0.370	10.7
Zinc Phosphate: Manganese	$\beta$ 3ZnO: P <sub>2</sub> O <sub>5</sub> : Mn	0.674	0.326	7.0
Zinc Selenide: Copper	ZnSe: Cu	0.652	0.347	17.0
Zinc Cadmium Selenide: Copper: Chloride	(ZnCd)Se: Cu: Cl	0.662	0.338	11.0
Zinc Cadmium Sulfide: Silver: Chloride <sup>3</sup>	(ZnCd)S: Ag: Cl	0.663	0.337	12.6
Yttrium Vanadate: Europium	YVO <sub>4</sub> : Eu	0.675	0.325	9.5
Yttrium Oxysulfide: Europium	Y <sub>2</sub> O <sub>3</sub> S: Eu	0.660	0.340	13.8

1. This notation defines color in accordance with that established by the Commission Internationale de l'Eclairage (C.I.E.).

2. The differences between these two phosphors are in silver content, flux composition, and firing temperature.

3. These phosphors differ primarily in their cadmium content.

### Early phosphors

The listing under the color red illustrates how RCA's research and development activity operates in seeking to optimize all design specifications. The first phosphor on the list—cadmium borate: manganese—satisfied all requirements except one of the most important: quality of emission. The emission of the borate phosphor was much too orange. For that reason it was replaced by zinc orthophosphate: manganese whose color was ideal. The lower lumens/watt value of the phosphate results from its redder color and a somewhat lower intrinsic conversion efficiency, a severe handicap that led to much research to find a replacement. The phosphate was commercially acceptable, however, and was used as RCA's standard red in those early years when color was trying to get off the ground.

### Zinc selenide: copper

The next phosphor to receive considerable attention was zinc selenide: copper. This phosphor is almost a classic example of one whose initial promise was very high but which was subsequently found to lack many of the required characteristics. Zinc selenide: copper has an outstanding lumens/watt value, although its hue is a bit too orange.

### Zinc cadmium selenide: copper

An improved red emission is obtained by addition of cadmium selenide to form solid solutions of zinc cadmium selenide. When this is done, however, the lumens/watt value of the compound is significantly decreased; the percentage decrease is greater than should be expected on the basis of color change alone. It has been concluded, therefore, that the solid solution has an intrinsic lower conversion efficiency than zinc selenide alone. Although disappointing in some characteristics, the zinc cadmium selenide has a final lumens/watt value that is still much higher than the phosphate it was designed to replace. A major disadvantage of zinc-cadmium selenide is its process instability; in water, at room temperature, a slow decomposition occurs. At the elevated temperatures of tube and screen bakes, the water vapor evolved during decomposition of the organic binder attacks the phosphor at such an accelerated rate that an effi-

ciency loss of approximately fifty per cent occurs. Although a coating capable of slowing decomposition was developed, the close controls required in both manufacture and screen processing forced RCA to drop zinc-cadmium selenide as a commercial product.

### Silver-activated zinc-cadmium sulfide

A silver-activated zinc cadmium sulfide of high cadmium content eventually replaced the zinc orthophosphate: manganese, primarily because of its higher conversion efficiency, but also because its persistence matched that of the other two sulfides more exactly. All of the brightness gain indicated in Table I was not realized because the sulfide suffered mild degradation during tube processing and showed a slight color shift on drive, a drawback not present in the phosphate. The plus features of the sulfide were considered to far outweigh its disadvantages, and for many years it was the standard red component in RCA color tubes.

### Europium-activated yttrium vanadate

The europium-activated yttrium vanadate replaced the sulfide for reasons not readily apparent from Table I. Again, it was adopted on the basis of a series of compromises, the sum total of which made it superior to the sulfide. One prime disadvantage was its cost, some ten times that of the sulfide. Advantages included no color shift with high current and no current saturation; persistence was in line with the green and blue sulfides. The lumens/watt values shown in Table I appear to put the vanadate at a disadvantage in relation to the sulfide. After processing into tubes, however, the vanadate shows a very slight improvement over the sulfide, because the sulfide efficiency is degraded during processing while the vanadate is not. This is a good example of why the acceptance of a phosphor must be based on its performance in the tube and not on a simple powder test.

### Europium-activated yttrium oxysulfide

Shortly after the yttrium vanadate: europium went into production, RCA's research efforts led to the discovery of europium-activated yttrium oxysulfide, a phosphor with a much higher efficiency than the vanadate. The oxysulfide is as stable as the vanadate in

all respects, has processing stability, shows no color shift on drive, and no current saturation.

A new process compatible with factory equipment had to be invented for the production of the oxysulfide (here the staff of the David Sarnoff Laboratories helped considerably). Firing conditions capable of yielding proper color and particle size had to be developed, rigid control procedures established, and impurity levels discovered. The Pilot Plant went into production of the material to establish production routine, and actually made many hundreds of pounds of product without a single reject lot, to determine reliability, costs, and other commercial considerations.

### Future improvements

From RCA's viewpoint, a phosphor is not a commercial success until it has performed satisfactorily in a marketable cathode-ray tube. To perform satisfactorily a phosphor must fulfill two categories of design parameters, one dealing with intrinsic luminescent properties, the other with application characteristics. Future improvements exclusive to RCA will become increasingly difficult because intense competition has increased not only the number of investigators throughout the world, but the sophistication of the approach to the discovery of new phosphors.

### References

1. Garlick, G. F. J., *Luminescent Materials* (Oxford Univ. Press, New York, 1949).
2. Leverenz, H. W., *Introduction to Luminescence of Solids* (Wiley, New York, 1950).
3. Goldberg, P., *Luminescence of Inorganic Solids* (Academic Press, New York, 1966).
4. Kallman, H. P., and Spruch, G. M., *Luminescence of Organic and Inorganic Materials* (Wiley, New York, 1962).
5. Kroger, F. A., *Some Aspects of the Luminescence of Solids* (Elsevier, New York, 1948).
6. Curie, D., *Luminescence in Crystals* (translated by G. F. J. Garlick, Wiley, New York, 1960).
7. Leverenz, H. W., "Luminescence" *Encyclopedia Britannica* (1966).
8. Pallita, F. C., *Elect. Tech.*, Vol. 6 (1968) p. 39.
9. Ouweltjes, J. L., *Modern Materials* (edited by B. W. Gosser, Volume 5, Academica Press, N.Y., 1965) pp. 161-257.
10. Garlick, G. F. J., *Brit. J. Applied Physics*, Vol. 13 (1962) p. 541.
11. Larach, S., Shrader, R. E., Yocum, P. N., *RCA reprints PE-276, PE-280, and PE-291*.
12. Henderson, S. T., "Luminescence," *Cambridge Symposia, Brit. J. Applied Phys.* Vol. 6, Supplement 4 (1955) p. 51.
13. Brill, A. and Klasens, H. A., *Philips Res. Rpts.* Vol. 7 (1952) p. 401.
14. Brill, A., Klasens, H. A., *Philips Res. Rpts.* Vol. 10 (1955) p. 305.
15. Brill, A., Wanmaker, W. L., *Philips Tech. Rev.* Vol. 27 (1966) p. 22.
16. Hardy, A. E., *IEEE Transactions BTR* 11, No. 2 (1965) p. 33.

# Gases and getters in color picture tubes

Dr. J. C. Turnbull | Dr. J. J. Moscony | A. Month and J. R. Hale

Picture tubes, like other oxide-cathode electron-tube devices, require a high vacuum for prolonged operating life. Unfortunately, the inside tube surfaces become gas sources and destroy the desired vacuum. This problem results from high-energy electron beams striking the tube screen and the shadow mask, in the case of color picture tubes, and liberating various gases from these surfaces. At the same time, high-energy, back-scattered primary electrons strike and liberate gas from the surface of the conductive funnel coating. The use of a barium getter in picture tubes forms a film on the interior tube surfaces, which reacts chemically with stray gases to form stable, solid, barium compounds and thus maintain the desired vacuum. This paper describes the use of getters and their function in color picture tubes.



**J. C. Turnbull**  
Color TV Chemical and Physical Laboratory  
Electronic Components  
Lancaster, Pa.

received the BS in Physics from M.I.T. in 1934 and the PhD in physics from Brown University in 1938. Between 1938 and 1942 he worked on glass development and research at the Preston Laboratories. During World War II, he was employed by M.I.T., Princeton, and Harvard to work on high power, high frequency transmitters and modulators. He joined Electronic Components in 1945 and from then through 1954 was involved in glass and ceramic work in the Chemical and Physical Laboratory. Thereafter, he was involved with the development of the metal kinescope and with the development of both the metal bulb and the glass bulb versions of the shadow-mask color kinescopes. Since 1958 he has been leader of the Applied Physics Group of the Chemical and Physical Lab investigating thermionic cathodes, getters and related phenomena which affect performance and life of electron tubes.



**J. J. Moscony**  
Color TV Chemical and Physical Laboratory  
Electronic Components  
Lancaster, Pa.

received the BS in Chemistry from St. Joseph's College in 1951. He worked with the Electric Storage Battery Co. as an analytical chemist, served two years in active duty with the U.S. Army and then worked for Waterman Products Co. as a Chemical Engineer in the development of phosphor screening methods for cathode ray tubes. He joined RCA, Defense Electronics Products in 1957, where he assisted in the development of thermo-electric materials for refrigeration purposes. In 1958 he received the MS in Chemistry from St. Joseph's College. In 1959 he joined RCA Industrial Tube Products, Space Components Engineering, where he worked on a variety of topics related to thermionic energy conversion. As a recipient of a David Sarnoff Fellowship, he attended the University of Pennsylvania from 1962 to 1965 where he earned a PhD in Synthetic Inorganic Chemistry. He then joined the Color TV Chemical and Physical Laboratory of EC and has been working on mass spectrometer analysis of residual gases in vacuum and also on getter and cathode developments. Dr. Moscony has had nine papers published and holds one patent. He is a member of the American Chemical, American Physical and American Vacuum Societies.



**A. Month**  
Color TV Chemical and Physical Laboratory  
Electronic Components  
Lancaster, Pa.

received the BS in Chemistry-Physics in 1950 from the City College of New York and continued graduate studies in Physics at the Polytechnic Institute of Brooklyn and CCNY. Prior to joining RCA he was Engineering Leader of the Spectroscopy Instrument Section of the Process and Instruments Company and then the Manager of the Instrument Model and Glassblowing Shop of Emil Greiner Company. He joined RCA in 1957 as a Spectroscopist for the Microwave Chemical and Physical Laboratory in Harrison, N.J. In 1959 he assumed responsibility for Analytical and Metallurgical Analysis and Physical Testing for the laboratory. He joined the Electron Physics Group in Lancaster Color TV Chemical and Physical Laboratory in 1964. At Lancaster he investigated the factors affecting operating of color TV tubes and was responsible for the use of the first high yield exothermic getters in the color TV tubes. Mr. Month received the EC Engineering Award in 1967 for his work in increasing the reliability and life of color picture tubes. He is presently engaged in the design and development of future color TV picture tubes. He is a member of the American Chemical Society and American Physical Society; has authored technical papers; and has several patents pending.



**J. R. Hale**  
Color TV Chemical and Physical Laboratory  
Electronic Components  
Lancaster, Pa.

received the BS degree from the New York College of Ceramics at Alfred University in 1961. He was employed as a Development Engineer by the Ferro Company and worked on low temperature glass formulations through 1962. Currently, he is engaged with various glass technology problems, getter design, heater-cathode reliability problems and investigations relative to solder glass technology. Mr. Hale is a member of the American Ceramic Society, The National Institute of Ceramic Engineers, The Society of Glass Technology, and The Society of Rheology.

Final Manuscript received.

**T**HE GETTERS used in black-and-white picture tubes evolved from the early loop getters which were mounted and flashed onto the neck area of the tube above the electron gun. These getters were stable in air and used a barium-aluminum alloy which contained approximately 50% of each metal.

The alloy was in the form of a wire clad with nickel or stainless steel; the wire was ground down on one side to expose the alloy for easy flashing. The getter wire was welded to a metal loop (see Fig. 1) to facilitate heating by a high-frequency source. This heating causes the barium metal to be flashed from the alloy by evaporation. The ring getter shown in Fig. 1 is an improved version which allows a larger quantity of barium to be flashed with a minimum expenditure of RF energy. This getter has a stainless-steel channel to which the barium-aluminum alloy material is pressed.

Ring getters can be exothermic or endothermic. The exothermic ring getter is made by mixing nickel powder with the barium-aluminum alloy powder. When heating of the getter starts, the nickel and aluminum form an alloy and release heat to help to bring the getter quickly to the flash temperature. The endothermic getter does not include the nickel-powder addition.

#### Getters in shadow-mask picture tubes

Getters used for shadow-mask color picture tubes evolved along the same lines as the black-and-white tube versions. The first color picture tubes (type 21AP22, 70° deflection, large neck tubes) were produced with six loop getters mounted above the gun in a circle. These getters had a total maximum yield of 90 mg of barium and were flashed radially outward with a high-frequency coil onto a limited area of the neck. Later, a number of different types of getters were used in this tube as part of a transition that led to a ring getter 36 mm in diameter, located above the gun mount and flashed upward and away from it. This getter provided a large area of flash on the

2-inch (diameter) neck of the tube. Barium fill was 150 mg and actual yield was maintained above 100 mg. By observation of the disappearance of metallic barium, it was estimated that 50 mg of barium were typically consumed during the first few thousand hours of tube operation. The good performance of this single getter system has been demonstrated by the excellent life of the 70° deflection color picture tubes.

#### Two-getter systems

A greatly increased flash area was achieved by using a getter system mounted in the funnel and directed to flash across the bulb onto the funnel and mask areas. Two 130 mg endothermic getters were used in this system. As shown in Fig. 2, one was mounted in the tube neck, and the other in tube funnel. The system had adequate getter-capacity on the oxygen capacity test (described later), however, experience showed it to be more difficult to control the flash of two getters and that the flashing produced higher methane pressure<sup>1,2</sup> than with a single getter. Although the methane disappeared during tube scanning, it caused short-term emission instability after cathode aging.

#### Large exothermic funnel getters

RCA's getter-vendors were asked to develop, to RCA specifications, a single, large getter for the 90° deflection tubes. An exothermic getter was preferred because it is easier to flash than a large endothermic getter. (Large endothermic getters can present the problem of liquid aluminum spilling from the channel during flash. This problem is not present with endothermic getters because a solid nickel-aluminum matrix is formed during flash.) A goal of a minimum of 135 mg of barium-flash yield was set to achieve the same performance as the two-getter system. Experience with factory flash capabilities indicated that the getter fill would have to be in the range of 175 to 185 mg, about twice the amount as in the largest exothermic getter of 25-mm size.

Based on RCA's specifications, one vendor developed an exothermic getter

with 185 mg of fill. The antenna mounting system needed no changes to position this getter in the funnel. This getter flashed better than the 127-mg endothermic getter that it replaced. The starting time (time from the application of RF to initiation of the flash) was  $7 \pm 1$ s with a total RF application time of 30 seconds, and the average yields in production exceeded 150 mg. This getter is now being used in the smaller color picture tubes.

Another vendor produced a large getter having 240 mg of barium fill. This getter, also shown in Fig. 3, has a number of features which departed from the conventional ring-type getters. First, it used a greater exposed area, relative to the weight of fill, than other getters. This was achieved by forming a solid ring of getter material and pressing the ring into a separate external retainer ring. This external ring also aided the RF heating of the getter material. Second, a reflector was incorporated which became hot during flash and re-radiated the barium that normally deposited on the glass surface as back flash. Third, a ceramic substrate was substituted in place of metallic supports in the glass funnel around the getter support to minimize localized over-heating and cracking. This substrate eliminated glass problems and reduced the distance that the getter extended above the surface of the glass, resulting in more efficient coupling to the RF unit. Fourth, the getter used gas doping with nitrogen. This allowed the getter to release nitrogen just before flashing and, thereby, to momentarily increase the pressure and confine the flash area.

The performance of the 240-mg getter has been favorable. With gas doping, it was found that RF generators with frequencies above 450 kHz caused ionization of the gas released during flash and that getter yield was below normal. However, when the frequency was reduced to 300 kHz, ionization was not visible. This getter is used in the larger color picture tubes, and has provided an average yield of 210 mg.

#### Control criteria for getters and getter flash

Getters delivered to RCA are checked for barium fill, barium yield under controlled flash conditions, and gas content. During the inspection for barium fill, the getter material is

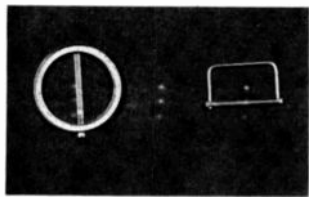


Fig. 1—Endothermic getters: loop getter (left), ring getter (right).

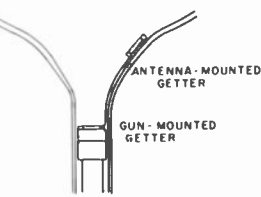


Fig. 2—Two-getter system used on the 90° deflection color picture tube.



Fig. 3—Exothermic getters: 185-mg getter (left), 240-mg getter (right).

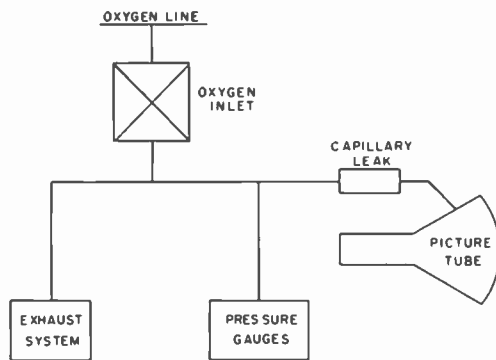


Fig. 4—Oxygen capacity test system.

broken out of its channel and inspected for barium content by chemical analysis. Barium yield is determined by the weight-loss method in which longer than average flashing is used so that most of the barium is removed from the channel. Gas content is determined by an ASTM test,<sup>3</sup> in which the pressure peak during flash is recorded in a system of known volume.

In production, barium yield must be controlled and conveniently evaluated. The weight-loss method is not wholly suitable because the initial weight of the getter, in an arbitrarily selected production tube, cannot be accurately determined. However, because the manufacturer maintains control over the amount of barium fill in each new getter, the approximate yield can be determined. This method of checking yield is used for endothermic getters. For exothermic getters a less time consuming approach is used, namely, X-rays are used to perform a residual barium analysis. This is achieved as follows: when a primary X-ray beam impinges on the face of a getter and its ring, the excited elements in the fill (barium, aluminum, and nickel) emit secondary or fluorescence X-radiation of discrete wavelengths. Quantitative analysis by X-ray fluorescence-emission spectroscopy is possible because the intensity of the wavelengths emitted is proportional to the concentration of that element in the sample. In this analysis, the barium  $K\alpha$  emis-

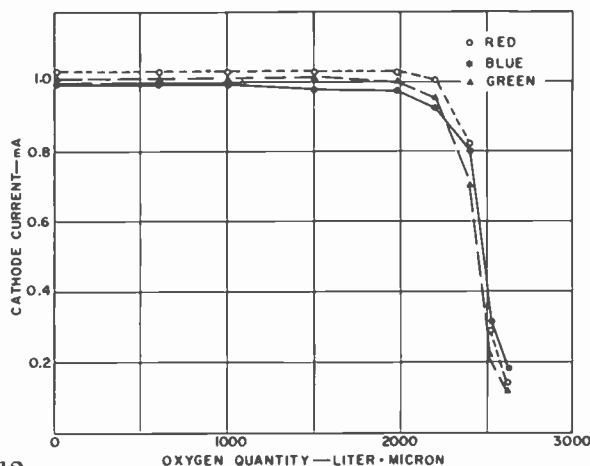


Fig. 5—Oxygen capacity test on a 70° tube.

Table I. Efficiencies of Various Getter Types

Getter Tube	Barium fill (mg)	Getter Efficiency (l- $\mu$ /mg Ba)	Average Oxygen Capacity (l- $\mu$ )
70° Tube			
Endothermic Neck Getter	150	20	2400
90° Tube			
Endothermic Neck Getter*	127	10	4500
Endothermic Funnel Getter*	127	40	
Exothermic Funnel Getter	185	40	6200
Exothermic Funnel Getter (nitrogen gas doped)	240	35	7350

\*Used in combination.

sion line is used to determine the amount of remaining barium in a flashed getter. Each determination is the average of two readings, with the getter rotated 90° between readings. This X-ray technique gives the amount of barium to within  $\pm 3$  milligrams and has been very useful in determining the best flashing techniques and in the discovery of faulty or poor flashing stations.

#### Evaluation of getter performance

Getter performance is best evaluated in an operating picture tube. The detrimental effect of oxygen on the oxide cathode and the high degree of activity of barium for oxygen led to a test method in which oxygen is introduced into a finished tube. (Oxygen is known to be present in picture tubes during scanning as is carbon dioxide<sup>4,5</sup>; the effects of these gases can sometimes be seen by oxidation of grid surfaces in tubes which are operated with insufficient getter yield.) When oxygen is admitted, cathode current is constant as long as the barium film is active and absorbs oxygen. When the film is depleted, the oxygen pressure rises and cathode current slumps.

For the purpose of this test method, a procedure was developed to break into the tube and admit oxygen gas. In this procedure, see Fig. 4, the funnel of a tube is partially drilled with a hollow, diamond-impregnated tool. Glass tubing from a vacuum station is sealed to the funnel with epoxy resin and the hole is broken through by impact with a magnetically controlled rod. Oxygen is let into the funnel from the manifold through a fixed leak. The latter is a section of capillary tube 1 mm in diameter and 1/4 inch long having a conductance (at room temperature) of 0.017 liters of oxygen per second. A second leak from an oxygen line keeps oxygen pressure in the manifold constant, usually at 4 microns—a convenient value to be checked with McLeod gauge. The rate of gas admission into the tube is normally 250 liter-

microns per hour. The quantity of oxygen that causes the cathode current to decrease to 80% of its initial value is taken as the oxygen absorption capacity (in liter-microns) of the getter. Fig. 5 shows a plot of cathode current as a function of oxygen quantity let into a new RCA-21FBP22 (70°-deflection) color picture tube. The current for all cathodes (red, blue, green) is constant up to 2000 liter-microns where it starts to slump. The 80% end point is about 2070 liter-microns for all three cathodes. A slower than normal rate of oxygen admission, 34 liter-microns per hour for 60 hours, was used to provide sharper end-points on the curves. The amount of barium flashed into the tube was 109 mg; therefore, the efficiency of the getter in the neck position of the tube was 19 liter-microns per mg of barium.

#### Oxygen capacity and getter efficiency

In a single getter system, oxygen capacity is a linear function of barium yield. The getter efficiency (liter-microns of capacity per mg of barium yield) depends on getter location and design and is sensitive to the distribution of the flash.

For a two-getter system, consisting of a neck getter plus a funnel getter attached to an antenna spring, oxygen capacity can be expressed by the following linear relation:

$$Q = aN + bF$$

where Q is getter capacity (liter-microns), N and F barium quantities (in mg), and a and b are constants. The chemical equivalent of oxygen reacting with barium to form barium oxide, BaO, is 67.7 liter-microns per mg of barium. This value is the maximum expected for the constants, a and b, for a getter film which reacts completely with oxygen to form BaO (assuming this happens before the cathode emission is affected). With this relationship, a least-squares fit of the data taken on many new 25-inch (90° deflection) color picture tubes gave actual values of a equal to 10

and  $b$  equal to 40 liter-microns per mg of barium. Results show that the funnel getter with its large area of flash approaches the theoretical value, while the neck getter with its restricted area is less than  $\frac{1}{4}$  as efficient as the funnel getter.

Getter efficiencies for the various types of getters used in color picture tubes are listed in Table I. These values are a function of flash area. The  $70^\circ$  neck getter has a large area of flash and greater efficiency than the  $90^\circ$  neck getter. The  $90^\circ$  endothermic and exothermic funnel getters have the same flash areas. The  $90^\circ$  exothermic gas-doped getter, also located in the funnel, has a more restricted area of flash and somewhat lower efficiency in terms of this test than the other  $90^\circ$  getters.

#### Getter depletion during tube operation

The oxygen capacity test can also be used for evaluation of getter depletion in tubes that have been operated. By use of this procedure, getter depletion is taken as the difference between the getter capacity of a used tube and that calculated for a new tube. Through the use of this test method, it has been found that oxygen absorption capacity of the 2-getter system in 25-inch tubes was depleted at the average rate of 3 liter-microns per hour during the first 300 hours of normal operation, and at the average rate of 1.5 liter-microns per hour during the first 1000 hours. Gas sources within the picture tube can be evaluated by similar measurements on picture tubes which are modified by omission of tube components. In one test, the mask, phosphor screen, and graphite-silicate funnel coating were omitted from a tube, and an operating tube made by aluminizing the funnel and face of the bulb, and by providing small-area patches to allow set up of the picture tube in a receiver. This tube showed no appreciable depletion of the neck flashed getter during hundreds of hours of tube operation, thus demonstrating that the omitted components were the important sources of gas.

#### Gas measurement in picture tubes

Mass spectrometer analysis of partial pressures of gas in tubes during their operating life can define conditions that limit cathode performance. A mass spectrometer developed for use in color picture tubes has the ionization source incorporated into the

electron-gun mount structure, making the partial pressure measurement refer to the same gaseous ambient to which the cathode is exposed. The analyser sector is attached directly to the neck of the tube; therefore, gas measurement can be made during scanning operation since one of the three guns in the mount is operable.

The picture tube mass spectrometer is used in a normally processed, sealed-off color tube which can then be operated and tested for gas pressures throughout a life test. These tests have shown the following: Prior to getter flash, the residual pressure in the tube is approximately  $5 \times 10^{-5}$  Torr, and consists mainly of nitrogen, carbon monoxide, and hydrogen. Several minutes after getter flash a significant drop in pressure occurs; the predominant gases are then methane, hydrogen and argon at a total pressure of  $5 \times 10^{-7}$  Torr. Upon subsequent processing, e.g., cathode aging, the total pressure continues to fall.

Results from initial scanning of the picture tube show an increase in nitrogen and carbon dioxide pressure; with a well flashed getter, however, the combined pressure of these gases does not exceed  $5 \times 10^{-9}$  Torr. With continued operation, the pressure in the tube is further reduced until after several hundred hours the total and partial pressures do not appear to change appreciably. At this point, the total pressure, caused chiefly by nitrogen and carbon monoxide, is  $5 \times 10^{-10}$  Torr. Thus, the total pressure in the tube decreased by a factor of about  $10^5$  Torr from immediately following exhaust (before getter flash) until after several hundred hours of operation.

The picture-tube mass spectrometer can also define getter performance. In this procedure gas is admitted into the funnel at a constant rate, simulating the gas sources from bulb surfaces. The steady-state change in pressure of the gettered gas is determined with the mass spectrometer.

Gettering action is described by the ratio between the gas inlet rate and the pressure change at the cathode. This ratio has the same units as pumping speed (liters per second), but it is not equal to the pumping speed of the getter for the gas under test, unless this quantity is very small. The ratio measures directly the ability of the getter

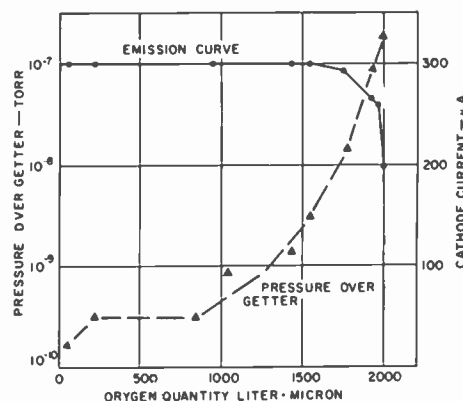


Fig. 6—Oxygen pressure over getter and cathode current as a function of quantity of oxygen absorbed.

to protect the cathode from the test gas and, therefore, its ability to protect the cathode during normal tube operation.

When the mass spectrometer is used to measure change in oxygen pressure as a function of a constant oxygen-inlet rate, and the resulting data is compared to the drop in cathode emission, the results are similar to those shown in Fig. 6. The color picture tube used for this test was a newly processed RCA-19EYP22 tube in which 50 mg of barium fill had been evaporated. From Fig. 6, it can be seen that the cathode emission current decreases to 80% of the initial value at a pressure of about  $2 \times 10^{-7}$  Torr. At this point the oxygen capacity is 2000 liter-microns. Many similar tests carried out on new 19EYP22 tubes and tubes which have been operated for thousands of hours indicate that the 80% emission level occurs when the pressure rises to the range  $5 \times 10^{-8}$  to  $5 \times 10^{-7}$  Torr.

#### Concluding remarks

Large barium getters have been developed to satisfy gas absorption requirements in color picture tubes. Tests evolved to assess gettering ability in production tubes can show whether a getter system is adequate throughout life operation of the tube, and can thus be used to define the getter system.

#### References

1. Moscony, J. J., *Evolution of Methane from Barium Films* (Supplemento al Nuovo Cimento Vol. V, No. 1, p. 7, 1967).
2. Michon, L. and Giorgi, T. A., *Studies of Gas Composition Within Finished Television Picture Tubes*, (Same p. 104).
3. *ASTM Gas Test of Barium Getters* (ASTM Tentative Proposed Practice for Testing Barium Flashed Getters, June 5, 1964, Rev. 6).
4. Collins, R. H. and Turnbull, J. C., *Evolution and Absorption of Gases in Electron Tubes* (Vacuum 10, p. 27, 1960).
5. Todd, B. J., Lineweaver, J. L. and Kerr, J. T., *Outgassing Caused by Electron Bombardment of Glass* (Journal Applied Physics Vol. 31, p. 51, 1960).
6. Moscony, J. J. and Turnbull, J. C., *A Mass Spectrometer for Gas Analysis in Color Television Picture Tubes*, (Supplemento al Nuovo Cimento Vol. V, No. 1, p. 93, 1967).

# Colorimetry and contrast performance of color picture tubes

G. M. Ehemann | W. G. Rudy

Although manufacturers use many technical terms to describe the quality of color television pictures, the ultimate appraisal is made on a purely subjective basis by the viewer. Therefore, it is more important to produce a picture that is "pleasing" to most viewers than to strive for an exact reproduction of an original scene which the home audience does not see. A viewer's subjective appraisal of a color picture depends upon the sensations he experiences as a result of various light stimuli. These sensations are produced by many properties of the light which can be measured and described in absolute values (e.g., total intensity, spectral energy distribution, hue, purity, brightness, contrast, and resolution). This paper discusses audience responses to chromatic stimuli of various hues, and relates the physical properties of these stimuli to the concept of picture "viewability."

VISIBLE LIGHT occupies the wavelength region between 4000 and 7000 angstroms. The spectral energy distribution of a light source is a detailed description of its color composition, i. e., the relative intensity of its light components distributed along this wavelength region. Each of the three phosphors used in color television is a primary emitter of light in a separate region of the visible spectrum, i.e., the three phosphors produce red, blue, and green light.

## Color mixing

The triad of red, blue, and green phosphors is important in color television because the proper mixture of these primary emitters produces white light. Addition of any primary color to the white mixture produces the hue of that color; subtraction induces the complement of the primary color. The primary triad, therefore, can generate a countless number of colors (the totality of which is called its *color gamut*), as well as white. (Although this discussion treats the primary triad as pure, spectral, or "rainbow" colors, it also applies to the phosphors used in commercial color television, which have less sharply peaked spectral distributions.)

The standard color mixing diagram shown in Fig. 1, which was adopted by the International Commission on Illumination in 1931, illustrates the pairs

of complementary colors generated by the primary triad. Because the proper mixture of complementary colors produces white, the straight line connecting each pair passes through the white, or neutral, point. The location of this point on the connecting line is an indication of the effectiveness of each primary color in neutralizing its complementary color. For example, blue light neutralizes its complement, yellow light, very effectively; red and green are less effective in neutralizing their respective complements, cyan (blue-green) and purple. (This property is described as relative luminance of each color, or as the luminance ratio between the complementary pairs.)

The neutralizing power of a primary color over its complement also affects a viewer's response to a field of that color placed in a luminous neutral (white) background. A neutral background of higher luminance (brightness) than the color area induces an apparent grayness into the chromatic field. The color at which the threshold of grayness is reached and "fluorence" (the appearance of fluorescence) begins to decrease is called a zero-gray color.<sup>1</sup>

Zero-gray colors for a given hue are described by their luminance and purity. The purity of a zero-gray color is the ratio of the luminance of the pure or chromatic hue-determining component to the total luminance of the color mixture (chromatic plus white additive) which complements



George M. Ehemann  
Chemical and Physical Laboratory  
Television Picture Tube Division  
Electronic Components  
Lancaster, Pa.

received the BE in Engineering Physics from Cornell University in 1964. That year he joined RCA's Chemical and Physical Laboratory at Lancaster and has been working on color measurement techniques and optical property studies of color television screens. In 1965, while on leave of absence, he earned the ME in Engineering Physics at Cornell University.



William G. Rudy  
Chemical and Physical Laboratory  
Television Picture Tube Division  
Electronic Components  
Lancaster, Pa.

received the BS at Dickinson College in 1943 and the MS in Physics at Carnegie-Mellon in 1948. He has had additional academic work at the American University at Biarritz, France, Newark College of Engineering, and Franklin & Marshall College. In 1948 he joined the Chemical and Physical Laboratory at RCA Lancaster and achieved senior engineering status in 1955. His major concern has been experimental work embracing conversion, cathode ray, and power tubes. His contributions resulted in improved performance in camera tubes leading to four patents, enhanced secondary electron emission in conversion tubes, and accurate and meaningful test methods for evaluating thermionic emission, residual gas, and life performance in cathode ray and power tubes. Presently, he is working in the field of colorimetry of color TV picture tube phosphors and has recently published a paper on the chromaticity of narrow-band emitting phosphors.

it in a two-component mix and desaturates it. Both can be varied independently of the luminous background.

An experimental technique was used to determine zero-gray color curves for blue, yellow, green, red, and cyan hues produced by a P22 television phosphor screen when the grid voltages of the three electron guns were adjusted to generate the proper primary excitations for the standard television white. For a desired hue of red, blue, or green, the grid voltage exciting the corresponding phosphor primary is increased either slightly or noticeably to produce low and medium purities, respectively. Full purity occurs when the hue-producing primary alone is excited.

For example, yellow and cyan hues are produced when their respective phosphor primary complements (blue and red) receive less excitation than that required to produce white. When the blue or red phosphor is unexcited, full purity results in the yellow and cyan hues, respectively.

Bright light having the color of a 3500°K black-body radiator was used to illuminate a reflecting baffle placed between the observer and the television screen; the light passes through the viewing aperture in the baffle without striking the screen, as shown in Fig. 2. The observer views the screen through the baffle illuminated by a luminous background, adjusts screen luminance until the zero-grayness threshold is reached, and records two measurements: the total luminance of the phosphor screen and the luminance of the hue-producing primary (in the case of yellow hues, the blue-phosphor luminance is recorded). The first measurement is the zero-gray color luminance, the second measurement allows calculation of color purity. Fig. 3 shows the results of such measurements for blue and yellow hues.

Blue colors, which easily neutralize their yellow complements, remain fluorescent until a high threshold value of background luminance is reached, while yellows lose fluorescence and appear to contain gray at a much lower threshold. Television-gamut greens and reds behave as the yellow colors, while cyans exhibit intermediate behavior.

The uniqueness of the zero-gray colors for blue hues lies in the behavior of required blue chromatic luminance as a function of color purity in the presence of a bright background. The blue chromatic luminance curve in Fig. 3 is flat at all color purities above a low threshold value; therefore, reduction of the white component does not require an increase in chromatic illumination, and the zero-gray threshold is maintained all the way to full purity as the white component is gradually reduced to zero.

Although a decrease in the white component of luminance in a yellow hue produces a purer yellow on the color mixing diagram of Fig. 1, for fixed background luminance near threshold, the induction of grayness offsets this physical gain in purity. As a result, additional chromatic yellow illumination would be required to produce the same total luminance of the original color to a viewer. At zero-gray threshold, therefore, total luminance of yellow hues remains constant for purities ranging from zero (completely white) to unity (pure yellow). Whether the "pure yellow" is spectral or within the television gamut of a broadband green is unimportant in matters concerning fluorence of yellow hues. So far as fluorence is concerned, phosphor efficiency rather than purity of emitted color is essential in the green and red primaries.

### Picture viewability

Viewability is best studied independently of a television picture so that the viewer can control some of the physical properties. When a television picture is simulated with projected color transparencies, the viewer can manipulate independently the color, the luminance (brightness), the resolution, and the ambient illumination to "create" the most desirable picture.

For each picture, the effects of the various factors influencing the viewer's judgment can be evaluated from a pattern produced by substitution of a RETMA resolution-chart transparency for the color transparency. The image provides a gray scale, broad black and white areas for high contrast, and resolution wedges. The gray scale, which has low contrast in both highlight

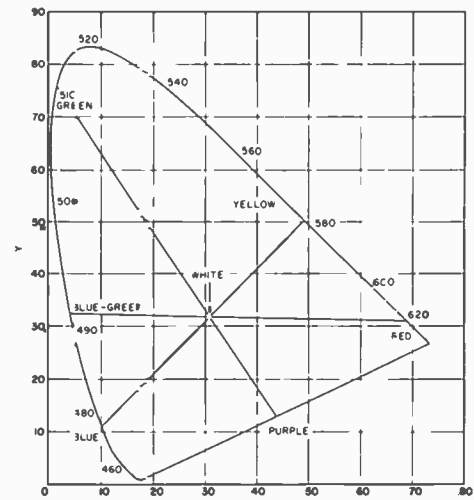


Fig. 1—Stacard ICI diagram showing spectral colors and their complements (the color of neutral equals that of a 7000°K black-body radiator).

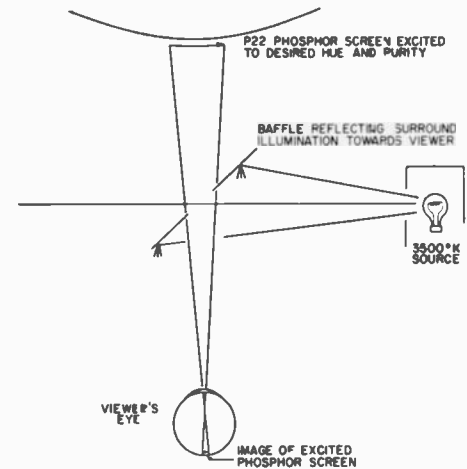


Fig. 2—Experimental determination of zero-gray colors.

and shadow areas, proves particularly useful.

One important factor is the picture brightness required for comfortable viewing at various ambient illumination levels. For example, the luminance required when pictures are viewed with 2.5 foot-lamberts reflected ambient illumination, comparable to that encountered in a moderately lighted room, is approximately 17 foot-lamberts. For prolonged viewing, the picture is judged uncomfortably bright at 40 foot-lamberts and too dim at 5 foot-lamberts. Fig. 4 shows the relation between the picture luminance for typical low and high brightness areas and reflected ambient illumination for satisfactory viewing.

Although the contrast and the resolution of a color picture are decreased by increases in ambient illumination, viewability can be conserved by increased picture luminance. As an example, a picture was set up with a reflected ambient illumination of 0.5 foot-lambert. The white luminance of

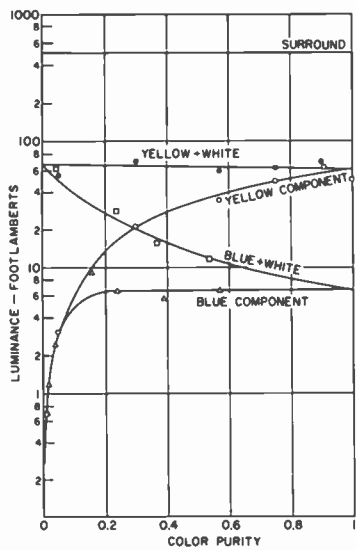


Fig. 3—The required luminance of blue and yellow hues and their respective chromatic components at zero-grayness threshold in a 500 fL surrounding.

the RETMA slide measured 25 foot-lamberts and the highlight contrast ratio was 50. When the ambient illumination was increased to 1 foot-lambert, the contrast ratio was reduced to 26. The viewer then changed the picture brightness to "recover" the excellent picture. However, instead of increasing the highlight brightness to 50 foot-lamberts to produce the original contrast ratio of 50, the viewer settled for a highlight luminance of about 40 foot-lamberts, and a contrast ratio of only 40, as shown in Fig. 5.

The conservation of viewability was studied by Luckiesh and Moss<sup>2</sup> using the black-and-white Snellen eye chart at various room light levels; their results are shown in Fig. 6. The percent contrast has been recalculated in terms of contrast ratio, which is the luminance ratio of the highlights to adjacent areas on the eye chart. These curves should remain valid for comparison to color television, in which a self-luminous phosphor screen and a protective gray glass are placed in an ambient setting.

The experimental highlight data for constant viewability shown in Fig. 5 correspond to the 110% normal-vision curve of Luckiesh and Moss in Fig. 6. However, the slope of the latter curve indicates that a decrease in highlight contrast ratio should not affect the viewability, while the slope of the experimental data indicates picture degradation with decreased contrast ratios. This discrepancy was resolved when the experimental shadow-area behavior (i.e., contrast ratio and luminance) was plotted in Fig. 5 for the same ambient conditions as those

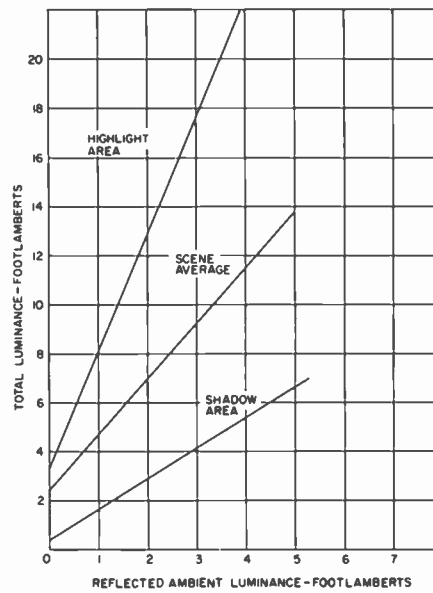


Fig. 4—Picture luminance for typical low and high brightness areas as a function of reflected ambient illumination.

placed on the highlights of the picture. This experimental curve nearly coincides with the 50% normal-vision curve of Luckiesh and Moss. This result indicates that the viewability conserved by the viewer is primarily in the picture shadow areas.

There is also agreement between the Luckiesh and Moss normal-vision data and the experimental data on induced grayness in a chromatic field. The Luckiesh and Moss curves for 50, 80, 100, and 120% normal vision are not associated with independently adjusted background luminance. In their work, the background is identical to the highlights. However, when zero-gray curves for blue and yellow hues in a background luminance of 500 foot-lamberts are replotted from Fig. 3 onto the Luckiesh and Moss plot, they show significant correspondence. (Color purity in Fig. 3 is converted to contrast ratio in Fig. 5. The contrast ratio for color mixtures of chromatic light and white light composing the hues of Fig. 3 is the ratio of the total luminance of the hue to that of the white component.)

For dim colored areas such as blue on a projected picture, the zero-gray curve for blue shifts to the left in Fig. 5 (and produces smaller threshold luminance for the same contrast ratio) as a result of the much lower background luminance values (0.5 and 1 foot-lambert) used in the experiment. The experimental curve of constant viewability in the blue background then agrees fairly well with the shifted zero-gray curve for blue color areas. These experimental results of constant viewability may

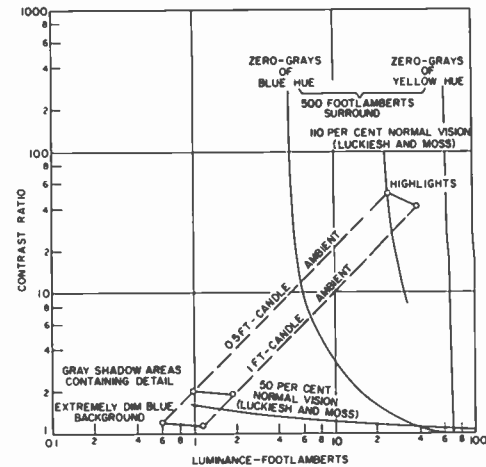


Fig. 5—Behavior of various areas in a scene judged equally viewable under different ambient conditions.

be altered if the dim background area is yellow, red, or green in hue because of the radical difference between the zero-gray curves for blues and for greens, yellows, and reds in the low-contrast-ratio region, where the fluorence of the latter hues is less sensitive to contrast ratio. Vertical lines in Fig. 5 would then represent constant viewability as determined by the zero-gray condition of the green, yellow, or red hue. It is also possible, however, that detail in the shadows must be conserved for any hue, or even for true grays; this condition would lead to horizontal lines of constant contrast ratio at the highlight regions as well as in the shadow regions for constant viewability of a picture.

Detail resolution and picture fluorence are not necessarily incompatible, therefore, since both are enhanced by gain in picture luminance. For a scene with dim, unstructured chromatic background mixed with ambient illumination, however, a compromise may be necessary between increased background fluorence and a slight loss in detail resolution in other shadow areas of the scene as the ambient luminance is increased. If picture fluorence were much more critical than detail resolution, constant viewability of pictures with green, yellow, and red shadows would require constant luminance, and the viewability curves would be vertical or nearly so in the highlight-area behavior of Fig. 5. Pictures containing detail in green, yellow, and red shadow areas would not suffer in this respect. Because the increase in picture luminance recovers both fluorence and

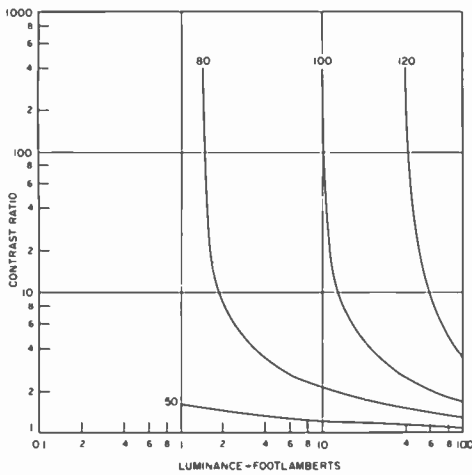


Fig. 6—Constant viewability curves of Luckiesh and Moss.

shadow-area detail (except for dazzling background luminances), and because both are desirable in a given area of a scene, the viewability is limited by shadow detail provided no dimmer unstructured chromatic background exists.

Fig. 7 shows the effects of reflected ambient illumination on shadow detail contrast for a specific case of two adjacent picture elements in a shadow area with luminances  $L_1$  and  $L_2$ , where  $L_1$  is twice the value of  $L_2$ . (At zero ambient, the contrast would equal 2.) The average scene luminance is defined as the sum of the average luminance of the two picture shadow areas and the reflected ambient.

As an example of the use of Fig. 7, the following conditions are assumed:

- Average scene luminance 7 foot-lamberts (i.e.,  $L_1 = 4$  foot-lamberts);
- Reflected ambient luminance 4 foot-lamberts;
- Screen reflectivity 1.0;
- Glass reflectivity 0.04;
- Faceplate transmission 0.5.

When no faceplate is used, the contrast is 1.33. With the faceplate, the reflected ambient luminance is reduced by 75% (doubly attenuated) and the area luminances  $L_1$  and  $L_2$  by 50% (singly attenuated). The result is a 64% decrease in average scene luminance but a 12% increase in contrast. (Although this latter figure seems insignificant, the eye is capable of discerning a 2% shift at this brightness level.) In a television receiver, the loss of brightness can be compensated by an increase of video drive. If the video

drive is quadrupled to produce the original average scene luminance of 7 foot-lamberts, the contrast increases by 35% to 1.8.

Table I shows the effect of the faceplate transmission on contrast for the above example, without video-drive compensation. Decreasing faceplate transmission decreases luminance, but increases contrast.

In color television, the white light that mixes with and desaturates a color is related to the background luminance by a factor that involves the television faceplate transmission. Zero-gray colors of the various hues are produced in the picture shadow areas, and the purity of these threshold colors is controlled by the faceplate transmission.

In the case of zero-gray colors of yellow, red, and green hues, varying faceplate transmissions also cause zero-gray areas of the scene to be redistributed, even when the product of the picture signal luminance (video drive) and glass transmission remains fixed. If glass transmission is decreased to enhance the contrast ratio, the blue threshold colors return to the original distribution in the picture after video-drive adjustment. In the case of the other hues, video drive must be further increased until the total picture luminance is the same as that for the original high glass transmission.

For constant ambient luminance and video drive, highlight-area behavior is directly related to shadow-area behavior as the glass transmission varies. For different faceplate transmissions, contrast and luminance in the highlights have been compared with the experimentally determined conditions for constant viewability. If a particular scene has dim achromatic detail upon a still dimmer and unstructured blue background, Fig. 8 shows that 40% transmission is a reasonable value for practical use. Values lower than 40%, including the 24% value for optimum contrast, reduce picture viewability primarily because of decreased luminance. Transmission higher than 40% produces a substantial increase in the reflected ambient illumination and a consequent loss in detail contrast. The contrast loss can be recovered by an increase in the picture brightness with video drive; however, resolution will

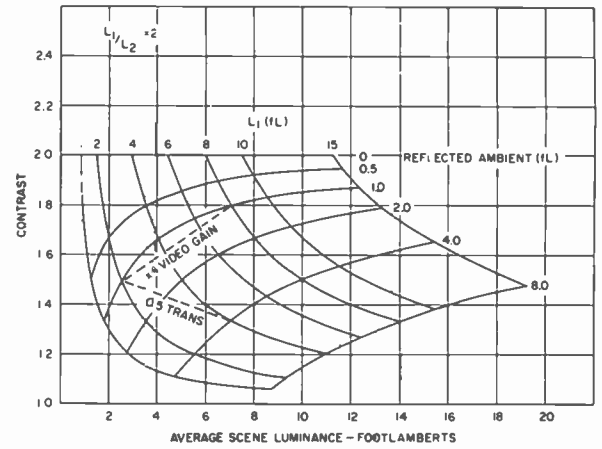


Fig. 7—Effect of reflected ambient illumination on shadow-area detail contrast for two picture elements with luminances  $L_1$  and  $L_2$ .

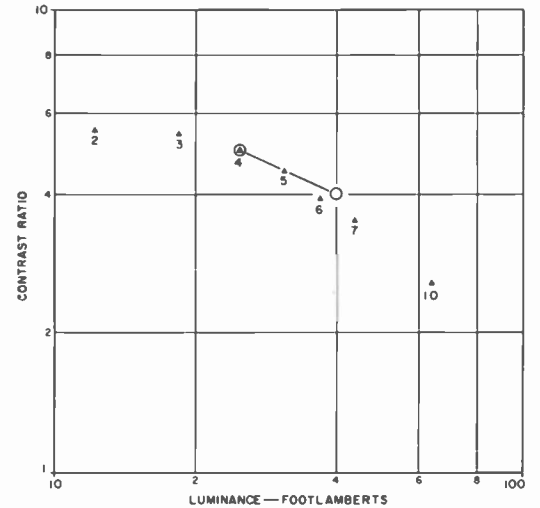


Fig. 8—Effect of glass transmission choice for fixed operating conditions as compared to experimental segment of constant picture viewability drawn for highlight region.

decrease as a result of beam blooming and beam power requirements will increase.

## References

1. Evans, R. M., and Swenholt, B. K., "Chromatic Strength of Colors: Dominant Wavelength and Purity," *J. of Optical Soc. of Amer.* (Nov 1967).
2. Luckiesh, N., and Moss, F. K., *The Science of Seeing* (D. Van Nostrand Co., New York, N.Y., 1943) p. 133.

Table I—Contrast and average scene luminance change as a function of faceplate transmission for a scene of low brightness and low contrast ( $L_1/L_2 = 2$ )

Faceplate Transmission	Re- flected ambient Lumi- nance (fL)	$L_1$ (fL)	Ave. scene lumi- nance (fL)	Contrast
1.0	4.0	4.0	7.0	1.33
0.8	2.56	3.06	4.85	1.37
0.7	1.96	2.68	3.97	1.40
0.6	1.48	2.30	3.20	1.44
0.5	1.08	1.92	2.52	1.47
0.4	0.75	1.53	1.90	1.50
0.3	0.49	1.15	1.35	1.54
0.24	0.32	0.92	1.00	1.60

# Autotest—automatic production-test and process-control system for color picture tubes

W. E. Bahls  
F. C. Fryburg  
A. C. Grover, Jr.  
J. F. Stewart  
N. A. Teixeira  
E. D. Wyant

**The automatic production-test and process-control system permits more efficient and more accurate testing of mass-produced color picture tubes than was heretofore possible. Therefore, this system offers the possibility for both improving the quality of the manufactured product and reducing the cost of the testing procedure.**

**A**N IMPORTANT STEP in the production of a complex, mass-produced product such as color picture tubes is the final testing. Formerly, color picture tubes were tested at a number of test stations, each manned by an operator. Because of the many different tests that had to be made, testing required many people, much test equipment, and a considerable amount of time, and was relatively expensive. In addition, because of the production deadlines the number of tests that could be performed was limited. Finally, because many people and pieces of testing equipment were involved, maintenance of calibration was difficult. It sometimes occurred that tubes which should have been rejected were not discovered and tubes which were perfectly good were rejected.

## THE SYSTEM

The system includes five test stations, each testing different tube parameters and all under the control of a digital computer of the stored-program type. It also includes means for automatic indication which shows whether a tube has passed all tests and, if not, the tests which it has failed and, in some cases, the reprocessing steps which should be taken. The computer performs immediate (on-line) analyses of the tube parameters which have been measured during the testing procedure. In addition, it performs subsequent statistical

analyses of the data to determine the deficiencies or potential weaknesses in the manufacturing process so that corrective action may be taken. Fig. 1 is a functional flow diagram embodying not only the test capability of the system but also its ability to provide some control over the processes (exhaust and aging) immediately before testing and the analysis and/or reprocessing subsequent to testing.

## PRODUCTION PROCESS

The manufacture of color picture tubes involves many different steps, including manufacture of the mask, application of the screen to the faceplate, production of the gun assembly, joining of the faceplate to the remainder of the glass envelope, sealing of the gun assembly into the glass envelope, evacuation of the tube, and the like (Fig. 2).

During the manufacturing process, each tube is identified by a number. This identification number, and identification of certain critical steps in the manufacturing process, are recorded by punching a data-processing card, which travels with each tube. For example, in the manufacturing process there are a number of different machines employed for evacuating the tubes. The identifying number of the machine and the evacuating cart used for processing a particular tube are recorded on the data-processing card for that tube. The tube class and the tube type are also recorded.

After the above manufacturing steps have been completed, tubes of different types and classes are transferred from different processing equipment and/or conveyors to the final processing conveyor. Each tube undergoes certain processes which activate the cathode coating of each gun. Such process functions are possible because each tube is located on a separate aging/test car-

rier which (through its aging socket and spring contacts) provides the electrical interface between the tube and the process equipment.

## FACTORY AUTOMATIC ELECTRICAL TEST COMPLEX

### Data Entry Stations

When the tube leaves the aging area (Fig. 3) the aging socket is removed and the test socket is connected. In addition, the data card which travels with the picture tube is placed in the card reader. (As previously men-

**Frank C. Fryburg, Program Director**  
Color Autotest Project  
Electronic Components  
Lancaster, Pa.

received the BS in Physics from Pennsylvania State University in 1949 and the MBA in Industrial Management from the University of Pennsylvania in 1951. He joined RCA in February, 1951 as a Manufacturing Trainee. He has served in Lancaster, Pa. as a Parts Manufacturing Engineer, Color Parts Quality Manager, and Color Cost Reduction Administrator. He is currently an Engineer in TPTD Systems, Quality and Reliability Assurance Engineering. In the summer of 1964 he was appointed Program Director for the Color Autotest Project. He is presently President of the Board of Commissioners in Manheim Twp., Lancaster County and is a past National President of the Sigma Pi Fraternity.



tioned, this card includes such vital information as the tube class, the tube type, and the identification of the equipment used to process the tube). After the card is placed in the card reader and the reader is closed, an operator depresses a button on the reader control panel to indicate the test status of the tube. The button depressed indicates whether the tube has been tested previously. If all such data have been properly entered, they will then be read into the computer. A signal is then returned to the card reader from the computer indicating that the data have been read and recorded; this signal opens the card-reader mechanism. The operator then removes the card and returns it to the tube.

In the meantime, the computer is processing the information read in from the data entry station. Some of this information is maintained in high-speed memory. The balance is stored on magnetic tape for later off-line use. The information retained in high-speed memory includes the tube class, the tube type, and the position number of the carrier on which the tube is riding. This information is vital to the performance of the tests in the subsequent five test stations.

#### Shorts and Leakage Test Station

When a tube reaches this station, an electrical connection is made between the tube to be tested and the specific test station. In addition, a signal is generated which produces an interrupt to the computer signifying that there is a tube in the station ready to test. The computer, having kept track of each of the 120 carriers included in the test loop at any given time by means of an interrupt analysis system, is then able to determine the number of the carrier in the station and, therefore, the class and type of the tube to be tested. With this information, the computer then determines the tests to be performed on the tube while it is in this station.

It should be noted that once the engagement of the contactor blocks of the test carrier and carriage is completed, both the tube and the carriage continue to move along the conveyor. This joint movement continues for a period of 10 seconds which is the maximum time available to perform all of the tests on that tube. At the end

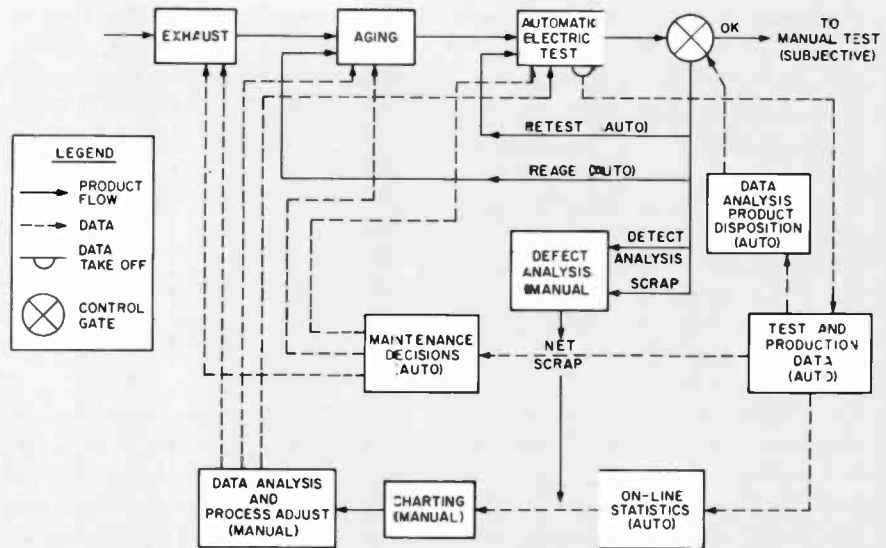


Fig. 1—Functional system diagram of the automatic production test and process-control system for color picture tubes.

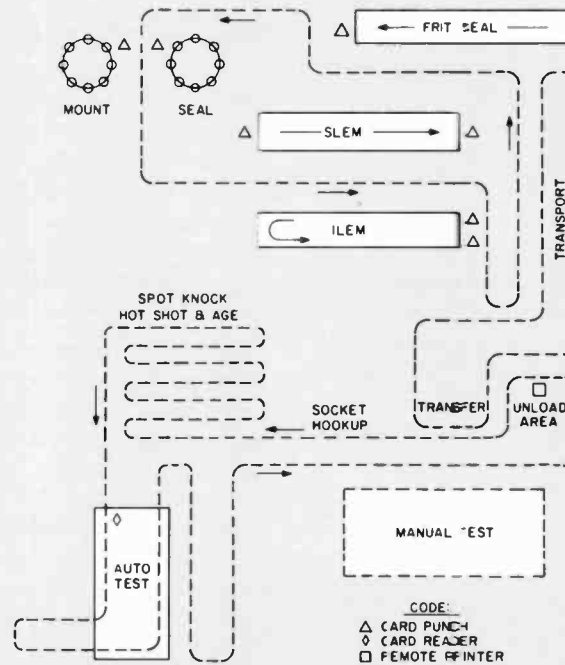


Fig. 2—Factory process flow.

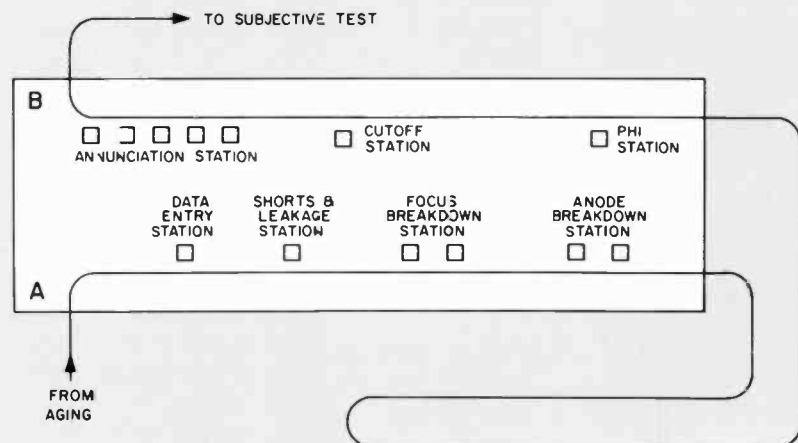


Fig. 3—Factory automatic electrical test complex.

of the 10-second period, the contactor blocks are disengaged and the test carriage returns to its starting position to pick up the next tube carrier.

Because of the high-speed switching capability of this system, the shorts and leakage station has been so designed that it is capable of performing a maximum of 42 individual tests on each tube. In actual practice, the total test routine has been broken down into 13 group tests and 29 individual tests. During a group test, voltages are applied to several elements and a measurement circuit is tied in to one additional element. The leakage current between that element and those with applied voltages is then measured. If this leakage exceeds a predetermined value, the computer then performs the individual tests. With this method, it is possible to test good tubes in a minimum amount of time and, simultaneously, to produce detailed information on tubes that exhibit leakage. Finally, it is noted that this feature not only tests the elements in a given gun, but can also test similar elements between guns.

This station, as well as all other stations, was designed for maximum flexibility. This system can apply a wide range of voltages to each element of the tube and also read a wide range of leakage currents. Such a capability is currently sufficient for measurement of all known color-picture-tube types and it is expected that it will handle all future types being considered for production.

#### **Focus Breakdown Station**

This station is the next one in the autotest sequence. From the standpoint of test-carriage to tube-carrier contact, its operation is similar to the previous station. In addition, however, it contains a sensing device which is placed over the face of the tube. This test station performs an over-voltage test. In other words, during the entire test period that voltages are applied, the beam current is completely cut off by a high bias voltage, and excessive voltage is applied to the focus element. The purpose of this test is to determine any instability in the form of arcing or stray emission between the accelerating element and the focus element of the tube.

Tube arcing is detected through a special transducer device in the anode

circuit of the system. Thus, when arcing occurs the current level flowing in the anode lead changes significantly. This change in current is detected and converted into a digital form which is stored and subsequently transmitted to the computer. Detection of stray emission is accomplished through photosensitive devices installed in the detector housing which, in turn, is placed on the tube face during the entire test period. The photocells sense the light which develops as a result of stray emission.

Finally, it should be noted that these devices continue to count arcs and detect stray emission during the entire test period. The final readings sent to the computer constitute a summation of all arcs and stray emission developed during this test cycle.

#### **Anode-Breakdown Test Station**

This test station is next in sequence and is quite similar to the focus breakdown station. The primary difference is that the over-voltage in this particular case is applied to the anode rather than the focus element. Therefore, the primary source of arcing or stray emission is between the focus and anode elements of the tube.

Experience has shown that although these two test stations appear to be performing a very similar test, the tube-processing characteristics are such that problems can develop in the anode-breakdown or in the focus-breakdown area independently of each other. Thus, both of these tests must be performed to insure a good quality of the product to be shipped. Finally, it should be noted that the system has the capability, through computer control, to provide different over-voltages for the anode and/or focus element as different tube classes are tested.

#### **Phi Station**

This station, although next in the process, is some distance away from the anode-breakdown station. Such a delay permits the tube to cool. These tests are performed at minimum rated heater voltage after a short warmup. The first test in this station is cutoff-compensated emission current, commonly referred to as Phi. The test is performed in two parts:

- 1) The voltages to produce emission-current cutoff are applied to the gun.

- 2) The bias voltage is programmed to 0 by the computer; the measurement device records the emission current, and the computer compares this value against the predetermined limits.

The emission-current cutoff is determined through a series of tests known as search tests. These tests are performed with a fixed negative bias applied to the control grid and a predetermined value of positive voltage applied to the accelerating grid. At this point, the cathode current is measured and examined in high-speed memory which determines whether the next voltage step applied to the accelerating grid should be more positive (increase in current) or less positive (decrease in current) to reach the cutoff point. This process continues until cutoff is reached. This series of steps is performed three times to check the three guns in the tube.

A second important test in this station measures the gas content of the tube. In this test, the search concept is again used; a negative control-grid bias is programmed through a series of steps by the computer until a predetermined cathode current value is achieved. After the search test, two additional current measurements are made and their values are recorded in high-speed memory. A subtraction between two values is made and their net difference, usually in microamperes, constitutes the gas reading.

The final test at this station is anode continuity. As the name implies, it determines the continuity from the anode element of the mount through the bulb spacer and graphite coating to the button on the side of the funnel, where the high-voltage circuitry in the receiver will be eventually connected. Unless good continuity exists throughout this entire circuit, the tube will not work properly and will frequently exhibit a ragged raster.

#### **Cutoff Station**

This is the last test station in the system. There are two major tests at this station, each performed at normal heater voltages. The first is the emission cutoff test performed on each of the three guns. The  $G_2$  voltage obtained after the successful completion of a series of search tests is compared with a predetermined limit. In the second test, the bias voltage is pro-

grammed to zero and the maximum emission current is read and checked. These tests are then repeated for the other two guns in the tube. Finally, the last test in this station measures the actual heater current.

#### **Annunciation**

When a tube has completed all tests in the five test stations, it moves into the annunciation station. For each tube, this station provides specific colored tape markers to indicate whether a tube has satisfactorily completed all tests and, if not, what further processing is required.

At this point, it should be noted that in the data entry station, a 75-bit section of high-speed memory is set aside for the tube before it proceeds through test stations. This section is commonly referred to as the binary failure image and during the entire autotest cycle it provides the means of recording all failures of the tube in question for each of the 75 tests.

Once a tube reaches the annunciation station, the computer scans the binary failure image table for that tube to determine its test status. If the scanning reveals that the tube has passed all tests, a green label is applied to the tube with the first of the five tape markers. If, however, the tube has failed one or more tests, the computer determines the failures in the order of importance by means of a previously established priority annunciation table.

With this information, the computer commands one of the four remaining labels to be applied to the tube and, thereby, signifies one of the four alternate processes the tube will undergo: RETEST, REAGE, DEFECT ANALYSIS, and SCRAP.

A remote printer located at the conveyor unloading point is connected to the autotest system. This printer provides detailed information to the tube analyst which indicates the tests that any individual tube failed. Experience has shown that these print-outs are proving invaluable for establishing the cause of tube failure.

#### **PROCESS CONTROL FEATURES**

##### **Condemnation**

When the tube reaches the data entry station, certain key-process data are read from the card into the computer

which stores this information in high-speed memory. These data identify with the tube the key manufacturing processes used in its production. As the tube passes through the autotest cycle, pertinent test results are analyzed by the computer and recorded against specific pieces of production equipment on which the tube was manufactured. If this analysis reveals that a particular piece of manufacturing equipment has been producing bad tubes, the computer will display this result and the equipment will be removed from production. Although such condemnation practice has been in use on a manual basis within picture-tube plants for many years, it is anticipated that the additional high-speed capabilities available through the autotest system will improve the effectiveness of the condemnation procedure and will, thereby, reduce the number of faulty tubes generated from defective equipment.

##### **Data Analysis**

Another process-control feature of this system is its ability to analyze and summarize certain key variables collected during the test process. In addition, the system can provide regular reports of complete test results by the tube class and by type of defect. Through these analyses, it is anticipated that valuable information will be provided to both factory and laboratory engineering personnel which will aid them in their continuing efforts to improve tube processing and tube design.

#### **DESIGN FEATURES**

##### **Accuracy**

Analysis of this equipment clearly indicates that it is far more accurate than any equipment previously used in factory testing. In many respects, it provides a level of accuracy superior to existing laboratory equipment. Two key areas providing a major portion of this improved accuracy are the power supplies and the measurement circuits. In addition, another important feature of this system is its capability for continuous self-check which insures that all test equipment is calibrated and functions properly.

##### **Flexibility**

A major investment of this magnitude cannot be justified unless adequate

assurance of the long range use of this equipment is provided. For this reason, considerable care in the original system design and in the subsequent design of the hardware and software was devoted to the idea that long-range flexibility would be maintained. From the standpoint of hardware design, measurement ranges, voltage ranges, and the like, system capabilities were extended well beyond the requirements of existing tube types. Therefore, it is anticipated that as future tube types are developed, they can be readily adapted to this system without major modifications in the hardware.

The software design also included provisions for changes. In essence, the system was designed to provide a generalized test routine. As each new class of tubes comes into being, a test file must be developed for it. This file can be prepared by personnel familiar with testing but with little or no familiarity with computer programming. In this manner, it is anticipated that new tube classes can be introduced into the system without any significant program changes. This fact has been substantiated already through recent development of the Einzel-lens test file for use with the Autotest system. This development was accomplished with no changes in the software.

#### **SUMMARY**

The automatic production-test and process-control system described has computer-controlled capability for all functions. This capability allows the control of all five test stations, the performance of up to 75 tests on any given tube, and the testing of many tube types on successive carriers. These three features should allow the Marion plant to test all future types and classes of color tubes. In addition, the color Autotest unit can perform all electrical tests of color picture tubes with a higher degree of accuracy than any existing equipment. Finally, the process-equipment condemnation and the data analysis are expected to yield improvements in factory performance. Thus, with improved process control, more accurate test equipment, and a more uniform testing facility, the Autotest system in the Marion plant produces a highly reliable and excellent color picture tube.

# Vidicon photoconductors

J. F. Heagy

Of the many compounds and elements that exhibit photoconductive properties,<sup>1</sup> three have emerged as most suitable for use in vidicons: antimony trisulfide ( $Sb_2S_3$ ), lead oxide ( $PbO$ ), and antimony oxysulfide. The first two are used in commercial applications; the third is used in special applications only. This paper briefly describes the development, applications, and properties of these photoconductors.

IN A VIDICON CAMERA TUBE, the target consists of a layer of semiconductor material called a photoconductor. The electrical resistance of this photoconductor varies when light, X-rays, or electrons are incident upon it. When the camera-lens shutter is opened for a specified time, a charge pattern is formed on the photoconductive layer that corresponds to the image being viewed by the camera. The photoconductor is then scanned by an electron beam to transform this pattern into a video signal.

To perform adequately, a photoconductor must exhibit adequate sensitivity, fast response, adequate spectral response, low or uniform dark current, and chemical stability in a vacuum. In addition, the discharge time of the photoconductor, or the time required for it to return to cathode potential, must be long compared with the time between two successive scans. For commercial TV applications, the discharge time, or RC time constant, must be greater than 1/60 second.

## Antimony-trisulfide

The first commercial vidicon, the RCA-6198, was introduced in March, 1952.<sup>2</sup> Antimony trisulfide was used as the photoconductor because it had been discovered that evaporation of  $Sb_2S_3$  at a rather high pressure (10 to 1000 microns) in an inert gas, such as argon, produced response to blue light superior to that which could be achieved with any photoconductive material previously used and also reduced lag and dark current.<sup>3,4</sup> (Lag refers to persistence, the delay in change of photoconductivity with changes in light intensity measured in percent of initial value of video signal current after illumination is removed from the photoconductor; dark current refers to the current that flows

when there is no radiation incident on the photoconductor.) The antimony-trisulfide photolayers were evaporated in the tube envelope, and exhibited relatively high, nonuniform values of dark current. This was corrected by special shading controls in the camera.

Photoconductor performance was improved by use of an indium seal that permitted vacuum sealing of the faceplate to the glass envelope, or bulb, of the tube. This technique allowed the photoconductive layer to be prepared before the faceplate and photoconductor were sealed within the vidicon. Many faceplates would then be coated in one process, with the result that photoconductive layers were more uniform than those obtained by evaporation within the tube envelope. In this process, as many as twenty targets were prepared at one time by passage of the faceplates over an evaporation boat in a long, cylindrical bell jar. Two passes were made, one in a high gas pressure to obtain a porous layer and one in a hard vacuum to obtain a hard layer. The resulting vidicons were more sensitive than previous vidicons because the uniform dark current exhibited permitted the target voltage to be increased. The RCA-7038 vidicon which resulted from this process became the standard tube for use in film-chain broadcast equipment. The next improvement in antimony-trisulfide photoconductors was the development of a solid-porous-solid layer arrangement that increased the sensitivity of the vidicon by a factor of two with no significant increase in lag. As a result, vidicons could be used in applications in which insufficient lighting conditions had previously prohibited their use. However, the response was still too slow for studio telecasting.



J. F. Heagy  
Camera Tube Design  
Industrial Tube Division  
Electronic Components  
Lancaster, Pa.

received the BS in Physics (*cum laude*) from Franklin and Marshall College in 1957. In 1963, he received the MS in Physics from that institution. In 1959, after two years of teaching, Mr. Heagy was employed by RCA as a type engineer in Vidicon Tube Manufacturing. Since 1963 he has been engaged in photoconductor development work in the Camera Tube Design Group. In this assignment, he developed the high sensitivity photoconductor now used on practically all RCA commercial vidicons and customized vidicons. He developed the photoconductor for vidicons used to monitor radar displays, and was instrumental in the development and improvement of the photoconductor and reticle configuration used in Ranger 8 and 9. Both of these developments resulted in the granting of U.S. patents. In 1964, he received an RCA Engineering Achievement Award in recognition of his contributions to the advancement of the vidicon state-of-the-art. Mr. Heagy is a member of Phi Beta Kappa.

## Lead-oxide

The lead-oxide photoconductor was introduced in 1964.<sup>5</sup> Fig. 1 shows a photograph of the RCA-C23803 lead-oxide vidicon—the Vistacon. Lead-oxide vidicons exhibit extremely low dark current and fast response, and thus are suitable for use in studio color cameras. Because these vidicons have a very low noise level as compared to that of image orthicons under normal studio lighting conditions, and are also simpler to operate, the lead-oxide-vidicon color camera has gained wide acceptance in broadcasting.

Because lead-oxide layers undergo extreme chemical change in a normal room environment, great care must be taken of the layer after it is evaporated. Standard vidicon manufacturing procedures in which the photoconductor is deposited on a faceplate in one physical location and the faceplate is assembled to the gun mount in another location are not practical because of the possibility of exposure

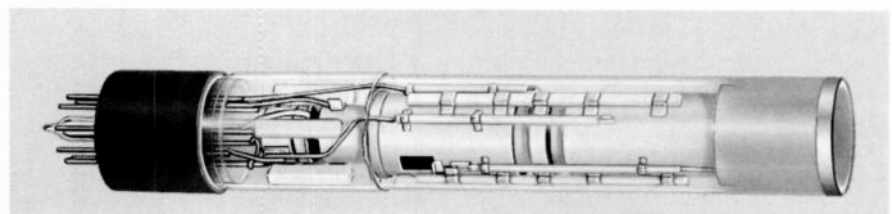


Fig. 1—RCA-CA23083  
lead-oxide vidicon,  
or vistacon.

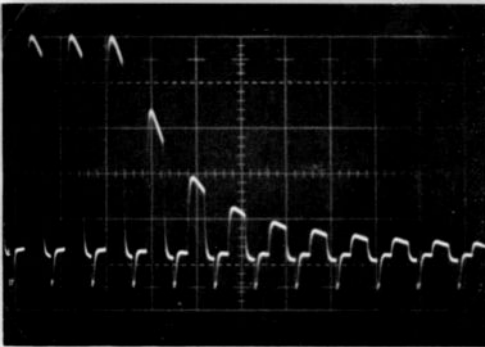


Fig. 2—Decay curve of video signal after illumination is removed from antimony trisulfide photoconductor in RCA-8134 vidicon (lag is 28%).

of the photoconductive layer to air between operations. The photoconductive layer is also susceptible to gases driven off tube parts and glass when they are heated during tube processing. Consequently, most of the gun and tube processing must be completed before the lead-oxide photoconductor is transferred to the gun mount.

Because of the chemical delicacy of a lead-oxide photoconductor, it is desirable that the layer be scanned at various stages of tube processing to evaluate its photoconductive properties. Routine vidicon processing steps in which glass or gun parts are heated may have a severe chemical effect on the lead-oxide layer and significantly alter its photoconductive properties. Lead-oxide photoconductors also tend to undergo significant changes during the first 100 hours of scanning; in general, the photoconductive properties improve. As part of the quality-control procedure, tubes are operated for 100 hours and then "shelf-aged" for a period of approximately four weeks. If a tube performs satisfactorily after this period, it is classified as a useful tube and will have a probable scanning life of several thousand hours.

#### Lead-oxide vs. antimony-trisulfide

Table I compares the electrical properties of antimony-trisulfide and lead-oxide photoconductors. Measurements for antimony trisulfide were made on an RCA-8134 vidicon, and those for lead oxide on an RCA-C23083. Figs. 2 and 3 show the decay curve of a 100-nA-peak video signal after removal of illumination from the 8134 and the C23083. Fig. 4 shows the transfer characteristics of both tubes.

It is evident from Table I that the two photoconductor types differ in

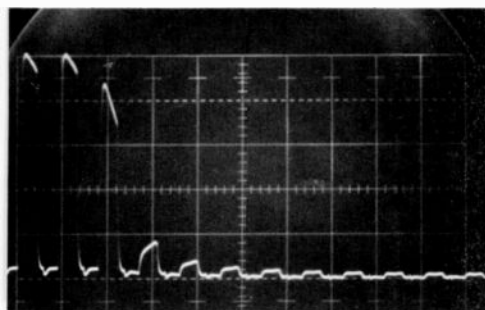


Fig. 3—Decay of video signal after illumination is removed from lead-oxide photoconductor in RCA-C23083 visticon (lag is 6%).

many respects electrically. However, the basic difference between the two photoconductors is the barrier-layer construction used in the lead oxide type, which produces a low dark current and a high electric field in the photoconductor. The major advantages of lead oxide targets, therefore, are the extremely low dark current and fast response. Because the dark current of antimony trisulfide targets is very temperature-dependent,<sup>6</sup> operation of cameras using antimony trisulfide vidicons may be quite unstable if the ambient temperature varies as much as 5 to 10°C. The dark current of a lead oxide vidicon is relatively unaffected by the same temperature change; even when the dark current is doubled or tripled, it is still in the nanoampere range and is a very small part of the total signal.

The low lag of the lead-oxide photoconductor makes it suitable for tubes used in studio and outdoor broadcasts where earlier vidicons exhibited too much lag and smearing of scenes. Lead-oxide vidicons are therefore replacing the image orthicons which were used almost exclusively for live color cameras before 1964.

Some disadvantages of the lead-oxide photoconductors are lack of sensitivity to dark reds (6500 to 7000 angstroms) and unity gamma (where gamma is the slope of the light transfer curve shown in Fig. 4). The lack of sensitivity to dark reds has not proven to be a major problem in actual use. However, because of the high gamma value, bright areas of a scene make it difficult for the scanning electron beam to reduce the signal on the photoconductor to cathode potential. As a result, moving highlights of a scene may smear if the electron-beam strength is insufficient to discharge the signal.

The dependence of vidicon sensitivity on target voltage is much greater when antimony trisulfide is used for the photoconductor than when lead oxide is used. The sensitivity of a lead-oxide vidicon almost reaches a plateau at 50 volts for a fixed illumination; in addition, its dark current is relatively unaffected by target voltage. In an antimony-trisulfide vidicon, the sensitivity is proportional to the square of the target voltage, and the dark current is proportional to the cube of the target voltage.

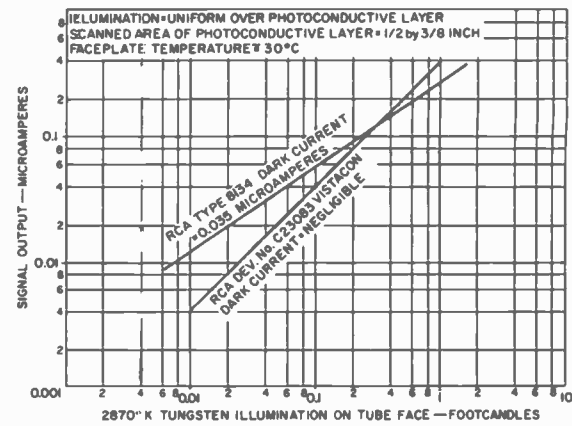


Fig. 4—Transfer characteristics of a lead oxide and an antimony trisulfide photoconductor.

#### Antimony-oxysulfide

Photoconductors other than antimony trisulfide and lead oxide are used in tubes intended for unique applications in which different scan rates and lag are required. For example, the RCA-C74113 and 4500 vidicons are made with an antimony-oxysulfide photoconductor. This photoconductor can provide a sensitivity of 500  $\mu\text{A}/\text{lumen}$ , but also has a lag of 60 to 90% after removal of illumination, and is therefore totally unacceptable for broadcast use. However, it is quite adequate for slow-scan TV applications such as the TIROS and RANGER spacecraft.

#### References

1. Bube, R. H., *Photoconductivity of Solids* (John Wiley and Sons, 1960) pp. 281.
2. Weimer, P. K., Forgue, S. V., Goodrich, R. R., "The Vidicon Photoconductive Camera Tube" *Electronics* Vol. 23 (May, 1950) pp. 70-73.
3. Cope, A. D., Goodrich, P. R., Forgue, S. V., "Properties of Some Photoconductors, Principally Antimony Trisulfide" *RCA Review* Vol. 12 (1951) pp. 336.
4. Forgue, S. V., "Porous Antimony Trisulfide." U.S. Patent 2,744,837 filed June 1, 1951 and Zworykin, V. K., Ramberg, E. G., Flory, L. E., *Television in Science and Industry* (Wiley & Sons, Inc., 1958).
5. DeHaan, E. F., "A Photosensitive Device and Its Manufacturing Process," Belgian Patent No. 645,119, March 12, 1964.
6. Johnson, R. E., "Vidicon Performance in Extreme Thermal Environments" *RCA Review* Vol. 27, No. 3 (Sep 1966) pp. 367-369.
7. DeHaan, E. F., Van der Drift, A., Schampers, D. P. M., "The 'Plumbicon,' A New Television Camera Tube," *Philips Tech. Rev.* 25, No. 5 (1963-64).

Table I—Comparison of lead-oxide and antimony-trisulfide photoconductors

Photoconductor Property	Antimony Trisulfide	Lead Oxide
Operating target voltage (V)	30	50
Dark current (nA)	35	0.3
Sensitivity ( $\mu\text{A}/\text{lumen}$ )	200	500
Lag (% of initial value of 100 nA signal 1/20 s. after illumination is removed)	28	6
Amplitude response to a 400 line square-wave TV test pattern at center of picture	25	20
Average gamma (slope of transfer characteristic for a signal output current between 20 and 200 nA)	0.65	0.95

# The image isocon — an improved image orthicon

E. M. Musselman | R. L. VanAsselt

This paper discusses the basic operation of the image isocon, with emphasis on the electron optics of the reading section which distinguishes the operation of the isocon from the orthicon. The improvement achieved by low-dark-current operation of the isocon is demonstrated by comparison of the image-isocon and image-orthicon performance. In addition, image isocons designed variously for use in studio, X-ray, and low-light level applications are briefly described.

THE IMAGE-ORTHICON CAMERA TUBE has been used in broadcast television for more than twenty years. It has good sensitivity and resolution, and can televise scenes containing very bright objects because of the well-known knee in its transfer characteristic. The image orthicon is also surprisingly rugged, very stable in operation and not damaged by inadvertent overlighting. The new electronically conducting glass targets now incorporated in these tubes provide long life and freedom from raster burn.

The image orthicon, however, operates with a high dark-current level that leads to some undesirable characteristics in the resulting picture quality. Variations in this dark current produce background non-uniformity. In addition, the dark current adds noise, particularly to the signal from low-light areas of a scene, and this noise limits the dynamic range. Finally, beam setting is critical because excess beam adds directly to the dark current and produces excess noise.

A recently developed variation of the image orthicon, the image isocon, provides performance that far surpasses that of the image orthicon. In particular, the signal-to-noise ratio, dynamic range, and background uniformity are improved, while the desirable characteristics of the image orthicon are retained.

## Image-isocon history

The image isocon was invented by P. K. Weimer<sup>1</sup> in 1947. Because the electron-optical requirements for isocon operation were more sophisticated than for image-orthicon operation and problems with tube set-up were encountered,

commercial development of the isocon was not continued. In 1958, however, requirements for special applications revived work on the image isocon. During 1960-61 a group at the RCA Laboratories in Princeton, N.J. completed important fundamental work<sup>2</sup> on isocon operation which provided the groundwork for engineering development of the tube. The work has continued,<sup>3</sup> and tubes have been designed for use in a number of unusual television applications—for example, astronomical image recording on a remotely operated telescope<sup>4</sup>.

Recent development of the image isocon had three basic objectives as follows:

- 1) Higher signal-to-noise ratio, particularly in the dark areas of the picture, than that produced by an image orthicon of equal size and target-mesh spacing;
- 2) Retention of the superior resolution, sensitivity, and low-lag characteristic of the image orthicon;
- 3) Simplified tube set-up and operating procedures, similar to those for the image orthicon, so that the image isocon can be readily utilized by persons familiar with image-orthicon cameras.

Because the magnetic components are an integral part of the electron optics of the tube, the Camera-Tube Development Group at Lancaster cooperated closely with the Camera Advanced Development Group of the Commercial Electronic Systems Division at Camden to develop the combination of tube plus focus and deflection components.

## Image-isocon operation

Fig. 1 shows a cross section of a typical RCA image-isocon system. The outer coil structure and the faceplate coil provide a uniform axial magnetic field over the entire length of the tube. Motion of electrons in the tube is



**R. L. VanAsselt**  
Image Orthicon Product Engineering  
Industrial Tube Division  
Electronic Components  
Lancaster, Pa.

received the BS in Physics from Birmingham-Southern College in 1948 and the MS in Physics from Ohio State University in 1949. From 1949 to 1952, he was an Associate Professor of Physics at Birmingham-Southern. From 1952 to 1956, he was a research physicist with Monsanto Chemical Corporation, working primarily in infrared spectroscopy. Since 1956, Mr. VanAsselt has been with the Industrial Tube Division of RCA at Lancaster, Pa., principally concerned with image orthicon target development. He was instrumental in the development of the MgO target and the semi-conducting glass target. He also played a large part in the development of the 3-in image isocon. Mr. VanAsselt is a member of Phi Beta Kappa and Sigma Pi Sigma.



**E. M. Musselman**  
Image Orthicon Product Engineering  
Industrial Tube Division  
Electronic Components, Lancaster, Pa.

received the BSEE from the University of Pennsylvania in 1948. He joined RCA Lancaster in 1948 as a manufacturing engineer. He was promoted to Manager, Camera Tube Factory Engineering in 1956. In 1959, he was made Manager, Developmental Types and Facilities for the Pickup Tube Factory. Mr. Musselman was assigned to Storage Tube Product Development in 1960. In this capacity he was responsible for the design of scan converters, including transmission type, participated in the development of the 7-in display storage tube and designed a compact 5-in display storage tube. He is co-holder of a US Patent for "Insulated Mesh Assembly for Vidicons", and also holds a patent on an improved target support structure for pickup tubes. Most recently he served as project engineer on the development of a ruggedized 3-in image isocon. Mr. Musselman is a member of Eta Kappa Nu, Tau Beta Pi, Sigma Tau and IEEE.

most easily discussed in terms of three regions: the image section, the target/scanning-beam section, and the separation section.

#### Image section

Operation of the image section is identical to that of an image orthicon. When an optical image is formed on the photocathode, photoelectrons from each point of the image are accelerated toward the target and focussed by the axial magnetic field. These photoelectrons arrive with sufficient energy to produce secondary electrons and charge the target positively. The secondary electrons are collected by a fine-metal mesh close to the target on the side facing the photocathode. The target is a thin glass membrane with critical physical properties. It must be sufficiently thin and resistive so that the charge pattern produced by the photoelectrons is not degraded significantly during a frame time by lateral leakage.

The charge pattern on the target is detected by the scanning beam, which deposits enough electrons on the target to neutralize the charge acquired during each frame. The time constant for the conduction of this charge through the target should not be much longer than a frame time; this requirement sets an upper limit to target resistivity. The mechanism for extracting the signal from the scanning beam is discussed later.

#### Target/scanning-beam section

The image isocon differs essentially from the image orthicon in the target/scanning-beam section and the separation section. To understand this difference, it is necessary to describe what happens in both an image orthicon and an image isocon when the primary beam strikes the target. As shown in Fig. 2, when the electrons in the primary beam approach the target, three events occur:

- 1) Some electrons enter the target and neutralize positive charges in the stored picture.
- 2) Some electrons strike the target and are scattered.
- 3) The remaining electrons do not quite reach the target and are specularly reflected.

The current distribution at the target satisfies the node equation:

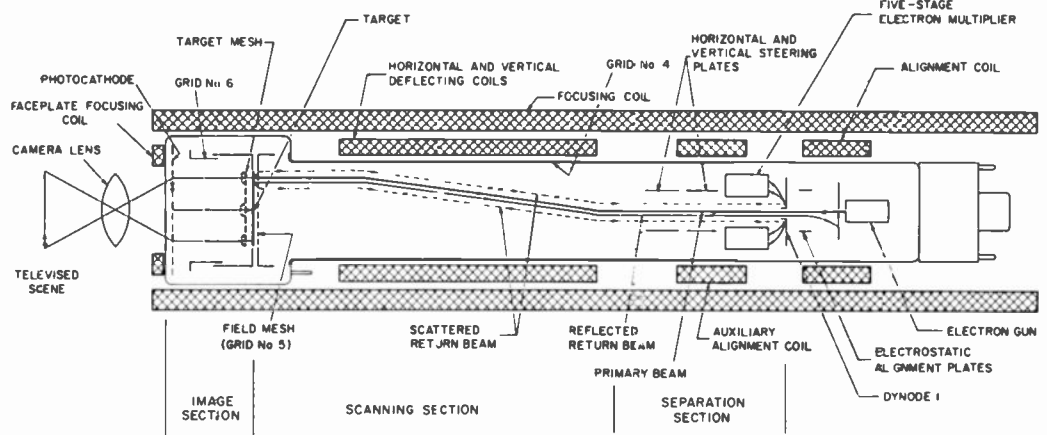


Fig. 1—Schematic diagram of image isocon and associated magnetic components.

$$I_p = i_c + i_s + i_r \quad (1)$$

where  $I_p$  is the primary current from gun to target,  $i_c$  is the current conducted into the target,  $i_s$  is the scattered electron current, and  $i_r$  is the reflected electron current.

In both the image orthicon and image isocon, the scattered electrons and reflected electrons constitute the return beam. In the image orthicon the video signal is obtained by directing the entire return beam into the multiplier. The output current can be represented as the sum of the reflected and scattered electron currents times the gain of the multiplier, as follows:

$$i_{\text{anode}} = M(i_r + i_s) \quad (2)$$

In the isocon, the return beam is split and only scattered electrons are permitted to enter the multiplier. (The direct relationship between scattered-electron current and conduction-electron current is utilized and the scattered electrons are used to form the video signal.) As will be shown later, the separation of scattered electrons and conduction electrons results in a portion of the scattered electron current being lost. For the same image-section construction and multiplier gain, however, the isocon signal current is slightly greater than the signal current from an image orthicon.

Fig. 3a compares the signals from the image isocon and the image orthicon when the primary beam is adjusted to just neutralize the charged target. A few gray-scale chips are shown together with the electron currents generated at the target as the beam scans a line through this pattern. As discussed previously, the orthicon signal is composed of both scattered electrons and reflected electrons.

Rearranging Eq. 1 and substituting in Eq. 2 yields the following equation for output current of the orthicon:

$$i_{\text{anode}} = M(I_p - i_c) \quad (3)$$

Because the primary beam current  $I_p$  is constant, the signal current is a function only of the conduction electron current.

The polarity is negative and the signal is riding on top of a large dark current, which adds noise. The isocon signal, on the other hand, is derived from the scattered electron current. No dark current is present (if perfect separation is assumed) and the noise is related only to the amount of signal current.

Fig. 3b shows the advantage of the isocon when excess primary beam current is used. Although the orthicon signal remains the same, the dark current and noise increase. The isocon signal and noise, however, remain unchanged because the excess reflected electron current is separated from the scattered electrons before they enter the multiplier.

#### Separation section

Separation of the scattered-electron beam from the reflected-electron beam is achieved simply by placement of a hole in the first dynode of the electron multiplier, as shown schematically in Fig. 1, and with greater detail in Fig. 4. As shown, the beam of reflected electrons is always contained within the envelope of the scattered-electron beam. The electron optics of the reading section is designed so that, when the composite beam strikes the first dynode, the reflected electron beam passes through the hole and is discarded, while a large fraction of the scattered-electron beam strikes the first dynode and generates secondary

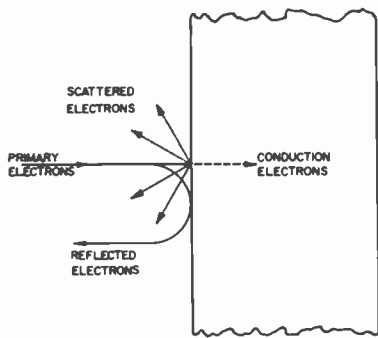


Fig. 2—Current distribution at target.

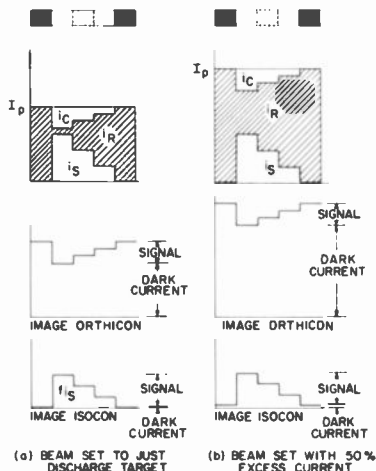


Fig. 3—Target current as a function of light level and beam setting.

electrons which are directed into the second stage of the electron multiplier.

Although the concept is quite simple, the return beam must have certain critical characteristics for proper separation to occur:

- 1) The diameter of the scattered-electron beam (at an antinode) must be large as compared with that of the reflected-electron beam.
- 2) The return beam must not contain any residual scan.

To fulfill the first requirement, it is necessary to add some transverse energy to the primary beam. Fig. 5 shows the cross section of the return beam at an antinode for various light levels within a scene. In Fig. 5a, the primary beam is aligned with the magnetic focus field and the target is perpendicular to the field. At low illumination levels, as shown by the extreme left-hand representation, the maximum transverse energy of the scattered electrons is small and the diameter of the scattered electron beam is essentially equal to that of the reflected-electron beam. As a result, a condition called "black clipping" occurs in which both the scattered electrons and reflected electrons pass through the hole in the separation electrode.

This condition is corrected by adding a small amount of transverse energy to the primary beam just after it leaves

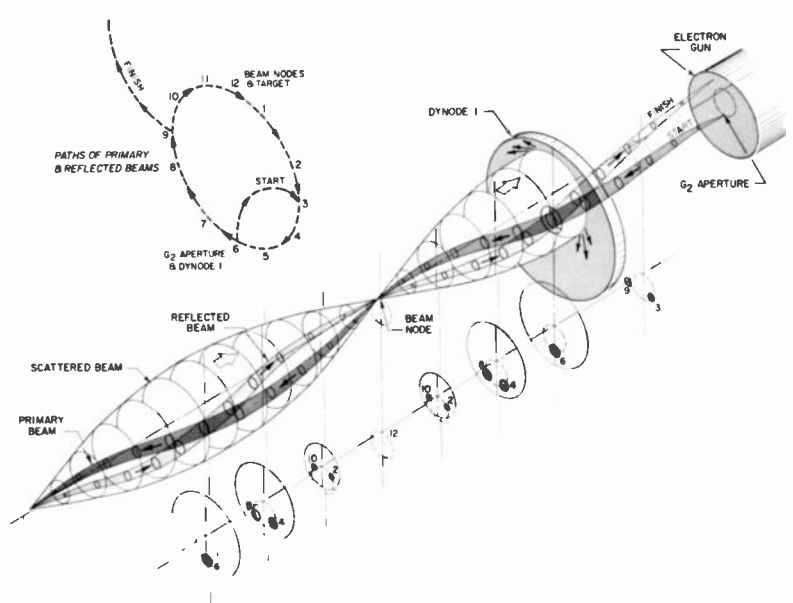


Fig. 4—Idealized trajectories of image-isocon beams.

the gun. The primary beam then spirals toward the target, and the reflected-electron beam spirals away from the target. The scattered-electron beam, however, leaves the target aligned with the axial magnetic field. The primary and reflected beams still cross at the antinode, but the spot is displaced from the center of the scattered beam. Fig. 5b shows the cross-section of the return beam for the same light levels when transverse energy of 0.5 eV has been applied to the primary beam. The low-transverse-energy scattered electrons which represent the low-illumination signals are spread out over a large diameter at the antinode, while the diameter of the reflected beam is unchanged. Scattered electrons can therefore be captured from all light levels, and a linear gray scale is obtained.

It would appear that if greater transverse energy were given to the primary beam, greater ease of separation would result. However, excess transverse energy increases the axial velocity distribution of the beam electrons as well as the radial velocity distribution, and the beam becomes less effective in discharging the target, causing lag.

The second requirement for proper separation of scattered electrons from reflected electrons is that the reflected beam must always return to the same point in the separation plane regardless of what part of the target is being scanned. In image-orthicon cameras, a small amount of residual scan<sup>2</sup> is present at the first dynode of the multiplier and information about the surface of this dynode is present in the video

signal. For an isocon to work properly, this residual scan must be very small, approximately 0.01 cm or less. A practical solution was obtained by design of a deflection yoke that, in combination with the new RCA image-isocon electrode configuration, provides uniform landing of the beam across the target and essentially zero residual return-beam scan. This yoke is an important part of the system of tube plus deflection and focus components needed to generate good isocon pictures.

### Tube Alignment and Adjustment

Proper operation of the image isocon requires that the electron beam be accurately directed to the target and back through the separation aperture. The primary beam is started on a helical path and directed through the separation aperture by the combined effect of the alignment plates and alignment coils (shown in Fig. 1). The alignment-plate differential voltage is preset to a value specified for the tube, and the alignment-coil currents are adjusted to center the primary beam in the aperture. These adjustments of the primary beam correspond to the center of the range for which video signal is obtained and cause the primary beam to spiral out from the center of the separation aperture toward the target. The reflected beam spirals back, as shown in Fig. 4, and criss-crosses the primary beam through the same area at an antinode in an ideal system. Thus, the reflected beam should continue back toward the multiplier and exit through the center of the separation aperture. The image isocon has

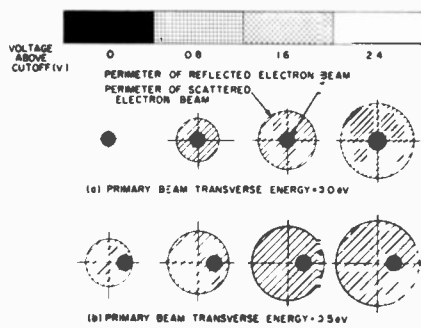


Fig. 5—Return-beam cross section at an antinode as a function of target voltage and transverse energy of primary beam.

steering plates, also shown in Fig. 1, to direct the reflected beam exactly through the center of the separation aperture. The use of these steering plates assures good separation while permitting reasonable tolerances in tube construction and positioning of the tube in the yokes.

The adjustment of the steering plates is made in two steps:

- 1) The correct polarity of signal is obtained by a coarse adjustment of the steering-plate differential voltages. (If the reflected beam strikes the first dynode a negative picture will be obtained.)

- 2) The target voltage is reduced close to cutoff, and any bright edges are eliminated by fine adjustment of the steering-plate voltages.

The bright edges result when reflected electrons are deflected at the target by sharp black-white transitions and acquire additional transverse energy.<sup>5</sup> At an antinode, these electrons are located just outside the perimeter of the reflected beam and can become a part of the signal. The separation aperture of the image isocon is large enough to allow these deflected electrons to pass through and be discarded with the reflected beam provided the reflected beam is accurately centered. The electrons striking the first dynode are then only scattered electrons and an isocon signal free of exaggerated edges is generated.

### Image-isocon performance

Low dark noise is an outstanding feature of the new image isocon. Fig. 6 compares the signal-to-noise performance of an image isocon with that of an equivalent image orthicon as a function of the light available in a scene. Because the noise in the image-orthicon signal is nearly constant for all light levels (the beam setting is not changed during scanning of a given scene), the signal-to-noise ratio is approximately a linear function of the

light level. In the isocon signal, however, the noise decreases with signal level and the signal-to-noise ratio varies approximately as the one-half power of the light level. The curves show that the dynamic range of the isocon is at least ten times greater than that of the image orthicon. This wide dynamic range of the image isocon also allows the camera to move from scene to scene without attention to the beam-current setting used.

The resolution and the amplitude response of the new image isocon compares very favorably with the best image orthicons operating in well designed yokes. This excellent performance results from the electron optical design in which the magnetic components and the tube structure are properly matched. Image isocons typically provide response of 80% at 400 tv lines without aperture correction. Corner response shows less than 20% dropoff and no dynamic correction is required. Limiting resolution is 1200 tv lines at an illumination of 0.02 foot candle on the faceplate. Picture geometry is excellent.

Slightly lower amplitude response results from use of fiber-optic faceplates and/or lower-capacitance target mesh assemblies. Fig. 7 compares amplitude response for image isocon and image orthicon.

High-resolution, slow-scan versions of the new image isocon have been made by increasing the glass-target resistivity (up to a factor of  $10^5$  above the range used for 30-frame/second television). Lateral leakage is minimized and long storage times are achieved without special cooling equipment. Applications requiring long integration time and good resolving power, such as astronomical observation, find the new isocon a useful tool.

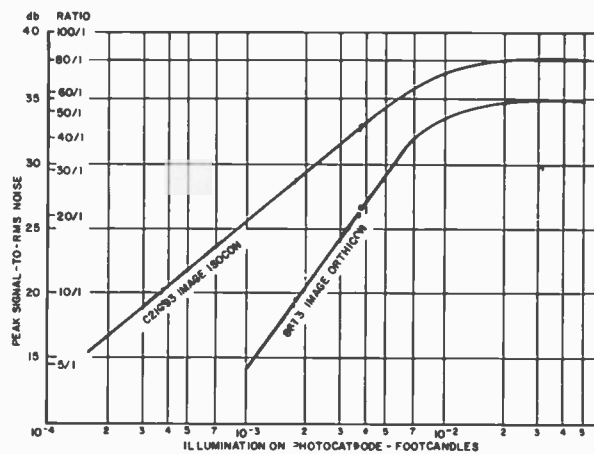


Fig. 6—Signal-to-noise ratio as a function of light level within scene.

Signal uniformity produced by the new image isocons is exceptional. The scan optic developed to reduce residual scan in the return beam also provides uniform landing of the beam with less than 0.1-volt variation across the target. The absence of scanning at the separation aperture guarantees uniform separation.

Background uniformity is excellent and dynode problems are eliminated. The positive-polarity, low-dark-current read-out makes variations in gain across the first dynode surface less critical. Also, the first dynode of the isocon is located at an antinode at which the current density is a minimum and the surface is not in focus. Finally, the absence of scanning at the first dynode means that no video information can be developed. Dynode problems have not been observed with the new image isocons.

Incomplete target discharge in one sweep of the scanning beam results in a residual signal characteristic called lag. The RCA Dev. No.C21093, an image isocon with a high-capacitance target-to-collector-mesh assembly, displays residual signals less than 10% of peak amplitude during the third scanning field when operating at a light level with highlights at the knee. The low-capacitance target of a newer type, the RCA Dev. No.C21095, offers further improvement in dynamic response. This performance is achieved when the tube is properly set up, i.e. with minimum transverse energy required for good gray scale given to the primary beam. This low-lag performance results in excellent motion-capturing capability similar to that obtained with the image orthicon.

### Application

The image isocon is a versatile camera tube. The specific requirements for a particular application can be met dur-

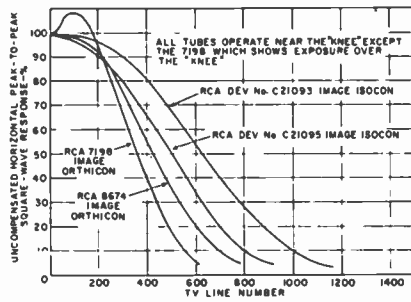


Fig. 7—Amplitude response as a function of TV line number.

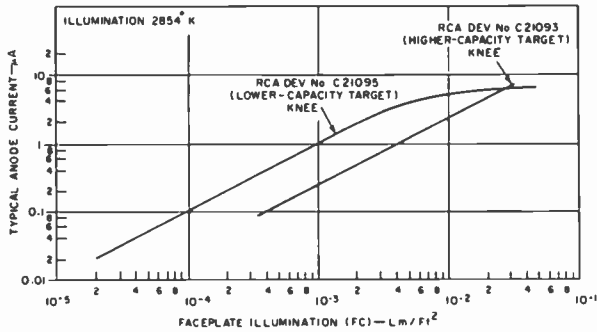


Fig. 8—Signal current as a function of light on photocathode.

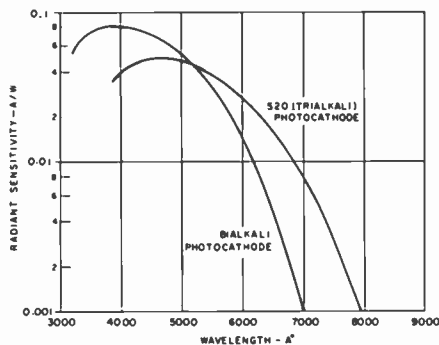


Fig. 9—Photocathode spectral response

ing manufacturing by adjustment or change of one or more of the following factors: target resistivity, target-to-collector-mesh capacitance, photocathode formulation, or face-plate materials.

In a typical television-broadcast application, for example, where there is ample and controlled studio lighting, the target of the camera tube is read-out repetitively every 1/30 second. This rate sets an appropriate value of target resistivity at  $10^{11}$  ohm-cm. A maximum target-to-collector-mesh capacitance, therefore, produces the desirable pronounced knee characteristic, as well as a very high signal current under the ample lighting conditions. This high signal current, in turn, requires minimum amplification in its subsequent processing. (It should be noted that

the process frequently employs "black stretch"—a gain nonlinearity designed to correct for an unsuitable gamma characteristic in the display device at the output end of the system. The low dark current and low noise of the image isocon make it uniquely suited to this form of signal processing.)

Signal output of the new image isocon is directly proportional to light received at the photocathode (unity gamma factor). The gray scale is therefore linear and provides excellent contrast between steps of varying illumination at all levels below saturation, as indicated in Fig. 8.

A spectral response emphasizing the visible portion of the spectrum can be obtained with this system by employing a conventional optical-glass faceplate in conjunction with a photocathode such as the potassium-cesium antimonide (bi-alkali) or the sodium-potassium-cesium antimonide (multi-alkali) types. Response of these photosurfaces is shown in Fig 9. The tube can also be made to respond to radiation in the ultra-violet region of the spectrum by use of suitable face-plate materials, such as quartz or lithium fluoride, and a UV sensitive photocathode.

For extremely-low-available-light situations, such as military surveillance, a multi-alkali photocathode is preferred in the camera tube because of its broad spectral range, which extends into the infra-red region. The tube uses a reduced target-to-collector-mesh capacitance to minimize smearing and therefore increase the dynamic resolution of images reproduced from fast-moving dimly lit scenes. If additional light amplifiers or spectrum converters are then required, a fibre-optic faceplate can be used to provide the optical coupling. The electron-conduction glass target, proven in image orthicons, has been utilized to provide long life, resistance to scanning burn, and resistance to highlight damage. Scan zoom can be employed without damage to the target. Three-to-one ratios are readily achieved by appropriate reduction of the scanning power.

An interesting application of the image isocon is its use in medical X-ray equipment. The intrinsically high sensitivity and resolution of the isocon permits continuous detailed observation of the

living subject with a minimum of radiation dosage. The requirements for the tube are similar to those for the low-available-light application: a real-time target performance and good response to low-contrast dynamic-scene material.

## Conclusions

The new RCA image isocon with its associated components produces pictures that are a distinct improvement over those obtained with image orthicons. Performance features of the isocon include the following:

- 1) Improved signal-to-noise ratio, particularly in the dark areas of a scene, which greatly increases dynamic range and allows gamma correction without degradation;
- 2) Excellent resolution both in limiting value (1200 tv lines) and in amplitude response;
- 3) Picture background free of dynode defects and shading;
- 4) Fast and easy setup procedure comparable to that for image orthicon operation but without the critical beam-setting problem associated with image orthicons;
- 5) Linear transfer characteristic and low lag attained simultaneously by use of optimum electron-beam transverse energy;
- 6) Very good picture geometry and uniform resolution.

The image isocon has inherited many good features from a long image-orthicon tube-development program. The burn-resisting and long-life electron-conducting glass targets developed for image orthicons are equally effective in the image isocon. The good mechanical and electron-optical features of the image mount developed for type 8673 image orthicons have also been applied to the image isocon. Mechanical development is continuing on the isocon and should provide sturdy structures capable of withstanding the severe shock and vibration of rocket launching.

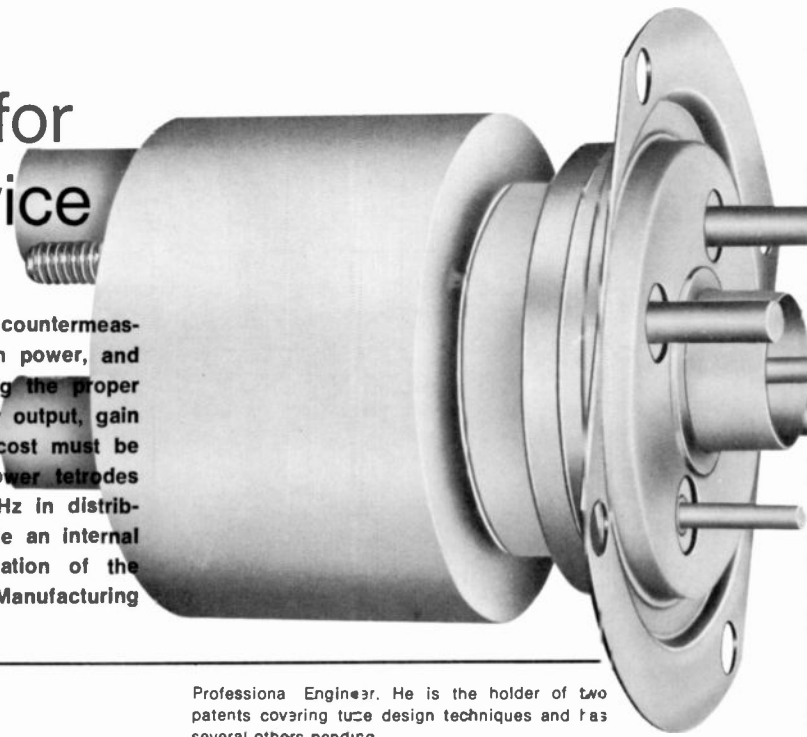
## References

1. Weimer, P. K., "The Image Isocon—An Experimental Television Pickup Tube Based on the Scattering of Low-Velocity Electrons" *RCA Review* Volume 10 (1949) p. 366-386.
2. Cope, A. D., Peterson, C. C., and Borkan, H., private correspondence (1961) p. 36-37.
3. Cope, A. D., and Borkan, H., "Isocon Scan—A Low Noise, Wide Dynamic-Range Camera Tube Scanning Technique" *Appl. Optics*, Volume 2 (March 1963) p. 253-261.
4. Cope, A. D., and Luedicke, E., "Camera Tubes for Recording Stratoscope II Telescope Images" *RCA Review* Volume 27 (1966) p. 41-56.
5. Weimer, P. K., *loc. cit.* p. 376.

# Ceramic-metal tetrodes for distributed-amplifier service

C. E. Doner | W. R. Weyant

Distributed amplifiers have become an important part of electronic countermeasures systems because they provide extremely broad bandwidth, high power, and high gain at frequencies up to approximately 400 MHz. In selecting the proper amplifier device for these systems, such factors as bandwidth, power output, gain efficiency, environmental requirements, reliability, size, weight, and cost must be considered. This paper describes two RCA ceramic-metal beam power tetrodes designed specifically for high-power, broadband operation to 400 MHz in distributed-amplifier services. Special design features of these tubes include an internal screen-grid bypass capacitor, low-inductance grid leads, ruggedization of the internal structure, and use of a monolithic heater-cathode assembly. Manufacturing techniques, process controls, and testing criteria are also discussed.



**D**ISTRIBUTED AMPLIFICATION is a method of combining the outputs of many amplifier tubes by substitution of input and output capacitances of these tubes as shunt elements in two artificial transmission lines (Fig. 1). This technique permits a large number of tubes to be operated in parallel over a very large bandwidth which is independent of the number of tubes in the amplifier.

Power tubes for use in high-power, high-frequency distributed amplifiers must have high transconductance, high current capability, low lead inductances, low input and output capacitances, low grid conductance, and a high degree of grid-to-plate isolation. These characteristics determine maximum operating frequency, bandwidth, efficiency, power output, power gain, and stability. Because these parameters are not all compatible, a tube designed for high-power distributed-amplifier service is optimized for the particular application.

## Forced-air cooled tetrode

The RCA 4624 forced-air cooled tetrode has been designed to meet the requirements of the distributed amplifier. This tetrode provides the highest practical power output with bandwidths as high as 200 MHz, and has an upper frequency capability of approximately 400 MHz. Many of the tube parameters which affect distributed-amplifier performance have been optimized in this tube.

**C. E. Doner, Ldr.**  
Circuit Product Engineering  
Industrial Tube Division  
Electronic Components  
Lancaster, Pa.

received the BSEE from Pennsylvania State University and joined RCA Lancaster in 1955 as a power tube application engineer. From 1959 to 1962, Mr. Doner worked as a design engineer responsible for development of several power tubes including a UHF ceramic-metal tetrode for high-power distributed-amplifier service. In 1962, Mr. Doner was appointed Engineering Leader in charge of a design group responsible for design and development of numerous power tubes including a 5000-watt tetrode for UHF television service. In 1963, he was appointed Engineering Leader in charge of Regular Power Tube Application Engineering. In 1966, Mr. Doner was appointed to his present position, responsible for the design and development of RF power generating devices including strip-line and cavity amplifiers and oscillators for CW, AM, FM, SSB and pulse applications from HF through UHF. Mr. Doner is a Registered

Professional Engineer. He is the holder of two patents covering tube design techniques and has several others pending.

**W. R. Weyant**  
Regular Power Tubes  
Industrial Tube Division  
Electronic Components  
Lancaster, Pa.

received the BSEE in 1955 from Indiana Institute of Technology. He joined RCA in 1955 as an engineer on the specialized training program, following which he spent nine years with the industrial design group in the receiving tube engineering activity of the Electron Tube Division in Harrison, N.J., working on the design and development of new electron tubes for specialized industrial and military application. He was also the responsible design engineer for industrial and military current products. In 1964, Mr. Weyant was transferred to regular power tube group, Lancaster Plant, where he is presently serving in a similar capacity. Mr. Weyant has contributed to the quality improvement of industrial tubes and holds related patents.



Seated at left is W. R. Weyant; C. E. Doner is on the right.

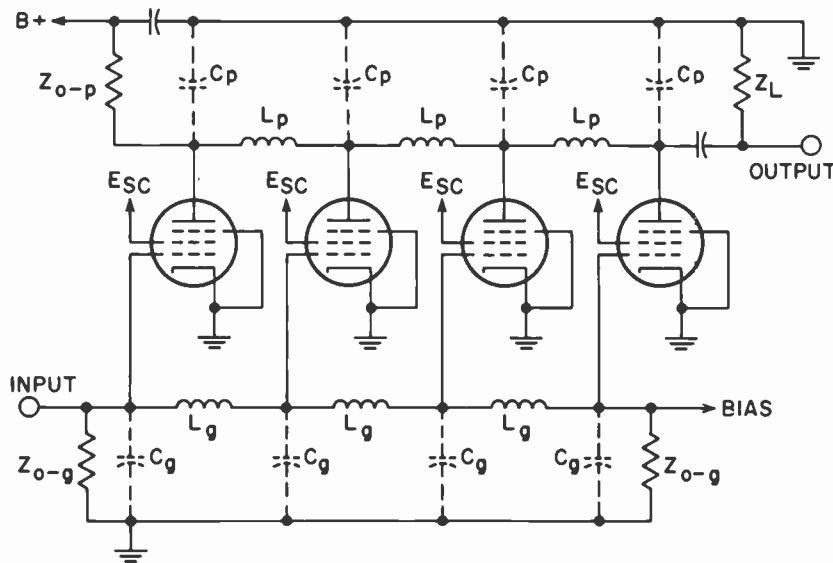


Fig. 1—Simplified low-pass circuit for a distributed amplifier.

#### Grid-cathode assembly

Design of the 4624 began with the cathode and the control grid because the input capacitance, being much higher than the output of power tubes, determines the frequency capability of the tube. For a bandpass distributed amplifier, the bandwidth,  $f_2 - f_1$ , is determined by the following relationship:

$$f_2 - f_1 = 1/\pi (L_p C_p)^{1/2} = 1/\pi (L_o C_o)^{1/2}$$

where  $f_2$  and  $f_1$  are the upper and lower cutoff frequencies, respectively;  $L_p$  and  $C_p$  are the series inductance and shunt capacitance of the plate; and  $L_o$  and  $C_o$  are the series inductance and shunt capacitance of the control grid.  $C_p$  and  $C_o$  represent the tube output and input capacitance, respectively.

A minimum practical value of  $L_o$  was estimated to be approximately 25 nanohenries. With  $f_2$  at 400 MHz and  $f_1$  at 200 MHz, the maximum permissible value of  $C_o$  is approximately 40 pF. After analysis of various cathode and control-grid configurations, it was determined that a cylindrical cathode design having a minimum area of 3 cm<sup>2</sup>, with a grid-to-cathode spacing of 0.008 in. would provide high current capability (steady-state plate current of 350 mA in class-A service) and high transconductance (25,000  $\mu$ mhos at 300 mA) and also meet the  $L_o$  and  $C_o$  requirements.

Fig. 2 shows a cross section of the 4624 tube (with the radiator removed). The cathode surface is the matrix unipotential type consisting of a layer of

sintered nickel powder cathoretically filled with emissive carbonates. This cathode produces high current densities, has a long reserve life, and resists damage from arcing. The diameter of the cylindrical heat dam attached to the bottom of the active area of the cathode is smaller than the active area to produce a minimum grid-to-cathode capacitance. A flat circular disc serving as an RF ground plane and as a part of the vacuum envelope is attached to the bottom of this heat dam. This design provides an extremely low cathode-lead inductance, which increases the upper frequency capability and reduces input conductance.

The RF ground plane, or cathode flange, is constructed with four holes for direct mounting to the amplifier chassis. An RF gasket provides a good RF contact between the flange and the

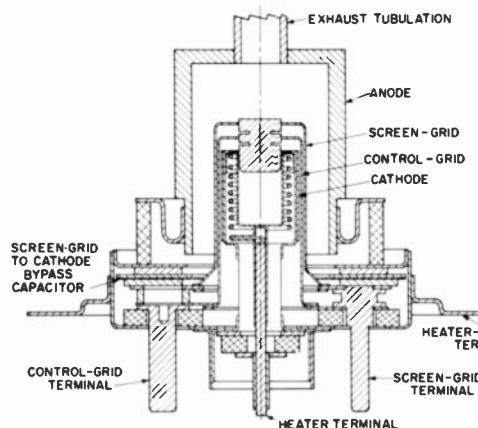


Fig. 2—Cross section of the 4624 tube with radiator removed.

chassis. The shape of the flange permits close spacing between tubes which reduces series circuit inductance to as low a value as practical.

The grid is cylindrical in the active area and is supported by three small ceramic insulating washers in the cathode ground plane. Fig. 3 shows the two diametrically opposed grid leads which are used for input-circuit connections for operation in a low-pass circuit configuration. In this connection, the low grid-lead inductance is utilized as a circuit element appearing as part of the series line inductance. This type of grid lead also provides lower seal capacitance than an all-concentric terminal arrangement such as that normally used in UHF power-tube design. The third grid lead provides a connection for a shunt inductor for operation in a bandpass distributed-amplifier circuit. In this operation the inductance of the lead is again a useful part of the circuit.

The heater is of monolithic construction and consists of an insulated tungsten helix connected to a molybdenum heater rod at one end and to the heater cup at the other. The heater element is held firmly in place by sintered nickel powder filling the void between the heater cup and the cathode. This arrangement provides an extremely rugged heater.

#### Screen-grid bypassing

The screen grid is bypassed to the cathode inside the tube envelope to minimize screen grid lead inductance. The screen grid consists of a cylinder in the active area attached to a flat washer-like support. This washer forms one electrode or plate of a radial



Fig. 3—Two diametrically opposed grid leads for input-circuit connections in a low-pass circuit.

bypass capacitor in which a 0.003-inch-thick mica washer serves as the dielectric. Another metal washer forms the other electrode and attaches to the cathode ground plane. A wire-mesh gasket, compressed during tube assembly, holds the capacitor parts in a direct contact. This bypass design produces an extremely low value of screen-grid lead inductance which reduces undesirable feedback effects to a minimum.

A single screen-grid lead is brought through an insulator in the cathode flange for application of DC screen-grid voltage. For low-frequency operation, where the 600-pF internal capacitor does not provide sufficient bypassing, additional capacitance may be added externally to this lead. At frequencies when this becomes necessary, the inductive reactance of this lead is negligible.

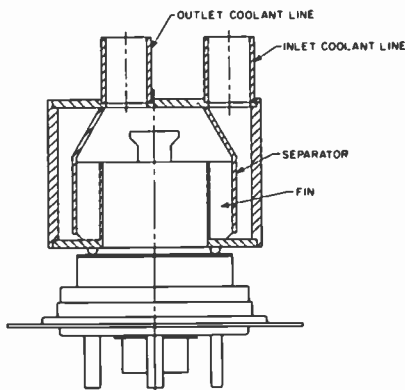


Fig. 4—Single-pass low-pressure cooler for the RCA 4636.

The control-grid-to-screen-grid spacing and the pitch of the grids were chosen to provide a screen-grid-to-control-grid amplification factor of 12. This relatively high value permits class-AB<sub>1</sub> operation (zero grid current) at full plate-current ratings with a DC screen-grid voltage of only 400 volts. Zero-grid-current operation is essential to prevent extremely high attenuation of the drive signal as it passes down the input line; low-screen-grid operating voltage is important for increased amplifier efficiency.

Both the control grid and the screen grid consist of drawn cups of a heat-tempered copper alloy. These electrodes are furnace brazed to the base pins and the respective grid flanges using a high-temperature silver-alloy solder; high-alumina spacers are used as insulators. A ceramic pin with anti-leakage grooves is also brazed at the

top of the assembly to assure ruggedization and alignment of the control grid with respect to the screen grid and the cathode. The grid wires are formed by electrical-discharge machining and are further refined by electro-polishing which provides a ruggedized structure of precise alignment.

#### Plate design

Factors affecting plate design include the plate-curve "knee" characteristics, DC plate voltage, and plate cooling and output capacitance. The final design has an output capacitance of approximately 6.5 pF. This relatively low value enhances the high output-power capability because output power is inversely proportional to output capacitance.

The five-piece plate assembly consists of the pinchoff tubulation, a heavy OFHC copper cup for uniform heat distribution, a Kovar stress-isolating ring, a high-alumina (low-RF-loss) ceramic insulator, and a copper-clad Kovar flange that serves as a connection to the ground plane. This assembly is fabricated by means of a furnace braze at 800°C.

In the final assembly of the tube, the ground plane and the screen-grid bypass capacitor are formed when the OFHC copper backup washers, the gold-evaporated mica dielectric, and the gold-plated wire-mesh gasket (which provides the proper compressive force and contact area) are placed on the screen-grid flange. The plate assembly is then heliarc-welded to the cathode flange.

The tube is evacuated to approximately  $10^{-6}$  Torr, and its plate temperature is raised to 450°C. The cathode is then activated, and current is drawn to the various tube elements to provide high temperature for proper outgassing. After this step is completed, the tube is "tipped off" (sealed by a metal closure of the tubulation) and "aged" for stabilized operation. The tube is then dynamically tested at input frequencies of 30 and 600 MHz; shock-tested at 30g, 11 milliseconds; vibration-tested at 10g, 500 Hz; and life-tested at 600 MHz.

#### Higher-power tube

The 4624 is designed for forced-air cooling and has a plate power-dissipating capability of 400 watts. With recent requirements for 1000-watt dissipation, however, air cooling becomes impractical because the high air volume needed requires high blower power. As a result, an intense-liquid-cooled version of the 4624 was designed to increase power output while maintaining frequency characteristics and compact size. Fig. 4 shows the single-pass, low-pressure cooler used for this tube, the RCA 4636. This cooler operates with Coolanol-35, a silicate-ester base dielectric fluid, at temperature from -50 to 135°C. The coolant enters through the  $\frac{3}{8}$  inch lines and passes through a restriction (for increased surface velocity at the higher-thermal-density areas) in the finned area. At an inlet temperature of 105°C and a dissipation of 750 watts, the required flow of Coolanol-35 is 0.75 gal/min at a pressure drop of 0.3 lb/in<sup>2</sup> (gage).

The 4636 is tested for a zero-bias current of 1.4 A to assure satisfactory performance at a plate current of 600 mA in class-A, distributed-amplifier operation. Typical operation of the 4636 in an 11-tube bandpass distributed amplifier covering a frequency range of 107 to 187 MHz is shown in Table I. The values shown are for the output tube at an operating frequency of 141 MHz and a plate-line impedance of 250 ohms.

Table I represents only one of many possible modes of distributed-amplifier operation. Although a broad discussion of theoretical and practical techniques of distributed amplification is beyond the scope of this paper, numerous excellent papers have been written on the subject.<sup>1-3</sup>

#### References

- Ginzton, E. I., Hewlett, W. R., Jasberg, J. H., and Noe, J. D., "Distributed Amplification," *Proc. of I.R.E.*, (Aug. 1948).
- Medds, S. K., *An Experimental Distributed Power Amplifier*, Naval Research Laboratory Report 4985, Washington, D.C., (Aug. 20, 1957).
- Grimm, A. C., Internal Correspondence (Feb. 26, 1957).

Table I—Performance of RCA-4636 in 11-tube bandpass distributed amplifier

DC plate voltage	1800 V
DC screen-grid (grid-No. 2) voltage	400 V
DC control-grid (grid-No. 1) voltage	-60 V
Steady-state plate current	475 mA
Steady-state screen-grid current	10 mA
Steady-state control-grid current	0 mA
Peak RF drive voltage	55 V
Tube power output	365 W
Useful power output (from 11-tube distributed amplifier)	2000 W

# Klystron for the Stanford two-mile linear accelerator

A. C. Grimm | F. G. Hammersand

The completion of the two-mile linear accelerator at the Stanford Linear Accelerator Center in the fall of 1967 provided physicists with the largest and most costly research tool yet built in the U.S. The accelerator center (Fig. 1) constructed at a cost of \$114 millions, provides the physicist with a 20 GeV electron beam and research facilities to probe the interior of atomic nuclei in his quest to understand the fundamental nature of matter. This paper describes the development of this linear accelerator with particular emphasis on RCA's role in developing the high-power klystron for this application.



Fig. 1—The Stanford Linear Accelerator Center. Electrons begin their acceleration at the upper right and end their flight in one of the target areas of the "switch yard" in the lower left.

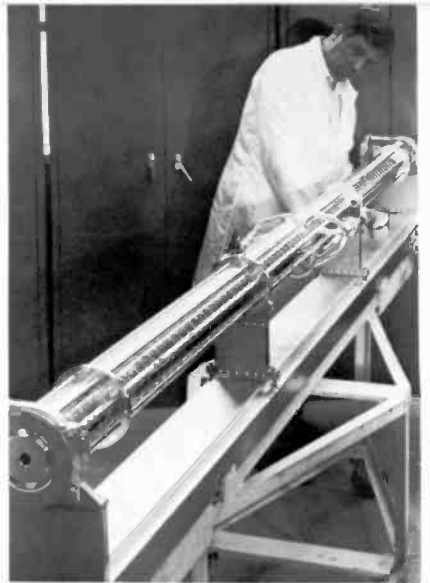
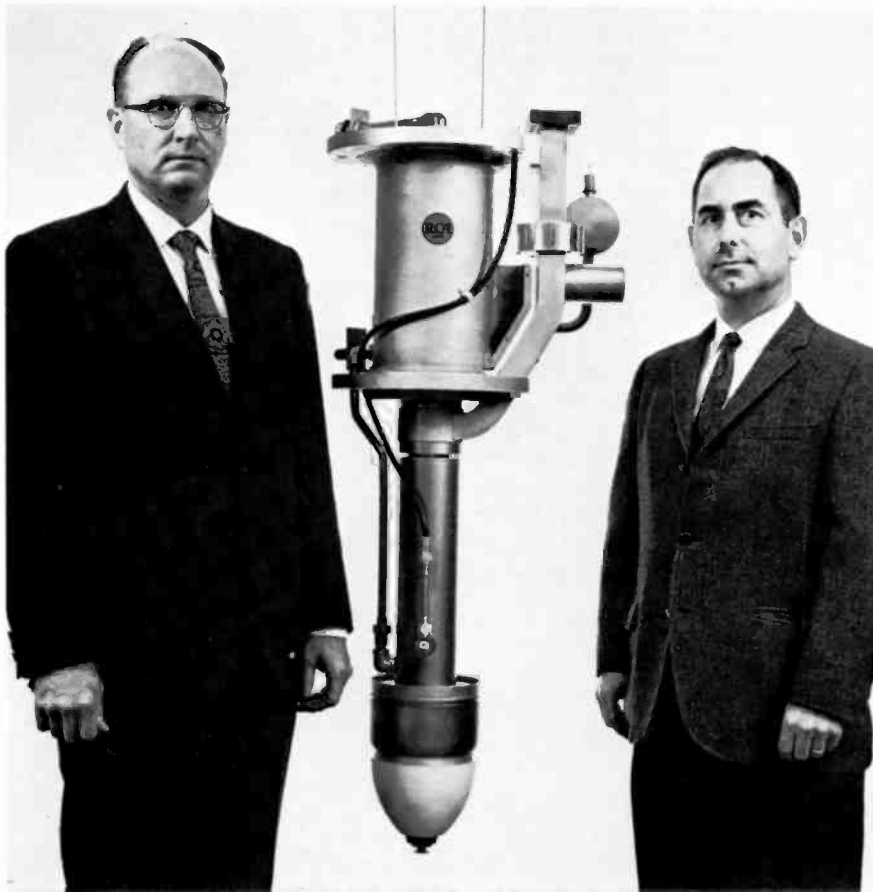


Fig. 2—A 10-ft section of accelerator waveguide.

**A. C. Grimm, Adm.**  
Industrial Market Development  
Industrial Tube Division  
Electronic Components  
Lancaster, Pa.

received the BSEE from the Polytechnic Institute of Brooklyn in 1940. Upon joining the RCA Tube Division in 1940, Mr. Grimm was assigned to the development of receiving and small power tubes. In this assignment from 1940 to 1951, he advanced to engineering leader. From 1951 to 1953, Mr. Grimm directed the advanced development effort on the RCA color kinescope. He was promoted to Product Manager for the Color Kinescope Product Group in 1954. In 1955, he was named Manager of Advanced Development in the Power Tube Group. In this capacity he was responsible, among other programs, for the development of the RCA 8568 klystron used to power the Stanford two-mile linear accelerator. From 1960 until he was appointed to his present position in 1967, he was manager of engineering and operations manager for RCA super power tubes. He has been issued six patents on electron tubes and associated devices, and he has published several papers on the developmental aspects of vacuum tubes. He is a member of Tau Beta Pi and Eta Kappa Nu, and is a senior member of the Institute of Radio Engineers. He is a registered professional engineer in the State of Pennsylvania.

**Fred G. Hammersand, Mgr.**  
Super Power Device Engineering  
Industrial Tube Division  
Electronic Components  
Lancaster, Pa.

received the BSEE and MSEE degrees from the University of Washington in 1949 and 1956 respectively. Since joining RCA, Lancaster in 1951, he has been responsible for the design, development, and application of many gridded, gas, klystron, and magnetron tubes. This experience includes the design of electron guns for round and sheet electron beams, RF interaction circuits for gridded, klystrons, and magnetron tubes and tube and gun structures for the production and conservation of gas plasmas. Mr. Hammersand became a member of the A1230D klystron development team in December, 1960. In April, 1966 he assumed group leader responsibility for the development of super power klystrons, magnetrons, and low frequency gridded tubes. In February, 1967 he became manager of Super Power Devices Design Engineering. Mr. Hammersand is a registered Professional Engineer in the state of Pennsylvania; a member of the IEEE, Tau Beta Pi, and Zeta Mu Tau; and an associate member of Sigma XI.

The two authors, A. C. Grimm (left) and F. G. Hammersand, are standing to either side of the RCA 8568 klystron.

THE CONCEPT for the two-mile linear accelerator originated with a group of faculty members at Stanford University twelve years ago. Formal proposals were made to the Atomic Energy Commission (AEC) on September 15, 1961. After four years of political and scientific debate, Congress authorized the creation of a national laboratory for the accelerator to be called the Stanford Linear Accelerator Center (SLAC).

Construction of the Center began in July, 1962. In May, 1966, the electron beam was first activated. By January 1967, a beam energy of 20.16 billion electron-volts (20.16 GeV) and design beam currents of 30 mA peak were achieved. Beam currents of 45 mA peak have been reported recently.

### Operation of accelerator

In the SLAC system, a beam of electrons is accelerated through a two-mile-long waveguide comprised of more than 22,000 cavities brazed together in 960 ten-foot-long sections (Fig. 2). After being fully accelerated, the electron beam can be switched to any of three experimental stations by large electromagnets. Thus, one or more experiments can be conducted simultaneously by programmed beam switching.

The 20-GeV energy level is obtained by acceleration of the electron beam by 5000-megawatt (MW) bursts of 2856-MHz power supplied by 240 klystron tubes spaced at 40-ft. intervals along the accelerator. Each klystron provides a 21-MW burst of power for 2.5  $\mu$ s. The burst from each klystron is accurately phased so that the RF energy from the tube arrives at the accelerator in the proper time sequence to accelerate the electrons as they progress down the waveguide. In the future, additional klystrons can be added to the machine to obtain an even higher-energy beam. Provisions have been made in the initial design of the accelerator for a total of 960 klystron tubes.

The klystrons, modulators, and power supplies are housed in a building called the klystron gallery. This building is located approximately 25 ft above a concrete tunnel containing the accel-

erator waveguide. Earth fill separates the concrete tunnel from the klystron gallery and acts as a radiation shield to protect workers in the gallery from gamma radiation produced in the accelerator waveguide by stray electrons. A portion of the gallery with an RCA 8568 klystron in position is shown in Fig. 3.

The RF energy from each klystron tube is fed to the accelerator waveguide sections through precision WR284 OFHC copper waveguide. The pressure level inside the entire waveguide system is maintained at approximately  $1 \times 10^{-7}$  Torr. For minimum cost and maintenance, no vacuum windows other than those in the klystron tubes are used in the waveguide system. Waveguide vacuum valves are used instead to close off individual sections of the accelerator waveguide RF feed system when klystron tubes must be changed.

### Klystron requirements

Prior to Congressional authorization for the construction of the Center, the AEC had authorized limited funds for studies of the critical components for the system. The most important of these components is the klystron tube used to power the accelerator.

The physicist's need for a highly stable electron beam of low energy spread placed rigid requirements for stability on the klystron tubes. Using AEC study funds, engineers, and physicists at Stanford University designed and built several prototype klystrons and developed tube performance specifications more stringent than those required for military radar applications to assure satisfactory performance of the accelerator. Tube cost, efficiency, and reliability were also prime considerations because of the large number of tubes used to power the machine.

In mid-1960, industry was requested by SLAC to complete the design of the prototype tube so that it could be reproduced and rebuilt at modest costs, and to develop a permanent-magnet focusing system for the tube. Both RCA and Sperry-Rand Corporation were successful bidders. Each was awarded contracts to deliver six developmental tubes and to develop a permanent-magnet focusing system.

The tube, as originally conceived by Stanford, was a five-cavity, 24-MW,

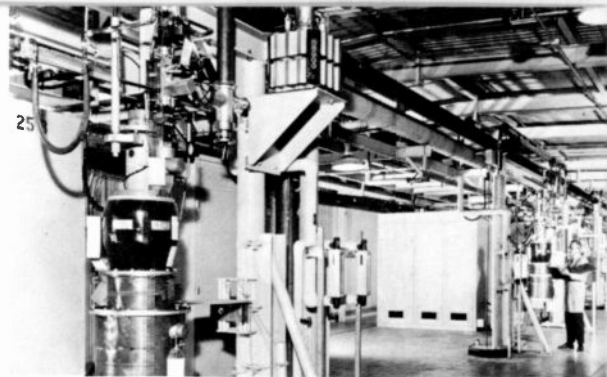


Fig. 3—A section of the Stanford Linear Accelerator klystron gallery using RCA-8568 klystrons.

2856-MHz pulse amplifier using a 2-microperv, 250-kV, 250-A electron beam. Double-waveguide output was specified at the time because there was some doubt that a single output window could reliably handle the full output power.

The basic electrical characteristics as listed in the original tube specification were as follows:

Operation	A	B
Frequency (MHz)	2856	2856
Peak power output (MW)	12	24
Average power output (kW)	10.8	21.6
RF pulse length ( $\mu$ s)	2.5	2.5
Beam voltage (kV)	195	248
Beam current (A)	172	247
Duty cycle	0.009	0.009
Gain (dB)	47	50
Efficiency (%)	35	38

Permanent-magnet focusing of the klystron electron beam was specified to reduce operating costs and to achieve a higher degree of reliability than possible with electromagnet focusing. The use of permanent magnets eliminated the need for 240 DC power supplies to energize electromagnets. The savings obtained included not only the cost of the DC supplies, but also the cost of electrical power consumption in excess of 250 kW that the electromagnets would otherwise consume and the cost of an increased heat-exchanger capacity of more than 250 kW needed to cool the electromagnets. Finally, the use of permanent magnets eliminated troublesome water-coolant connections that would otherwise be needed to connect electromagnets to



Fig. 4—A half section of the RCA 8568 klystron fourth cavity showing cavity loops and mode suppressors used to stabilize the tube.

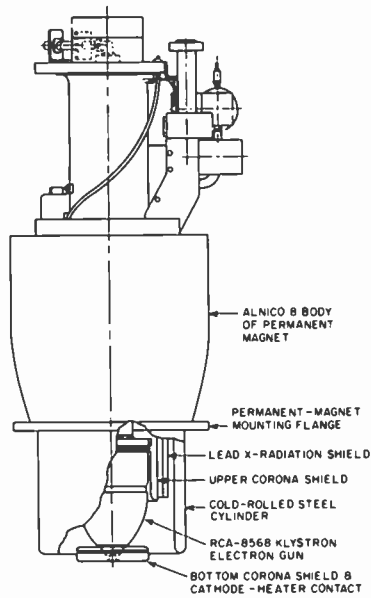


Fig. 5—Outline drawing of the RCA 8568 installed in a barrel type permanent focusing magnet. A cut-away view is shown of the electron gun region.

the coolant system. This arrangement reduced maintenance problems and improved the system reliability.

For additional reliability and ease of maintenance, it was specified that the klystron tube have only two coolant connections, operate in a stable manner at any beam-voltage level between 150 and 250 kV when operated at a fixed focusing field, and be interchangeable between focusing magnets, and that the output waveguide flanges align automatically with the mating flanges on the machine within a few thousandths of an inch. It was specified further that the X-radiation shielding for each tube occupy the minimum of space and that the shielding reduce the X-radiation level to a value of 5 milliroentgens at 24-in. from the tube axis to permit maintenance personnel to work safely in the klystron gallery when the klystrons were operating at maximum output.

Because the replacement of klystron tubes is a significant part of the operating cost of the machine, a design goal of 2000 hrs (minimum) was established for tube life. It was further specified that the tube be constructed in a manner that would permit it to be rebuilt at a fraction of the original cost.

#### Klystron development

During 1961 and early 1962, RCA redesigned the SLAC prototype tube to meet both the mechanical and electrical performance specifications. Six samples, designated RCA Dev. No. A1230D, were produced. These samples met the objective electrical performance specifications when they



Fig. 6—The RCA-8568 klystron installed in a barrel-type permanent magnet.

were electromagnetically focused. The tubes also met all the required mechanical specifications and had constructional features that made it feasible to rebuild them at low cost.

By the time the contract expired, satisfactory operation to 16 MW had been achieved by use of a prototype permanent-magnet focusing system. Although this performance was somewhat short of the goal of 24 MW, it was a record achievement and demonstrated that, with further refinement, permanent-magnet focusing was indeed feasible.

Encouraged by the results obtained by RCA, SLAC issued specifications in the request for production tubes to power the system requiring a power output of 21 MW with permanent magnet focusing. Sufficient evidence had been obtained at SLAC on resonant ring tests to suggest that a single RF window, coated with an extremely thin layer of titanium compounds, could handle the full peak and average power from a tube. Therefore, for minimum costs of both the accelerator and the klystron tubes, production tubes were specified to have only one RF window. This change reduced the number of vacuum valves and output flanges in the accelerator waveguide feed system by a factor of two and saved construction costs.

Experience gained as a result of the RCA work on the A1230D, together with similar work done at SLAC and Sperry-Rand, indicated that it would not be possible to construct a permanent magnet of reasonable size and cost to provide the requisite magnetic field to focus a tube like the A1230D. It was evident that a practical magnet

could be built only if the RF interaction length of the tube was shortened. This change would reduce the length of the magnetic path and bring the volume of magnetic material required to produce the needed field within practical bounds. Consequently, SLAC built a satisfactory tube approximately 3-in. shorter than the prototype.

On the basis of this information, the industry bid on production quantities of both tubes and permanent magnets in late 1962; again, RCA and Sperry-Rand were the successful bidders.

#### Production klystron—RCA 8568

The RCA 8568 klystron was designed to conform to the revised SLAC specifications. For this design, the A1230D was modified to use one output waveguide and window, and the RF interaction length was decreased by 3-in. to make permanent-magnet focusing practical.

Although the above modifications seem modest, they changed the stability characteristics of the tube drastically. Strong spurious oscillations in the frequency band between 5700 and 6300 MHz and 5-to-15-MHz ripples on the RF output pulse were chief among a host of instabilities observed in the modified A1230D. It took nearly eight months of careful analysis and patient cold-test work for final stabilization of the shortened design. During the course of this work, it was determined that the instabilities resulted from the following causes: RF feedback through the drift tubes; reflected electrons drifting counter to the normal electron beam; and electron-beam instabilities caused by transverse fields in the focusing magnets.

Solution of these instabilities included judicious perturbation of the various cavities, attenuation of the spurious resonances, improvement of the electron-gun optics, and development of permanent magnet with an extremely low transverse magnetic-field component. Fig. 4 shows one half of the fourth cavity, and illustrates the system of cavity loops and mode suppressors devised to stabilize the tubes. Similar mode suppressors are used in the other four cavities.

The barrel-type permanent focusing magnet for the RCA 8568, shown mounted on a tube in Figs. 5 and 6,

weighs approximately 1300 lbs. About 900 lbs of Alnico 8 are used to produce the field. A cold-rolled steel cylinder is located beneath the bottom pole plate of the magnet barrel to shape the axial magnetic focusing field in the region of the electron gun and to eliminate the bottom pole piece around the klystron tube.

The axial magnetic-field shape for the permanent magnet was originally derived from an electromagnet which had been used initially in evaluation of each tube. Thus, the early models of the permanent magnets featured a ring of bar magnets inside the cold-rolled steel cylinder to provide field shaping which more closely simulated the electromagnetic field. After several magnets were built, it was found that these bar magnets introduced non-symmetrical radial magnetic fields which degraded the klystron performance. When the bar magnets were removed, the klystron tubes performed better than they had in the electromagnet.

With early permanent magnets, non-symmetrical radial magnetic fields caused by transverse fields were a major cause of poor klystron operation. Even with an axial magnetic-field distribution approaching the electromagnet field, it was impossible to achieve comparable performance with a permanent magnet until the magnitude of the transverse magnetic fields was limited to less than 1% of the main axial field. Successful reduction of the transverse fields by RCA and the magnet supplier, Crucible Steel, made it possible for RCA to deliver the first full-performance klystron to the Stanford Accelerator Center by January, 1964, approximately a year before competition. The uniformity of both the tubes and the magnets has made it practical to interchange tubes and magnets at the accelerator site. No adjustment is needed on the magnets to obtain full performance from any tube operated in any magnet.

### Output windows

A unique output waveguide window was developed for the A1230D klystron<sup>1</sup> and was used without basic changes on the RCA 8568 klystron. This window is unique in that the ceramic-to-metal vacuum joint is achieved solely by means of pressure. A compression band made of high-

speed steel provides the pressure to compress an annealed, 0.010-inch-thick, OFHC copper sleeve against the smoothly ground edge of the ceramic window. This construction is economical and eliminates RF current losses that would otherwise occur in a brazed metallized joint.

The RF output windows in the RCA-8568 are subject to a phenomenon called single-surface multipactor. This phenomenon is manifested by localized window heating caused by bombardment of the ceramic by high-energy electrons that become trapped in the RF field near the window surface. The phenomenon is self-sustaining when the secondary-electron emission characteristics of the window surfaces exceed unity. If allowed to persist at the higher RF operating levels, multipactor causes the tube to fail as a result of window fracture, caused by overheating, or small vacuum leaks, caused by electron drilling.

Because both sides of the output window operate in vacuum environments, they are subject to the multipactor phenomenon. The problem has been eliminated by vapor-deposition of an RF transparent coating of titanium compounds on each window surface to reduce the secondary-emission characteristics of the window surfaces. Improved techniques are now being investigated as possible methods of improving the coating stability.

### Conclusions

This paper has discussed a few outstanding design accomplishments of the RCA-8568 klystron. Other accomplishments in this work include the design of a novel electron-gun construction for easy repair, a coolant system to meet the Stanford specifications for two coolant connections, X-radiation shielding to limit the X-radiation levels to 3 milliroentgens/hour, and a unique suspension design for mating the tube output flange to the accelerator.

More than 152 RCA-8568 klystrons have been operated on the Stanford machine since its completion in 1966. Although not all of the tubes have been operated at the maximum RF power level of 21 MW, statistical life-test studies at Stanford indicate little difference between life of the tubes at

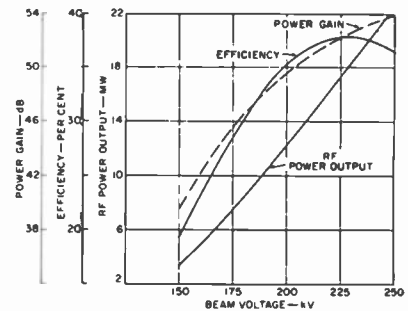


Fig. 6—The RCA-8568 klystron installed in a acteristics.

operating levels between 200 and 250 kV. On the basis of the current data, which is still incomplete because of insufficient tube failures, the projected life expectancy of the RCA-8568 is in excess of 11,000 hrs. Many tubes have operated for more than 10,000 hrs.

The RF power output, efficiency, and gain of a typical 8568 klystron with permanent-magnet focusing are shown in Fig. 7. Because of the fixed magnetic focusing conditions imposed by the permanent focusing magnet, the output-cavity design had to be compromised to meet the dual power-output specification; as a result, the operating efficiency of the tube typically peaks at 225 kilovolts.

Higher power-output levels than those shown in Fig. 7 have been realized with the RCA-8568 under experimental conditions. With normal pulse lengths, RF power outputs in excess of 25 and 30 MW have been obtained at RCA with beam voltages of 250 and 275 kV, respectively. The highest power output achieved experimentally with an RCA-8568 klystron was 105 MW at a beam voltage of 425 kV and a pulse width of 200 ns at MIT. The longest pulse operation was also achieved at MIT when a tube was operated at a peak power output of 10 MW for 50  $\mu$ s.

The RCA tube has received excellent customer acceptance. In the U.S., the RCA-8568 is used at the Stanford Linear Accelerator Center, the Brookhaven National Laboratory, the Cambridge Electron Accelerator, the Cornell University Linear Accelerator, and the Argonne National Laboratory. In Europe, the RCA-8568 is currently used at IKO in the Netherlands and at the University of Ghent in Belgium. A variant of the tube for operation at 2998 MHz is being built for the ORSAY accelerator in France.

### Reference

1. Teno, E., Hoffman, F. J., and Grimm, A. C., "Dielectric-To-Metal Compression-Band Seals".

# Environmental engineering laboratory

J. M. Forman | J. B. Grosh

RCA in Lancaster is a major supplier of power tubes, display storage tubes, vidicons, image orthicons, image converters, photomultipliers, and thermionic energy converters for industrial, military, and space applications. This paper discusses the facilities, responsibilities, and principles behind the RCA Lancaster Environmental Engineering Laboratory that supports these products. Customer-oriented environmental tube applications are also described.

CURRENT SPACE AND MILITARY SYSTEMS must operate reliably in widely varied environments. A single failure of a vital component may result in a costly loss of an airplane or a space vehicle. At the start of the jet age and the space era a large number of component failures were attributed to the hostile environment. As a result, a new technology—environmental engineering—was established. One objective of this technology is to subject system components to tests simulating the environmental conditions of their proposed mission; another objective is to analyze component failures and design various environmental protection methods and devices.

At present, many companies have major investments in testing facilities and technical personnel specifically directed towards the field of environmental engineering. Universities such as University of Pennsylvania, Massachusetts Institute of Technology, and the University of Michigan are offering environmental courses as part of their undergraduate and graduate curricula. In addition, a significant number of courses in shock, vibration, and acoustics are being offered by these same schools in engineering summer conferences. The Institute of Environmental Sciences, a technical society which has been in existence only ten years, currently has a membership of over 2,500.

## Evolution of the laboratory

The military, keenly aware of the accelerating dependence of their operations on electronics, and after having determined that electrical relays and

vacuum tubes in vibration and mechanical shock environments accounted for the vast majority of electronic system failures, began to take corrective action. As a result, military contracts, starting in 1955, required that various product design groups at RCA Lancaster devote considerable effort towards the ruggedization of electron tubes. Most of these contracts stipulated that the tubes operate satisfactorily while being subjected to a variety of environmental conditions. No single contract would support the cost of all the environmental equipment needed to perform the required design and qualification testing. Neither could the design activities send tubes, related electronic equipment, and personnel back and forth from the plant to outside environmental testing facilities without prohibitive delays and costs. The need for the environmental facilities was evident.

From 1955 to 1958, RCA Lancaster acquired a number of environmental equipments. More and more product lines gradually became involved in the use of these facilities. The custodians of these equipments, receiving an increasing number of requests from the design activities, spent more time providing aid in calibration, maintenance, design of suitable holding fixtures, selection of peripheral instrumentation, and guidance in mechanical tube design for the dynamic environments of shock and vibration.

It soon became evident that environmental problems were common to all electron tube types. As a result, the automatic transfer and integration of valuable design concepts from one product line to another were delegated to a single engineering group. Tech-

nical education and knowledge of this growing field were considered essential for better understanding and guidance to the various product lines. These factors played a major role in the evolution of a centralized environmental facility supported by an environmental engineering staff.

## Current facilities

The procurement of a wide variety of specialized laboratory equipments for simulation of stringent environmental field conditions led to the formation of a testing laboratory aimed at the evaluation of electron tubes. Auxiliary operational equipments of flexible design were engineered and built to accommodate numerous product-line types under rated or above-rated electrical test conditions. Analytical electronic instrumentation was also acquired or designed for monitoring tube performance under environmental conditions. Instruments such as spectrum analyzers, accelerometers, charge amplifiers, and level recorders were found useful, not only for environmental tube analysis but also for acoustic noise measurements and for dynamic analysis of the motion of machinery.

Natural, induced, and combined environments can be simulated by these facilities for a variety of tube test programs:

- 1) Design assurance testing and evaluation of partial assemblies or finished tubes;
- 2) Up-grading of existing products;
- 3) Pre-production qualification;
- 4) Reliability assessment and qualification;
- 5) Production sample testing; and
- 6) Qualification assurance testing.

These environmental test facilities produce simulated environments such as vibration, shock, constant acceleration, temperature, humidity, and altitude. Combined environments of temperature-humidity, temperature-altitude, and temperature-vibration are also available. All of these environmental equipments and related instrumentation in the Lancaster Environmental Engineering Laboratory are completely RCA owned.

## Current responsibilities

The environmental engineer provides consultation and technical guidance on tube design programs concerning environmental requirements. In this ca-

capacity, he offers engineering services on customer proposal preparation, including the development of environmental test programs to meet planned ruggedization goals for a particular electron tube, according to customer specifications. To accomplish this task, he must have a familiarity with electron-tube principles and environmental applications and a broad knowledge of environmental specifications and facilities with associated instrumentation. He frequently assists design, application, advanced development, and marketing personnel in the assessment and interpretation of customers' environmental demands. He is also responsible for the design, drafting, fabrication, and mechanical performance of the environmental fixtures required for tube analysis.

For developmental programs, the environmental engineer supported by trained technicians performs all environmental tests. It is likewise his responsibility to evaluate the environmental test results. From these analyses, he can furnish engineering guidance to the tube designer in overcoming tube, deflection-yoke, magnetic-shield or other component ruggedization deficiencies. A further responsibility of the engineer is the keeping of environmental facilities at a minimum by guiding the product lines toward standardization of test requirements. Periodic calibration and regular maintenance of the equipments and instrumentation is sustained by these engineers and technicians to assure the accuracy of their tests. The field of environmental engineering covers many scientific disciplines: thermodynamics, electronics, statics, dynamics, mathematical analysis, and the environmental applications of materials engineering. Finally, this engineer is equally responsible for assessing the state of the art of environmental knowledge in the areas covering new equipment, new testing methods and procedures, and the theory behind the test methods and procedures.

### Ruggedized tubes

Ideally, the development of ruggedized tubes would involve concurrent achievement of optimum environmental and electrical design objectives. Unfortunately, these objectives conflict; therefore a compromise is usually made between the initial and final de-

sign. This development is followed by a detailed quantitative definition of electrical and environmental limitations of the tube. The customers are not impressed by the term ruggedness unless it is backed by documented test conditions and definitive tube ratings.

Of the 450 tube types presently produced at RCA Lancaster about 100 electron tube types have been evaluated by the environmental laboratory in the last decade. A tabulation of some of the various kinds of field conditions associated with these products is given in Table I.

Table I—Ruggedized Conditions and Applications

#### Ruggedized Field Conditions

Aircraft shock during landing  
 Constant acceleration during missile take-off  
 Lunar landing (short duration high impact shock)  
 Shipboard shock impact from gun firing platforms  
 Low-pressure-temperature conditions of high altitude aircraft  
 Rocket engine random vibration forces  
 Turbulent airflow around supersonic aircraft  
 Ramjet screech  
 Helicopter mechanically induced excitations due to rotary components  
 Shock impacts of camera tube housing by high speed focal plane shutter  
 High impact shocks of naval ships that occur during a near miss of a torpedo which then explodes and sets the understructure of the ship into resonance.  
 Corona or breakdown created by low pressure environment during operational conditions.  
 Temperatures and humidities from the arctic to the jungle  
 Shock encountered in traversing rough terrain  
 Shipping and handling environments  
 Container drop tests  
 Railroad car or truck transportation

#### Ruggedized Tube Applications

Army, Navy and Air Force airborne equipment  
 Army half-track mobile equipment  
 Tactical ballistic missiles  
 Oil well logging  
 Sounding rockets  
 Satellites  
 Weather  
 Broadcast  
 Reconnaissance  
 Star-tracking for stellar navigation control of aircraft and missiles  
 Radar pulse compression  
 Airborne reconnaissance  
 Fire-control radar  
 Electronic countermeasures  
 Night vision  
 Airborne range finding  
 Television eye for:  
 Taxiing and landing of the supersonic transport  
 Viewing exhaust of the Saturn rocket  
 Observation of the earth and its resources  
 Observation of the launch of missiles  
 Weather radar for commercial aircraft  
 Underwater television for research and salvage operations

### Future prospects

In the coming decade, ruggedized and reliable electron devices will promote the use of electronics in many commercial fields. With the increasing use of electronic products in such non-electronic industries as chemical, food

processing, automobile, steel, crime detection, and educational institutions, environmental engineering will play a more vital part in the electronic industry.

**Jules M. Forman, Adm.**  
 Special Engineering Services  
 Industrial Tube Division  
 Electronic Components  
 Lancaster, Pa.

received the ME from Stevens Institute of Technology in 1940, was a teaching fellow at Stevens from 1940 to 1941, and did graduate work there from 1940 to 1942. He joined the Equipment Development Electrical Design Group at RCA Harrison in 1941; and transferred to RCA Lancaster in 1942, to the Special Equipment Engineering Group of the Life Test and Data Laboratory. Since 1942, he has designed numerous electromechanical electronic test sets, life test equipments, and has worked on the special application of electronic circuitry for small and large power, cathode ray, color, photo and image, and display storage electron tubes. He was promoted to Leader of Special Equipment Engineering in 1951. Since 1956 to 1962, his activity expanded to include Special Equipment and Environmental Engineering, having the additional responsibility for environmental engineering evaluation and testing of all new and improved tube ruggedization. From 1962 until his recent appointment, Mr. Forman was Manager, Environmental, Special Equipment & Specifications Engineering in the Electrical Measurements and Environmental Engineering Laboratory. Mr. Forman is a senior member of the IEEE, a member of the Institute of Environmental Sciences, a member of NSPE, and holds a Professional Electrical Engineering license in the state of Pennsylvania. Mr. Forman is also a Past President of Lincoln Chapter, PSPE, encompassing Lancaster, York, and Adam Counties.

**John B. Grosh, Ldr.**  
 Environmental Engineering  
 Industrial Tube Division  
 Electronic Components  
 Lancaster, Pa.

received the BS in Physics from Franklin & Marshall College in June 1953. He then joined RCA as a Junior Engineer in Specification Engineering. After two years in the service where he gained experience pertaining to missile telemetry and guidance systems, he returned to RCA in January 1956 and was assigned to the design of special electronic circuits and equipments in the Special Equipment Engineering Laboratory. Since 1957 he has been active in environmental engineering related to electron tubes. He had been Acting Engineering Leader of the Environmental Engineering Laboratory since October 1962, and was named Leader in October 1968. He is a member of Sigma Pi Sigma, Institute of Environmental Sciences, American Institute of Physics, and Society for the Advancement of Management.



In the photo, Jules Forman (right) and John Grosh apply the finishing touches to an environmental test fixture.

# Design of a 915-MHz power triode for microwave cooking

W. P. Bennett | D. R. Carter | I. E. Martin  
F. W. Peterson | J. D. Stabley | D. R. Trout

The microwave power system described in this paper uses a 915-MHz power triode as the power source to provide an economical unit that has general utility. This system provides a power output of approximately 900 W, and delivers more than 90% of full power to varying food loads. A large variety of foods have been prepared in the range. A 17-pound refrigerated turkey has been roasted in 70 minutes. A complete dinner for four, including chicken, baked potatoes, and a frozen vegetable, can be served in 25 minutes. Bacon is prepared to crisp condition in 2 minutes, and hot rolls and pastry require only seconds to heat. These results demonstrate that a completely different, less time-consuming method of preparing food is at hand.

## W. P. Bennett, Mgr

Advanced Development, Power Devices  
Industrial Tube Division  
Electronic Components  
Lancaster, Pa.

received the BSEE from Michigan State University in 1944 and has taken graduate courses in Physics and Chemistry at Franklin and Marshall College. Since joining RCA-Lancaster 23 years ago, Mr. Bennett has been engaged in the development of power tubes and associated circuitry. He joined RCA in 1944 as a Product Development Engineer, Industrial Tube Division at Lancaster. In 1956 he was promoted to Manager, Super-Power Tube Development and in 1958 was named Manager, Super-Power Tube Design and Application Engineering. He was appointed Manager, Regular Power Tube Engineering in 1962 and assumed his present post in 1963. Mr. Bennett was instrumental in the design and development of a family of small-power, ultra-high-frequency triode tubes, RCA Types 5588, 6161, and their derivatives. Mr. Bennett also directed an engineering group in the design and development of a family of ultra-high-frequency, high-power tetrodes capable of continuous output of 25 kilowatts and peak power output of 1 megawatt. Mr. Bennett is a member of Tau Beta Pi and a senior member of the IEEE. He holds four patents and has several applications pending. He is the author of numerous technical papers.

## D. R. Carter

Advanced Development, Power Devices  
Industrial Tube Division  
Electronic Components  
Lancaster, Pa.

received the BSEE from Drexel Institute of Technology in 1960 and the MS in Physics from Franklin and Marshall College in 1968. Upon joining RCA in 1956 as a co-op student, Mr. Carter had assignments in super power triode design, super power tetrode design, and regular power tube ap-

plication engineering. For the past seven years, he has worked on special power tube problems and radio frequency circuit design, utilizing computer techniques. In 1960 he was promoted to the position of Product Development Engineer. In this capacity he was assigned to work on the input circuit design of a new developmental coaxitron Type A-2696 which he successfully completed. He has since worked on other super power triode coaxitrons and tetrodes. In 1964 he was transferred to the Power Tube Advanced Development Activity and was assigned to the food electronics program, where he has been responsible for waveguide oven enclosure design and power triode oscillator circuitry. Mr. Carter is a member of IEEE, Eta Kappa Nu, and Sigma Pi Sigma.

## I. E. Martin

Advanced Development, Power Devices  
Industrial Tube Division  
Electronic Components  
Lancaster, Pa.

received the BSEE from Tulane University in 1950 and the MS in Physics from Franklin and Marshall College in 1968. Mr. Martin has been responsible for the early stress analysis and design of ceramic-to-metal compression-type seals and performed considerable experimentation in connection with the development of these seals. He has studied heat-transfer processes in power tubes, both analytically and experimentally. This work with both liquids and air, has led to significant improvements in the cooling of power tubes with liquids under extreme environmental conditions. Mr. Martin has participated in the design and development of numerous super-power tubes, particularly in connection with tube-processing, tube-circuiting, and tube-testing. He has designed a number of circuits including a multi-megawatt cavity for UHF pulse applications. More recently Mr. Martin has been concerned with the generation of high power through the use of transistors. He has also been concerned with modes of instability in transistors

under mismatched load conditions as well as the application of computers to the design of transistor amplifiers.

## F. W. Peterson

Advanced Development, Power Devices  
Industrial Tube Division  
Electronic Components  
Lancaster, Pa.

received the BSEE from the University of Arizona in 1949 and has done graduate work toward the MS in Physics at Franklin and Marshall College. Mr. Peterson joined RCA—Lancaster as a Specialized Engineering Trainee in 1949. Following completion of his training program he was assigned to the Power Tube Development group. From 1950 to 1954 he was responsible for the UHF circuitry used in evaluating the RCA-6161, 6181 and 6448 power tubes. In 1954 he was assigned to the Power Tube Design group as a Design Engineer where he was directly concerned with the design of the RCA-6816, 6884 and 7213. In 1956 he was appointed Leader, Medium Power Design group. In 1962 he was appointed Leader, Advanced Development, for Regular Power Tube Engineering. From 1963 to 1967 he was responsible for the RF generator development for cooking. Since 1967 he has led a task force team involved in cost reduction of the RF cooking generator. Mr. Peterson is a member of Tau Beta Pi, Phi Kappa Phi, Pi Mu Epsilon and Sigma Pi Sigma. He holds one patent in the electronics field and has submitted several additional disclosures. He presented a paper on the New Design Approach for Compact Kilowatt UHF Tetrode at the 1958 IRE Wescon Convention.

## J. D. Stabley

Advanced Development, Power Devices  
Industrial Tube Division  
Electronic Components  
Lancaster, Pa.

graduated from DeVry Institute of Technology in 1950. Upon joining RCA in 1951 Mr. Stabley was assigned to the Super Power activity under Lloyd Garner. His assignments include work on the RCA 5831 used in the Navy's Jim Greek transmitter. He also worked on the development of the A-2332, a shielding grid Triode, used by the A.E.C. in linear accelerator applications at Berkeley and the Lawrence Radiation Labs. In the late fifties Mr. Stabley participated in the design and application of several high power Radar and Switch tubes that had applications in the BMEWS, Nike Zeus and Tradex Radars. In the early sixties he was part of a team working under Navy contract to design, fabricate, and test the A-2696, a high power broadband coaxitron for shipboard operation. Since 1964 he has been engaged in the food electronics program where his responsibilities are in the area of enclosures, total system concepts, and customer contacts.

## D. R. Trout

Advanced Development, Power Devices  
Industrial Tube Division  
Electronic Components  
Lancaster, Pa.

joined the RCA Electron Tube Division in 1954 as an Undergraduate cooperative student. He acquired thirty months experience during this period as an electrical equipment designer. Upon graduation from Drexel Institute of Technology in 1958 with the BSEE he was assigned to the Super Power Tube Equipment Development group and was instrumental in the development and operation of several high-power high-frequency test facilities. He is currently doing graduate work at Franklin and Marshall College for his MS in Physics. Mr. Trout is a member of Sigma Pi Sigma.



The authors seated (left to right) are F. W. Peterson, I. E. Martin, W. P. Bennett, D. R. Carter, J. D. Stabley, and D. R. Trout.

**T**HE USE of microwave power to heat food has many benefits as compared with conventional methods. Its advantages include much faster heating time, less food shrinkage, better moisture retention, and several significant convenience factors. Because microwaves primarily heat the food, not the container which holds it, dishes may become warm but not hot enough to burn or to accumulate "baked" foods on the surface. As a result, food items may often be prepared, stored, heated, and served in the same dish, and the smaller number of dishes will be easier to clean. In addition, dishes and containers made of paper and plastic may be used to great advantage.

In spite of these advantages, the number of microwave ranges presently sold for use in the home is an almost insignificant percentage of the total range market. To increase this percentage, suppliers of microwave sources must give greater consideration to two requirements:

- 1) The economics of the microwave power unit must be compatible with the values of microwave heating as judged by the consumer.
- 2) The general utility and ease of use of the range unit without burdensome *do's* and *don'ts* must be consistent with the user price for the unit.

### Operating frequency

The best frequency for heating food is one which is high enough for the wave energy to be converted to heat energy by molecular motion in passing through the food, yet low enough to penetrate thoroughly into large items such as roasts or fowls. The infrared waves used in conventional ovens have very short wavelengths; they do not penetrate the food but are converted to heat energy in a very thin layer at the surface. As a result, the inner portions of the food can be heated only by a slow process of thermal conduction. Extremely long wavelengths, on the other hand, pass through food with essentially no heating effect. Either too short or too long a wavelength results in inefficient heating.

Two frequency bands assigned by the FCC are presently being used for microwave heating: 2450 MHz and

915 MHz. The longer-wavelength, lower-frequency band seems to strike a good balance for universal cooking. The superior penetration of the long-wave energy and its general usefulness in cooking and heating both large and small items are desirable features. In addition, because a 915-MHz power-generating device can be designed for operation at low voltages, the range power supply can be a simple, lightweight, inexpensive, transformerless unit that uses low-voltage solid-state devices. For these reasons, 915 MHz was selected as the frequency band for the design described.

### Microwave generator

The heart of a microwave heating system is the device employed as the microwave generator. A power triode was selected because of its potential low cost, small size, and light weight, and because of the proven production technology already established for this type of device. The 915-MHz triode power generator has the additional advantage of being able to tolerate both unusual loads (including metallic utensils) and the "no-load", or empty, oven condition. Fig. 1 shows a photograph of the power triode; Fig. 2 illustrates its construction.

The general design objectives for the microwave power triode were as follows: microwave power output of 1 kilowatt at 915 MHz, low-voltage (600-volt) operation, high efficiency, low cost, fast warmup, forced-air cooling, service life of 15 years, light weight, and small size. In addition, the tube would have to deliver essentially full power to a wide range of load impedances representing the nearly infinite variety of food loads anticipated.

A triode oscillator design was selected to meet these objectives. Unique input and feedback circuits were incorporated into the design so that the phase of the grid-cathode drive voltage could be properly fixed and the magnitude could be adjusted to optimize the efficiency of the oscillator.

The tube design features a massive copper grid block, wound with copper-alloy grid wires, to maximize heat transfer to external parts that can be maintained at low operating temperatures by forced-air cooling. The grid wires are mechanically peened into the

grid lands to assure good electrical and thermal contact. This feature greatly enhances the grid-dissipation limit to the extent that the tube can withstand operation even in the completely unloaded condition. The cathode area of 10 cm<sup>2</sup> is divided into 36 equal sections to keep the span of the 0.0015-in. grid wire very short.

Fig. 3 shows the component parts of the grid-block, cathode-block assembly. The gear-like grid block is manufactured economically by the use of cold-extrusion forming techniques which repeatedly produce parts to the close tolerances required. The one-piece extruded grid block contains 36 lands on which the grid wire is wound and 36 slots which serve as the bearing surface for one end of the cathode strands. An identical set of 36 slots for cathode seating are formed on the smaller cathode block. The grid and cathode blocks are guided on a common axis by a ceramic rod through the center of each block.

The total matrix-oxide cathode area of 10 cm<sup>2</sup> supplies a steady-state current of 0.5 A/cm<sup>2</sup>, as required for low-voltage (600 V) operation. This matrix-oxide cathode has been used extensively for years in many RCA power tubes. In the 915-MHz triode, directly heated strands are used to minimize cost and also to achieve fast warmup. The strands are directly connected to the grid block and cathode block in the tube. Direct connection is made possible by inductive "moats" in the grid block. This design greatly simplifies tube construction because only two insulating members are required in the vacuum envelope (the minimum required even for a diode), and the need for a DC bias supply is eliminated. The only electrical services directly required are a filament heating supply and the plate voltage supply. These features contribute substantially to the low-cost objective of the system.

The anode for the triode is also a cold-extruded copper cylinder which is formed with a thin-walled strain-isolation section on either end. The radiator consists of three concentric rings of corrugated copper strip brazed to the anode cylinder. In addition to providing the thermal heat path to the air stream, the fins of the radiator form part of the microwave circuit in the generator. Fig. 4 shows the mount as-

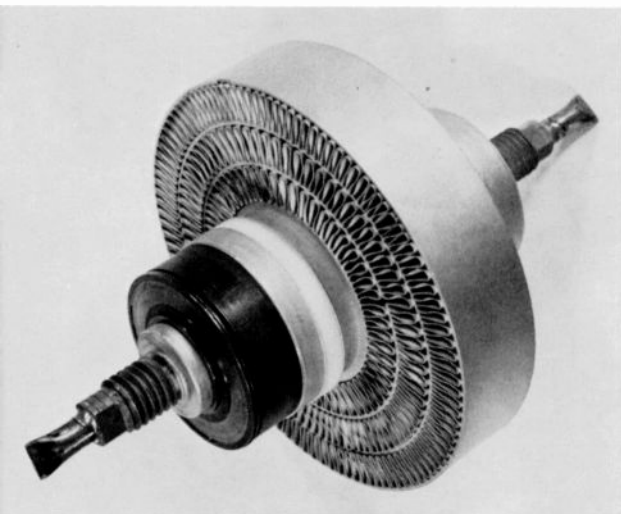


Fig. 1—Completed triode as an enclosed unit.

assembly ready for insertion into the anode-radiator assembly.

Processing of the tube during exhaust is conventional except that grid bombardment cannot be accomplished by application of positive grid bias because the cathodes are internally connected to the grid. Therefore, the grid is bombarded under microwave operating conditions. Consequently, a getter ion pump is connected to the tube until after a short period of microwave oscillator operation in a cavity similar to the one used for final generator assembly.

The microwave cavity for the oscillator consists of a coaxial cavity on either end of the tube with the anode radiator in the middle. The center conductor of the coaxial cavities is formed

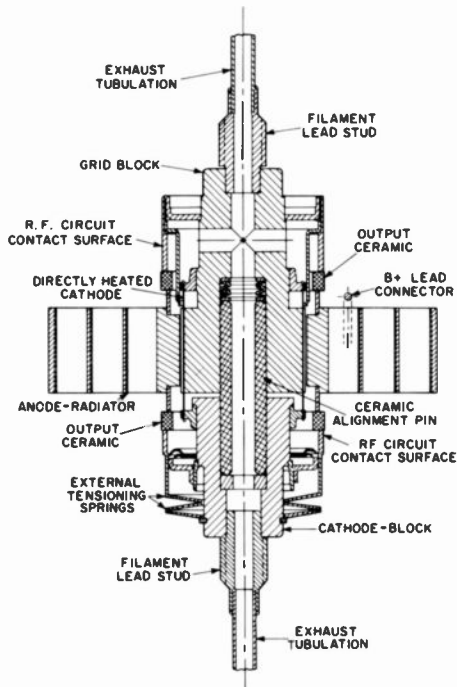


Fig. 2—Cross-section of the power triode.

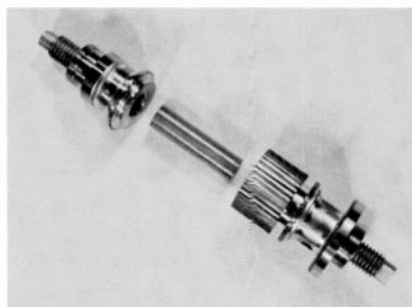


Fig. 3—Component parts of the grid-block, cathode-block assembly.

by the tube itself; the outer conductor is a 5-in.-diameter, 7-in.-long cylinder made of two identical, die-cast, aluminum half-shells that provide rugged, lightweight construction. Attached to each end of the tube are end-cup blockers (metal cylinders covered with an insulating sheet) which mate to the terminals of the tube, provide a microwave short for the end of the coaxial line, and form a DC voltage block on their outer diameter. The bottoms of the end-cup blockers consist of 36 radial fins which permit the free passage of cooling air through the entire coaxial cavity.

Air is directed into the cavity from the grid-block end, flows through the anode radiator, and exists past the cathode-block end. This direction of air flow provides cold air on the grid block which compensates for grid dissipation and prevents temperature unbalance between the grid block and the cathode block.

Adjustment of the electrical line length, established by the position of the end-cup blocker on the grid-block end of the tube, determines the operating frequency of the oscillator. Similarly, positioning of the end-cup blocker on the cathode-block end of the tube establishes the magnitude of the feedback voltage and thereby determines the operating level of plate current.

Microwave energy is capacitively coupled out of the cavity by means of a 1 $\frac{5}{8}$ -in.-diameter, 50-ohm transmission line that enters the cavity perpendicular to the axis of the tube in the region of the radiator. Fig. 5 shows the triode, with end-cup blockers and filament leads attached, positioned in the lower "half-shell". Fig. 6 shows a complete generator assembly, with the upper "half-shell" securely bolted to the lower "half-shell". This outer shell,

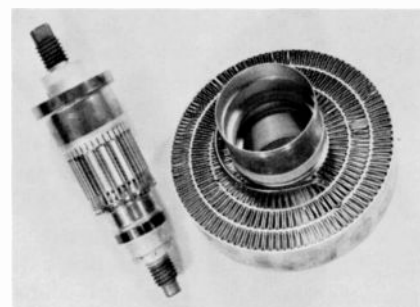


Fig. 4—Mount assembly ready for insertion into the anode-radiator assembly.

which contains the output transmission line, forms a complete shield that prevents the leakage of microwave energy. Because it is electrically isolated from all of the tube electrodes, it can be connected to the system ground. The generator weighs approximately 9 $\frac{1}{2}$  lbs., and occupies a small volume consisting of a 5-in.-diameter cylinder 7 in. long, and a 5 $\frac{1}{2}$ -in. length of 1 $\frac{5}{8}$ -in.-diameter coaxial transmission line.

### Triode microwave circuit

The microwave circuit for the tube can be described electrically as a quasi-Colpitts circuit. For optimum performance of the generator, the microwave circuit must control the magnitude and phase of the feedback signal and the system frequency. In the lumped-circuit model shown in Fig. 7, the values of  $C_1$ ,  $L_1$ , and the load Resistor  $R_L$  are controlled by the circuit external to the vacuum envelope. The grid-cathode circuit, built entirely within the vacuum envelope, is shown schematically as  $C_2$ ,  $L_2$ , and  $R_p$ . The capacitor  $C_2$  represents the active portion of the grid-cathode electrode capacitance. The inductor  $L_2$  represents a short length of transmission line terminated in a short circuit where the cathode is directly connected to the grid. The resistor  $R_p$  represents input losses caused by grid absorption and energy losses resulting from acceleration of the beam electrons into the grid-to-plate region.

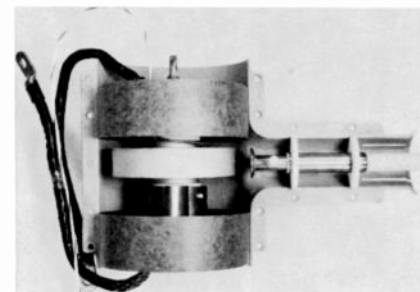


Fig. 5—The triode with the end-cup blockers and filament leads attached.

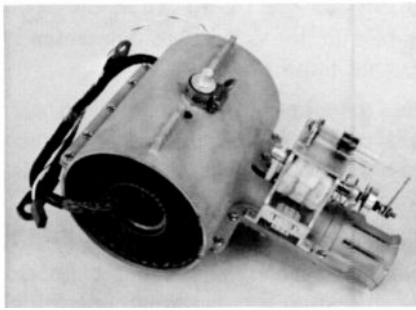


Fig. 6—A completed generator assembly.

In a microwave triode oscillator, electron transit time affects the boundary conditions that the circuit must satisfy. For optimum power generation, the fundamental plate current  $I_p$  of the tube must be in phase with the fundamental grid-to-plate voltage  $V_{gp}$  of the tube. The power generated  $P_r$  is given by

$$P_r = |V_{pr}| |I_p| \cos x$$

[The choice of  $V_{gp}$  instead of  $V_{pk}$  compensates for the normal  $180^\circ$  phase reversal at the output; therefore, the negative sign in the expression drops out.]

where  $x$  is the angle between  $V_{gp}$  and  $I_p$  (RMS values are used). At 915 MHz, the plate current  $I_p$  lags the grid-to-cathode voltage in time because of the electron transit time in the grid-to-cathode region. Therefore, the grid-cathode circuit is tuned precisely the right amount below the desired operating frequency so that the grid-to-cathode voltage leads the grid-to-plate voltage by a phase angle equal to the grid-to-cathode transit angle. This design compensates for the inherent transit-time lag, and thus accomplishes the desired objective of having  $I_p$  in phase with  $V_{gp}$ . Tuning of the grid-cathode circuit to 825 MHz optimizes the power generated at 915 MHz, as shown by the phase diagram in Fig. 8.

A test procedure was established to verify the transit-time correction. The passive resonant frequency of the entire circuit is the same as the oscillating frequency only if the transit-time compensation is correct. The amount of any correction necessary can be obtained from the difference between these two frequencies and the loaded  $Q$  of the circuit.

The dimensions of the circuit were calculated on a computer to avoid lengthy computations. Good correlation exists

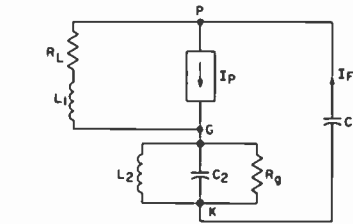


Fig. 7—Lumped-circuit model of the microwave circuit.

between the computer-predicted data and actual experimental data.

### Automatic power regulator

Adjustment of a coupling capacitor in series with the output transmission line permits the power output of the triode oscillator to be held at an optimum value even though the load impedance varies widely. Such control is feasible because maintenance of either constant steady-state plate current or constant RF voltage in the oscillator cavity produces optimum power output in the load. As the load is varied, therefore, the proper capacitor setting for optimum power can be determined by a control circuit such as that shown in Fig. 9, which senses a change in either of these parameters and adjusts the coupling capacitor to minimize this change.

The effectiveness of this control is illustrated by the performance diagram shown in Fig. 10. This diagram, which is essentially a Rieke diagram for a power-regulated oscillator, shows a set of power and frequency coordinates superimposed on an impedance plane (Smith Chart). It can be seen that 90% of full power can be produced with standing-wave ratios as high as 10 to 1; higher standing-wave ratios are seldom encountered, even in an empty oven.

Another feature of this control is that regulation can be applied to several discrete power levels. In most cases, two power levels are adequate and a switching arrangement is used to select the desired level. A lower regulated power level is achieved by a change of the reference level of the sensing signal to select a lower current- or voltage-level reference.

### Oven enclosures

One problem in the design of microwave ranges is the excitation of the proper voltage patterns in the oven. Any microwave oven enclosure is basically a waveguide resonator; therefore, the microwave energy fed into



Fig. 8—Oscillator phase diagram.

the oven forms standing-wave patterns which are determined by the boundary conditions: the oven dimensions, and the size, shape, and characteristics of the food load to be heated. Because of these standing-wave patterns, the effective heating voltage varies and some portions of the food are heated more rapidly than others. To avoid this non-uniform heating, it is common practice to move or change the voltage standing-wave pattern with relation to the food, and thus to equalize the heating effect throughout the item being heated.

There are always a number of different standing-wave patterns which are likely to occur, depending on the exact frequency of the power source and the perturbation of the electric field in the oven by the food load and other oven parts. These patterns (or modes, as they are often called) can be excited as a result of moving the food, pulling the frequency, or rotating a metallic stirrer inside the oven. The greater the number of modes or different field patterns in the oven, the greater is the diversity of heating patterns and the better the likelihood that the average heating effect throughout the food will be more uniform. A greater number of modes also reduces the range of impedances presented to the power source by different food loads.

Because the number of standing-wave patterns is relatively low in the 915-MHz band, a method was developed for moving the food in relation to the field patterns to provide uniform heating. In this method, proposed by Prucha,<sup>1</sup> the food load is slowly rotated in the oven on a turntable or "lazy susan". Either a dielectric material is used for the turntable, or the food is supported on an insulating platform 2 to 3 in. above a metal turntable.

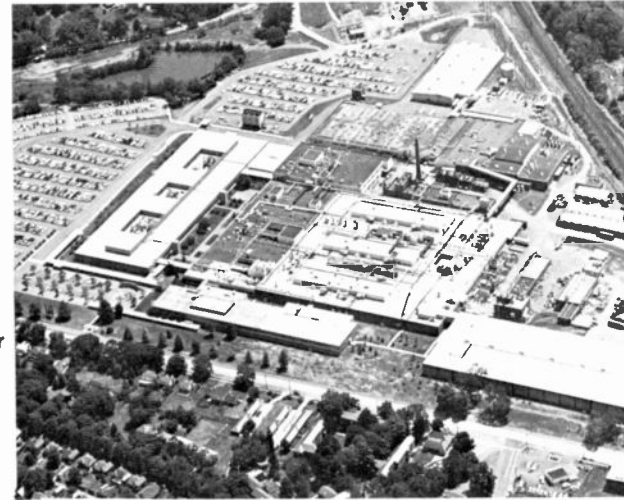
The voltage vectors of the field pattern excited in the oven enclosure should be predominantly in the horizontal direction. This excitation pattern is particularly beneficial in coupling power into thin food loads such as bacon. A simple and effective way of exciting such field patterns at 915 MHz



# RCA Lancaster—25 years of engineering excellence

At RCA's Lancaster plant—at the heart of Pennsylvania Dutch country—they certainly "know what good is." Lancaster engineers turn with just pride to their 25-year record of firsts in power, conversion, and color-tube engineering. Some of these firsts are given in the chronology below.

The Lancaster plant (shown at right) has grown from a 350,000-square-foot manufacturing facility in 1942 to a 1,400,000-square-foot complex employing over 5200 in applied research, design, development, and testing, as well as production. Their products vary from TV color picture tubes and RF cooking tubes used in home appliances, to giant high-power klystrons and magnetrons for government and industry, and to sensitive image orthicons, vidicons, and isocons for the entertainment industry and the space program.



## Cathode-ray and picture tubes

1943	Cathode-ray tube engineering department transferred from Harrison to Lancaster. At that time, it included all engineering on cathode-ray tubes such as radar, oscilloscope, flying spot, and projection types, as well as all pick-up tubes, such as iconoscopes, orthicons, and image tubes.
1949	Tri-color picture tube engineering began in Lancaster.
1950	RCA demonstrated first tri-color tube and a compatible all-electronic color television system to the FCC. Pick-up tubes set up as a separate department.
1951	First of several RCA symposia for presenting detailed technical and engineering information on its color tube to competing tube and set manufacturers.
1953	15GP22 flat-screen color picture tube put into production. Development of NTSC color system completed; adopted by the FCC.
1953 to 1954	Transfer of black-and-white picture tube design to the Marion, Ind. facility.
1954	21AXP22 metal color picture tube announced and demonstrated; the first tube to use lighthouse lens correction.
1955	Color tube applications set up as a department separate from color tube design.
1957	21CY22 introduced—the first color tube in all-glass bulb; it used "degroupping" lighthouse lens and graded apertures in steel masks.
1960	RCA introduced all-sulfide phosphors in color tubes, producing 50% increase in brightness (21FBP22).
1961	21FJP22 introduced—with bonded safety-glass.
1964	25AP22A introduced—first RCA 90° rectangular color picture tube.
1965	Introduction of Vanadate red.
1965 to present	Improvements in red-emitting phosphors (Vanadates and Oxysulfides); introduction of Einzel-lens gun.
1966	Development and introduction of "Perma-Chrome" tempera-tube compensation system.
1966	Einzel lens introduced in the 15-in portable color set.
1967	Development and introduction of Oxysulfide red—first "unity current ratio" color tube.

## Super power devices

1937	Super power tube research and development activity was started by L. P. Garner and Dr. P. T. Smith under Dr. V. K. Zworykin.
1943	Advanced Development Group established in Lancaster under L. P. Garner.
1947	The first commercial 1MW CW beam power triode, the RCA-5831, was marketed; the U.S. Navy bought the first tubes for their Jim Creek transmitter in Washington State.
1950 to 1955	Development of the RCA-6949. 500kW CW shielded grid beam triode for high-power communications, radar, and particle accelerator applications.
1953	The RCA-6448, the first UHF-TV high power beam tetrode tube, was announced.
1955 to 1958	Development of the RCA-6952, the first high power pulsed UHF radar beam power tetrode utilizing matrix oxide cathodes based on the electronic structures conceived for the RCA-6448.
1958 to 1961	The RCA Developmental Type A2346, the doubled-ended UHF triode now commercially available as the RCA-2054 and 7835, was developed for the Air Force. This structure provides the highest average power available in the world from gridded tubes suitable for UHF operation.
1961 to 1964	Development of the first coaxitron, integral-circuit high-power triode, under Air Force contract. Three Developmental Type A15038 Coaxitrons capable of 5MW peak power from 400 to 450 MHz were delivered.
1961 to 1964	The RCA-8568 30MW pulsed klystron for particle accelerator applications.
1964 to 1968	The development of heat pipes—devices for the efficient transfer of heat.
1966	Development of RCA-8684 25kW CW magnetron for industrial heating applications.
1966	Development of 100mW and 1W CW Argon lasers; a number of units have been produced and sold.
1968	Development of a 1kW CW klystron for operation between 4500 to 5000 MHz.

## Regular power tubes

1952	Development of the 6146 tube family for VHF mobile communications. The 6166 tubes were developed for VHF-TV transmitters. The 6181 tubes were developed for UHF-TV transmitters.
1956	The 6816 tubes were the first of the cermalox family that were developed.
1960	First conduction-cooled cermalox tubes developed.
1961	Ceramic-metal 8072 developed for UHF mobile communications.

## Conversion tubes

1962	Photocell facility moved to Mountaintop, Penna.
1965	Convex Expansion Program which included a Laminar Flow Clean Room (largest and cleanest in the world).
1966	Introduced long-life target image orthicon, increasing tube life four-fold. Great surge in image tube business because of night vision devices, increasing four-fold since 1955.
1967	TV guided missile business created an expanded vidicon tube market. Bi-Alkali photocathode was introduced to image orthicon and photomultiplier product lines. It vastly increased the general performance of these related types.

# The heat pipe, an unusual thermal device

R. A. Freggens | R. C. Turner

The transportation of unwanted heat to a suitable heat "sink" has proven to be a difficult design problem. Now, a unique device known as a "heat pipe" can transport large quantities of thermal energy to remote heat sinks with a temperature difference of only a few degrees. As an example of this unique ability, 11,000 watts of thermal energy have been transported through a one-inch diameter heat pipe over 27 inches long, with a temperature loss so small that it was difficult to measure. By comparison, a copper bar nine feet in diameter and weighing about 40 tons would be required to produce the same result. This paper describes the operation and design of heat pipes, and summarizes RCA's role in the development of these unusual thermal devices.

**R. C. Turner**  
Heat Transfer Devices Engineering  
Electronic Components  
Lancaster, Pa.

joined DEP's Missile and Surface Radar Division in 1958. He received the BSME from the Pennsylvania State University in 1961, and was reassigned to DEP's Astro-Electronics Division as a member of the Thermal Design Group. In this position he was involved in the thermal design and environmental testing of many of the spacecraft developed by AED, including Ranger, TIROS, Relay and Nimbus. In 1965, Mr. Turner was transferred to EC where he became a member of the Thermionic Converter Engineering Group of the Direct Energy Conversion Department. Since then, he has been responsible for the design and development of novel, fossil-fuel-fired, thermionic power systems for the Army, and a 500 watt, thermionic, radioisotope fueled space power system for the Air Force. He is currently responsible for the development of a 100-heat-pipe Rankin Space Power System Radiator for the Air Force. Mr. Turner has authored or co-authored several technical papers and has a patent pending for a highly accurate thermocouple device. He was awarded a certificate of commendation by NASA/JPL for, "significant contributions to the success of the RANGER 7 mission which secured the first high resolution photographs of the surface of the Moon," and received one of the 1967 Science awards from the Inventions and Contributions Board of NASA for "significant value to the advancement of the NASA Space Program."

**R. A. Freggens**  
Heat Transfer Devices Engineering  
Electronic Components  
Lancaster, Pa.

received the BS in Chemistry from Upsala College in 1951, and joined the Westinghouse Electron Tube Division as an engineer assigned to power tube development, responsible for the development of power tubes for audio, RF and high-voltage switch tube applications. His contributions included the design and improvement in electronic geometries and processing of high-power gridded tubes, with particular emphasis on the interaction between elements within the devices. Mr. Freggens joined RCA in 1966. Since then he has been responsible for the development of high temperature thermionic energy converters, employing heat pipes to transfer the primary thermal-energy from a nuclear heat source to a thermionic converter. He has been involved in special studies of molybdenum-lithium heat pipes for thermionic systems, under current in-house contracts. He has developed special low-temperature heat pipes employing aluminum and copper as the envelope material. He has also investigated the characteristics of these units to obtain compatible combinations of envelopes and working fluids for achieving reliable long-life operation. In addition, he has developed radial heat pipes for use in specialized applications. Mr. Freggens is a member of the IEEE, has been awarded one patent and has three patent applications pending.



In the photo, Mr. Freggens (seated) and Mr. Turner are examining various heat-pipes.

THE HEAT PIPE is basically a sealed two-phase system in which a fluid is continuously evaporating and condensing. The containment vessel shown in Fig. 1, is evacuated of all unwanted gases and sealed. A wick structure lines the inside wall from the evaporator end to the condenser end. Heat supplied to the evaporator causes vaporization of the fluid stored in the wick. The heat is then transported to the condenser end in the form of vapor flow, where it is recovered by condensation of vapor back into the wick. The cycle is completed when the condensate is returned to the evaporator by capillary action through the wick structure.

The purpose of the working fluid within the heat pipe is to absorb the heat energy injected into the evaporator section. This is accomplished by vaporization of the working fluid, a process that requires a large amount of heat energy, i.e., the latent heat of vaporization. (There is no increase in fluid temperature associated with this heat energy.) The vapor is transported to the condenser section by a slight pressure difference created between the ends of the pipe. When the vapor arrives at the condenser section, it encounters a slightly lower temperature than that of the evaporator. Consequently, the vapor condenses, releasing the thermal energy that had been stored as heat of vaporization.

For all practical engineering purposes, the heat pipe can be considered essentially isothermal along its length.

Final manuscript received October 17, 1968.

Table I. RCA heat pipe developments

Fluids		
Methanol	Ethylene glycol	Inorganic salts
Acetone	Mercury	Indium
Water	Cesium	Lithium
Dowtherm	Potassium	Bismuth
Naphthalene	Sodium	Lead
Vessels and wicks		
Glass	Stainless steel	Hastelloy X
Copper	Aluminum	Alumina
Nickel	Molybdenum (TZM)	
Geometries		
Cylindrical	Radial	"Y"
Double diameter	Serpentine	Double ended
Re-entrant	Star★	Flexible
Life continuing and undegraded		
Lithium-TZM	10,400 hours	
Sodium-Hastelloy X	17,000 hours	
Potassium-Nickel	15,000 hours	
Mercury-Stainless steel	10,000 hours	
Water-Copper	5,000 hours	
Water-Stainless steel	4,000 hours	

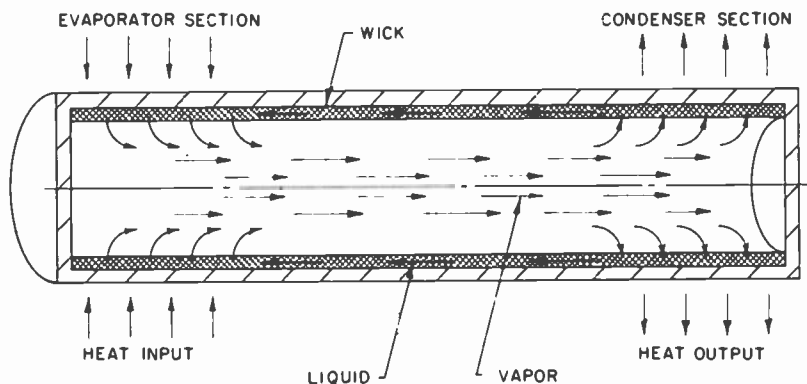


Fig. 1—Cutaway drawing of a typical cylindrical heat pipe.

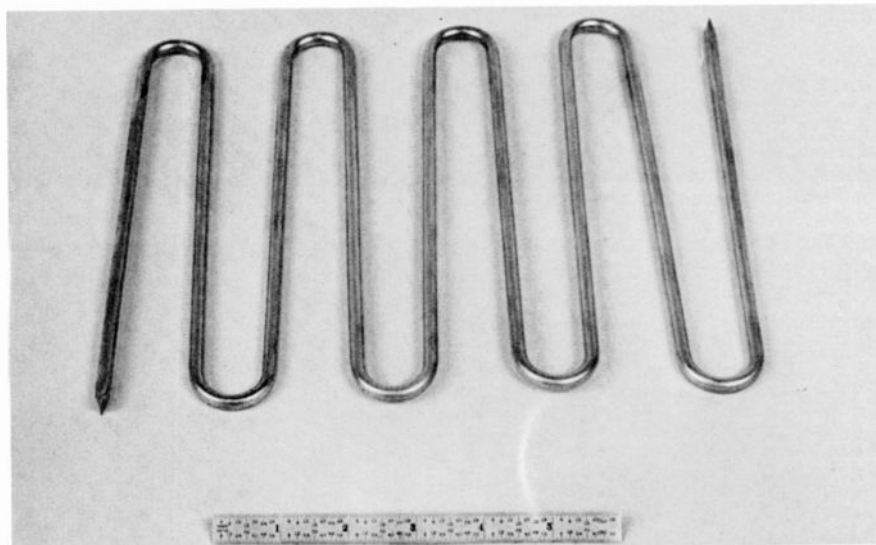


Fig. 2—"Serpentins" heat-pipe.

This nearly isothermal property is maintained even at high heat transfer rates and is responsible for the high effective thermal conductance.

### RCA developments

Since RCA began research on heat pipes in 1963, nearly 800 heat pipes of various sizes, temperatures, fluids, materials and power-handling capabilities have been built within the corporation. Table I lists some of the many working fluids and materials used for the containment vessels and wick structures. Although the name "heat pipe" conveys an image of a right-circular cylinder, they are not limited to this configuration. Heat pipes can be made square, rectangular, oval, spherical, serpentine, re-entrant, or in any configuration in which a two-phase, vapor-liquid system can exist. The various heat pipes developed at RCA Lancaster have included many of these shapes and configurations. Fig. 2 shows a "serpentine" configuration that was used as a heat pipe for cooling an array of integrated circuits. This pipe is made from 1/4-inch copper tubing with water as the working fluid. It is capable of transferring 100 watts in spite of several 180-degree bends, and demonstrates the inherent flexibility in heat-pipe configuration.

Heat pipes have also been fabricated to transfer large quantities of heat while withstanding high voltage potentials applied between the evaporator and condenser ends. One such pipe is shown in Fig. 3. The containment vessel is made of glass, the wick is fiberglass, and the working fluid is a fluoridated hydrocarbon. The two tubes extending from the pipe are employed to measure the thermal conductance by means of water-calorimetry. Although the thermal conductance is large, the heat pipe is electrically non-conductive.

Because of the high thermal efficiency of the heat pipe, substantial savings can be realized with respect to electrical power as well as in weight, volume and area. As an example, the radial heat pipe shown in Fig. 4 was built to cool the collector of a klystron for a troposcatter communications system. Using a conventional fin-type heat sink, the fan required nearly 1000 watts of electricity. When the heat sink was replaced by the heat pipe radiator, adequate cooling was provided by a 100-watt fan.

In spacecraft applications, reduced

weight and volume is an obvious design objective. The heat-pipe panel shown in Fig. 5 was used to provide a high heat-rejection rate from a Rankine Space-Power System. The radiator subsystem incorporates 100 stainless-steel heat pipes (horizontal tubes) in which the working fluid is metallic sodium. The heat pipes are designed to remove heat from the condenser section of a potassium-filled "loop". In operation, potassium vapor leaving the last turbine stage of the power system enters the heat-pipe radiator at 1420°F and exits at approximately the same temperature as a liquid. The heat pipes radiate 50,000 watts of thermal energy, or the amount required to condense 216 pounds per hour of potassium from the vapor state to the liquid state. The entire heat-pipe subsystem measures only 23 inches by 43 inches and weighs only 17 pounds, about 1/3 the weight of a comparable conduction-type fin and tube radiator. It was developed for the Air Force Aero-Propulsion Laboratory at Wright Patterson Air Force Base, Ohio.

Heat pipes have also been developed for cooling solid-state devices such as

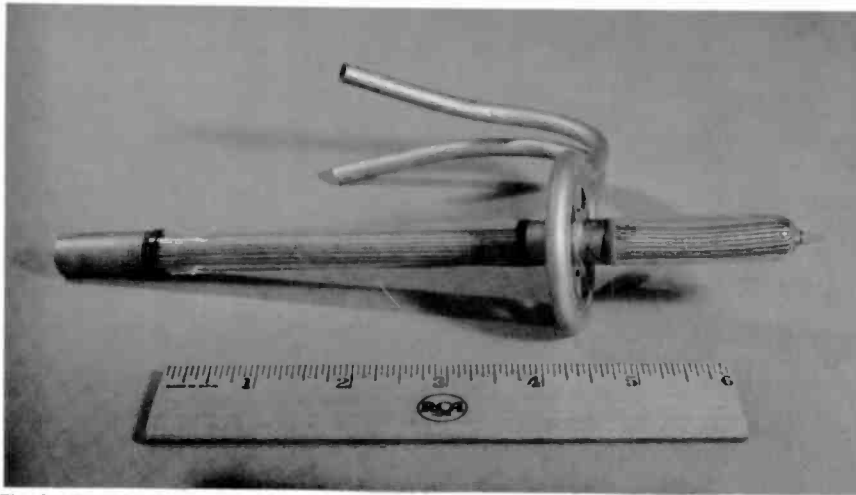


Fig. 3—Electrically insulated heat pipe.



Fig. 4—Radial heat pipe.

silicon-controlled rectifiers. The heat pipe shown in Fig. 6, for example, is capable of dissipating 1000 watts from the collectors of two 1N4044 silicon diodes, while maintaining a 100°C case temperature, with only 90 cfm of cooling air supplied by a fan. A comparable conductive-type heat sink would have required about ten times the sink volume in order to achieve the same power-dissipation capabilities.

It is also possible through a unique mode of heat-pipe operation to maintain constant temperature of a heat pipe in spite of large variations in transferred power. In this operational mode the heat pipe varies its access to the ultimate heat sink so as to maintain the constant temperature. The physical principles involved are the same as those by which an air pressure of one atmosphere establishes the boiling point of water as 100°C, i.e., if an overpressure of inert gas is used within the heat pipe it will establish an oper-

ating pressure and, because of the vapor pressure-temperature relationship, will establish a fixed operating temperature. The temperature of operation can be pre-set at the time of processing or modified as desired if a reservoir with variable volume is used.

Heat pipes designed to provide a constant temperature have wide application. As an example, they can be used to regulate the operating temperature of a semiconductor in the presence of a varying power demand or of a furnace with varying thermal loads.

#### Design factors

The heat pipe has been described in right circular form in most of the literature. However, as noted previously, there is no theoretical geometric limitation. In general, because heat is added to and removed from the heat pipe through the container wall by thermal conduction, the wall should be made as thin as possible. But, it

Table II. List of Symbols	
Symbol	Definition
$B$	Dimensionless constant related to the detailed geometry of the capillary structure
$R$	Universal gas constant
$T_o$	Heat pipe temperature—°K
$M$	Molecular weight of working fluid—g
$L$	Heat of vaporization—cal/g
$P(T_o)$	Vapor pressure of the working fluid at the operating temperature
$Q_o$	Heat transferred axially along pipe—cal/s
$e$	Fraction of wick volume occupied by liquid
$l$	Length of heat pipe—cm
$r_w$	Outside radius of wick—cm
$g$	Acceleration of gravity cm/s <sup>2</sup>
$r_e$	Radius of curvature of meniscus at evaporation—cm
$r_c$	Radius of curvature of meniscus at condenser—cm
$r_v$	Radius of vapor space—cm
$r_p$	Radius of wick pore—cm
$\sigma$	Surface tension of working fluid at temperature $T_o$ —dynes/cm
$\phi$	Wetting angle between working fluid and capillary structure—degrees
$\alpha$	Angle of the heat pipe to the horizontal—degrees
$\rho_o$	Density of the vapor phase of the working fluid at the temperature of operation g/cm <sup>3</sup>
$\rho_l$	Density of liquid phase of the working fluid at the temperature of operation—g/cm <sup>3</sup>
$\eta_e$	Vapor viscosity at operating temperature g/cm-s
$\eta_l$	Liquid viscosity at operating temperature g/cm-s
$m_o$	Mass flow rate = $Q_o/L$ = g/s
$\beta$	Fluid wetting angle at evaporation—degrees
$\delta$	Fluid wetting angle at condenser—

must be thick enough to support the difference between internal and ambient pressure. Long-term compatibility tests of the container wall with the working fluid help determine the exact thickness required.

The wick structure is composed of fine capillaries. The difference in the diameter of the capillary in the evaporator and condenser sections, coupled with the fluid surface tension, provides the driving force for fluid return. However, to achieve this force, the working fluid must "wet" the wick and walls of the heat pipe. Fig. 7 shows the effect of a small-diameter tube placed in a fluid bath. An attractive force between the liquid and the wall of the capillary tube combines with the surface tension of the liquid to move the liquid surface toward the unfilled portion of the tube. The cosine of the wetting angle,  $\phi$ , (the angle of contact between the fluid and surface) must be less than  $\pi/2$ . In the wick structure the driving force

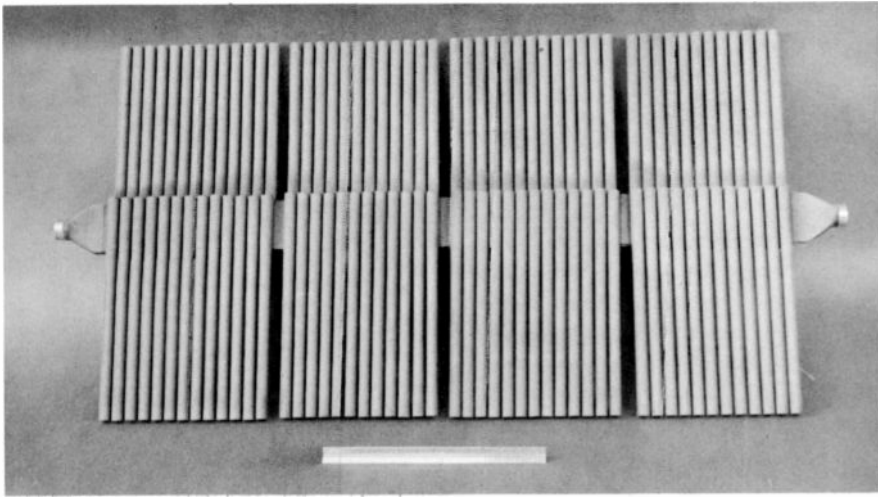


Fig. 5—Heat pipe panel used in spacecraft applications.



Fig. 6—Heat pipe which dissipates 1000 watts from the collectors of two type 1N4044 silicon diodes.

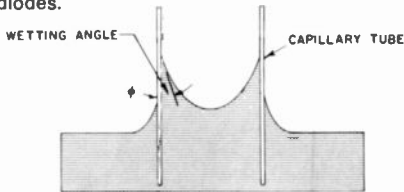


Fig. 7—Enlarged view of capillary tube placed in liquid bath to show the effect of capillary action.

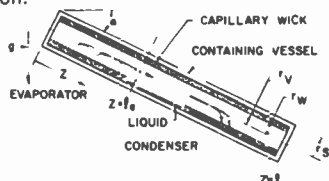


Fig. 8—Cylindrical heat-pipe structure.

is determined by this same wetting angle and the diameter of the capillary.

In the heat pipe, the capillary action in the wick sets up a difference of pressure between the evaporator and condenser ends that causes movement of the fluid through the wick. The pressure gradient can be determined from the expression

$$\Delta P_c = 2\sigma \left( \frac{\cos \beta}{r_e} - \frac{\cos \delta}{r_c} \right) \quad (1)$$

where the terms are as defined in Table II.

The fundamental requirement for operation of the heat pipe is that the system driving force (the capillary pumping pressure) equal or exceed the pressure

losses in the system. This relation may be expressed mathematically as

$$\Delta P_c \geq \Delta P_r + \Delta P_l + \Delta P_g \quad (2)$$

where  $\Delta P_r$  is the pressure difference of the vapor at both ends of the pipe,  $\Delta P_l$  is the pressure loss as a result of viscous drag of the liquid in the capillary tube, and  $\Delta P_g$  is the head pressure in the liquid caused by the force of gravity.

The first two pressure losses,  $\Delta P_r$  and  $\Delta P_l$ , represent two regions of the heat pipe: the vapor core and the fluid annulus, respectively. The flow of vapor in the central core of the heat pipe, as depicted in Fig. 8, is identical to fluid flow through a porous wall by injection or under suction.<sup>2,3</sup> This analogy assumes an incompressible liquid, laminar flow, and uniform injection or suction. Several vapor-flow expressions can be obtained based on the magnitude of the radial Reynolds number,  $R_r$ , as follows:

$$R_r = \frac{\rho_r r_c V_r}{\eta_r} \quad (3)$$

where  $V_r$  is the radial-flow velocity at the channel wall.

Based in the two ranges of the radial Reynold's number, the vapor-flow pressure loss can be expressed as

$$\Delta P_r = \frac{4\eta_r Q_r l}{\pi \rho_r r_c^4 L} \text{, for } R_r \ll 1, \text{ and} \quad (4)$$

$$-\left(1 - \frac{4}{\pi^2}\right) Q_r^2 \text{, for } R_r \gg 1.$$

$$\Delta P_r = \frac{8\rho_r r_c^4 L^2}{8\rho_r r_c^4 L^2}$$

The pressure loss ( $\Delta P_l$ ) associated with fluid flow through the wick from the condenser section to the evaporator section is based on the momentum

equation for steady incompressible flow. For long heat pipes in which  $r_w l$  is much greater than the outside diameter of the wick squared ( $r_w^2$ ), is given by

$$\Delta P_l = \frac{B\eta_l Q_r l}{2\pi (r_w^2 - r_c^2) \rho_l \epsilon r_p^2 L} \quad (5)$$

The gravitational term,  $\Delta P_g$ , is negative when the evaporation is below the condenser, positive when the evaporation is above the condenser, and zero when the pipe is operated in a horizontal position. The equation for head pressure caused by gravity is given by

$$\Delta P_g = \rho_l g l \sin \alpha \quad (6)$$

where  $\alpha$  is the angle of the heat pipe with respect to the horizontal position.

For small differences in pressure occurring in the vapor-phase region (between the evaporator and condenser sections), the resulting temperature difference, in degrees Kelvin ( $^{\circ}\text{K}$ ) can be calculated by use of the Clausius-Clapeyron equation:

$$\Delta T_r = \frac{RT_r^2 \Delta P_r}{MLP(T_r)} \quad (7)$$

There is one other factor which must be considered in the design of a heat pipe: The operating pressure of the working fluid. Heat pipes can operate when the vapor pressure of a work fluid is in the range of 0.01 atmosphere to several atmospheres. This pressure range sets the operating temperature range for each work fluid.

### Concluding remarks

The *heat pipe* has demonstrated its unique abilities to transport and dissipate thermal energy in a variety of sizes, and configurations, and over a wide range of operating temperatures. Currently, heat pipes are being used to cool semiconductors, electron tubes, and space power systems. The proven long life of the sealed heat pipe makes it attractive for unattended or inaccessible locations.

### References

1. Grover, G. M., Cotter, P. G., and Erickson, G. F., *Structures of Very High Thermal Conductance* (Journal of Applied Physics 35, 1964).
2. Yuan, S. W., and Finkelstein, A. B., *Laminar Flow with Injection and Suction Through a Porous Wall* (Heat Transfer and Fluid Mechanics Institute, Los Angeles, 1955).
3. Knight, B. W., and McInteer, B. B., *Laminar Incompressible Flow in Channels with Porous Walls* (LADS-5309).
4. Cotter, T. P., *Theory of Heat Pipes* (Los Alamos Scientific Lab Report LA 3246-MS, March 1965).
5. Hall, W. B., and Block, F., U. S. Patent Application No. 418946

# Ruggedization of camera tubes for space applications

J. G. Ziedonis

Television camera systems have played a major part in the exploration of our closer planets. The heart of these camera systems is the image-forming, light-sensitive device—the vidicon or the image orthicon. Such tubes must endure the most severe environment that electron tubes can be expected to meet: mechanical vibration and shock during the missile firing and lift-off. As a result, new design concepts have been developed for protection of vidicon tubes.

**I**N SPACE MISSIONS that use cameras with vidicons, high-resolution video pictures can be maintained only if the spacing among internal electrodes of vidicon remains the same as before the launch. Vidicons, therefore, are not only treated as light-sensitive electrical devices, but also as mechanical systems. All mechanical systems have resonances, and electron tubes are no exception. When an electron tube is subjected to mechanical vibration, some of its internal electrode resonances are excited. At these resonances, tube components may develop large relative displacements which may deteriorate tube performance or produce complete failure. The ruggedization of electron tubes, therefore, involves their redesign.

Mechanically, the electrode assembly represents a complex system with many degrees of freedom. During the design and ruggedization, two major design concepts must be considered: the internal electrode design and the effect of external equipment on the tube.

## Internal electrode design

In the design of internal electrodes of a tube, the following properties are important:

- 1) The electrically conductive materials used for electrodes should be antimagnetic because, when magnetic materials become magnetized, they distort the electron beam path. This requirement has only a few exceptions; e.g., the stem leads need not be antimagnetic.
- 2) All materials used inside the tube must withstand the 350 to 400°C tube-processing temperatures; annealing temperature of the materials must be well above the maximum tube-processing temperature to preserve the initially preselected stiffness.
- 3) The metals used must be weldable because the electrodes are usually spot-

welded, and good welds are crucial for a reliable, strong assembly.

4) The bulbspacers for electrode support must be designed to allow the electrodes to be inserted in the glass envelope without scraping the glass walls. Once inserted, these bulb spacers must rigidly support the electrodes. If the glass walls are scraped with bulbspacers, particles develop in the tubes which eventually get on the target or faceplate and interfere with tube operation.

5) The materials used should have very low vapor pressure. The internal electrodes operate in a relatively high vacuum,  $10^{-6}$  to  $10^{-7}$  Torr. Any degassing occurring after the tubes have been sealed may permanently damage the cathode and other electrodes.

6) The electrodes must be electrically insulated from each other.

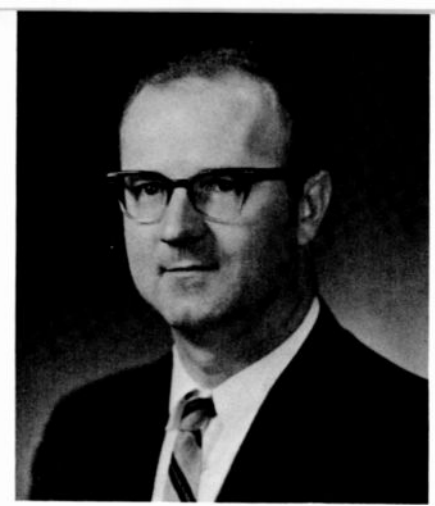
7) The electrode assembly should be sufficiently rigid to withstand the required vibration and shock environments.

## Effect of external equipment

Resonances of the camera and associated external equipment have considerable effect on tube performance. Any kind of resonance in the system that couples through the tube mounting severely excites the internal tube-electrode resonances. In many applications at low frequencies, especially below 500 Hz, the camera systems have caused poor tube performance. Rattling due to loose screws, loosely supported magnetic shields, and lens shutters, adversely affects tube performance.

## Ruggedization techniques

The internal electrode resonances are the major sources of tube performance deterioration. The thin, long, metal cylinders used in electron tubes have resonances below 2000 Hz. These resonances have low amplitudes of motion, but they are, nevertheless, responsible for mesh microphonics. The bulb-spacer and the gun-mount resonances are additional sources of tube prob-



Janis G. Ziedonis  
Advanced Development  
Medical Electronics\*  
Hoffmann-LaRoche  
Trenton, N.J.

received the BS in Mathematics and Physics from Muhlenberg College in Allentown, Pa. in 1959. Following graduation, he joined the environmental engineering department at the Electron Tube Division. He worked on electron tubes for space applications where he contributed to the design and development of vidicons and image orthicon tubes. He developed tube ruggedization techniques that were used on a wide range of conversion tubes including the all-ceramic vidicon and the 2- and 3-inch image orthicons. On a special project for Jet Propulsion Laboratories, Mr. Ziedonis analyzed the impact phenomena on the Ranger satellite cameras during their impact on the moon. This was accomplished by reviewing and analyzing the last 800 microseconds of the telemetry data, and performing experiments that simulated the last received video signals. Recently, Mr. Ziedonis transferred to RCA, Medical Electronics, Advanced Development Group, where he is responsible for the development and design of ultrasonic transducers for medical applications. He is a member of Sigma Pi Sigma, American Association of Physics Teachers, and American Institute of Ultrasonics in Medicine.

\*The RCA Medical Electronics activity has recently been sold to Hoffmann-LaRoche.

lems. These resonances are responsible for most severe mesh microphonics, loss of resolution, smeared pictures in slow-speed scanning systems, and the shorter life of the tubes.

Mesh microphonics occur when the thin mesh vibrates at its fundamental resonant frequency with respect to a fixed target or photoconductor. The video signal is modulated at the mesh resonant frequency. Although the mesh resonance in vidicon tubes is well above 2000 Hz, other electrode resonances excite the mesh. In 3-in. and 4 1/2-in. image-orthicon tubes, the mesh resonances are below 2000 Hz; these tubes should not be vibrated at the mesh resonant frequencies of 1700 Hz and 900 Hz.

The most severe environment for electron tubes is mechanical vibration. In most cases, the highest required vibration frequency is 2000 Hz. For satisfactory operation of tubes, bulb-spacer resonances should be well above the

highest vibration frequency; proper bulbspacer stiffness and location must also be determined.

Fig. 1 shows a typical, non-ruggedized, one-inch, hybrid vidicon tube. The analysis of electrode structure of this tube for dynamic environments is performed with a mechanical system representing the tube structure as shown in Fig. 2. Although the model in Fig. 2 is simplified, on the basis of theoretical analysis and experiments performed on actual tubes the following assumptions can be made:

- 1) Some of the interelectrode supports (such as the  $G_1-G_2$  and  $G_4-G_5$ ) are rigid within the 20-to-2000-Hz frequency range.
- 2) Normally, the tubes are rigidly mounted in the camera. If the tubes are potted in semi-flexible potting compound, they usually resonate below 2000 Hz; therefore, this resonance must be included in calculations.

When non-ruggedized vidicon tubes were subjected to mechanical vibration and shock, several major resonances were responsible for complete deterioration of the video signals:

- 1) *Electron-gun-mount resonances:* These resonances were present because of the soft bulbspacers that were initially used to support the electrode assembly. At these resonances, the electron beam was moved out of its electro-optical paths and loss of resolution occurred. These resonances were overcome when the heavy glass beads were replaced by brazed ceramic discs and the gun-mount was made considerably lighter.
- 2) *Electrode-support bulbspacer resonances:* Usually, the bulbspacers were overloaded with heavy electrodes which decreased the resonant frequency of the system. When the support bulbspacer resonance was excited, it, in turn, excited the mesh resonance. This resonance produced a distorted beam path and video-signal modulation. As a result, stiffer bulbspacers were designed and, the weight of the electrode assembly was reduced. These changes as shown in Fig. 3 reduced a number of resonances and, in some cases, eliminated them completely.
- 3) *Target-mesh resonances:* These resonances modulate the video-signal output. As a result, a new mesh processing technique was developed to reduce the mesh microphonics in the tubes. This process introduced considerably higher internal damping in the mesh, and almost doubled its resonant frequency to 4800 Hz. This design change enabled the mesh to withstand the most severe environmental requirements such as 3000-g-peak, 0.5-ms sine-pulse shock.

Vibration frequencies at which the non-ruggedized tube performance was

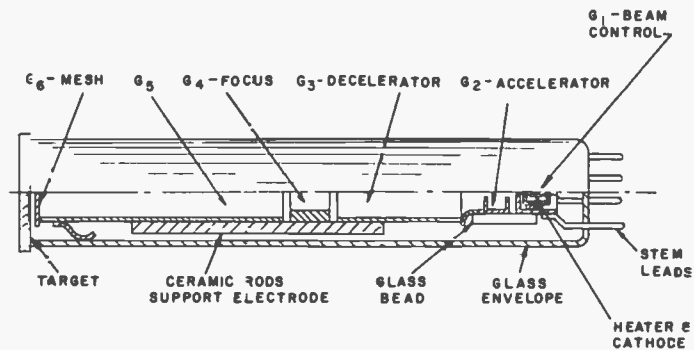


Fig. 1—Non-ruggedized one-inch hybrid vidicon.

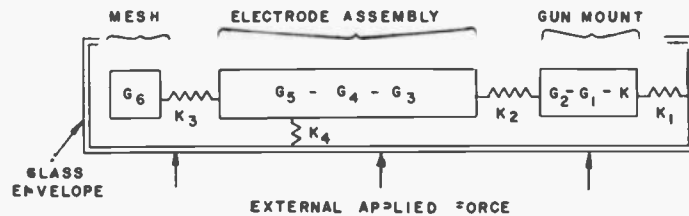


Fig. 2—Simplified equivalent diagram of one-inch hybrid vidicon.

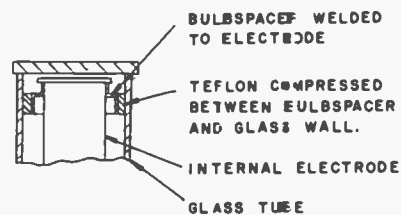


Fig. 3—Cylindrical bulbspacer for one-inch vidicon.

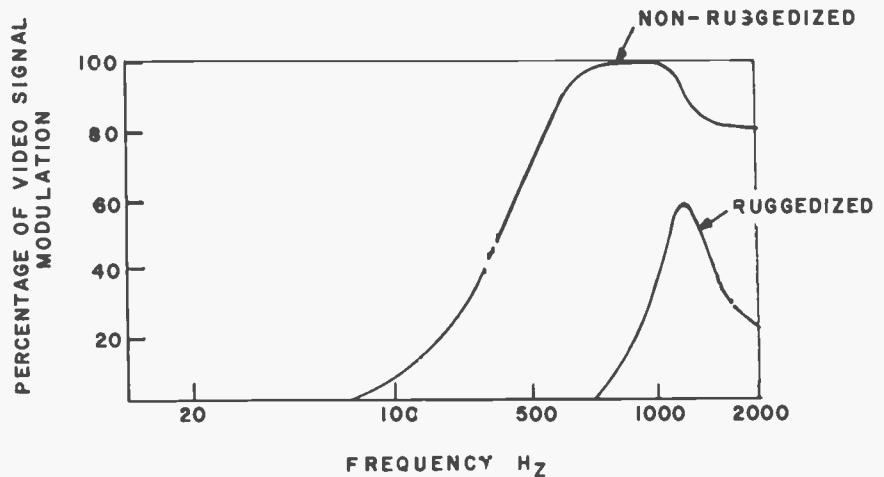


Fig. 4—Video-signal modulation during sinewave vibration test of non-ruggedized and ruggedized hybrid vidicons, 5g peak.

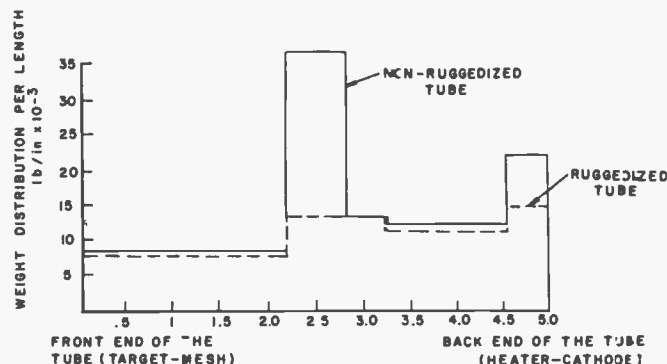


Fig. 5—Weight distribution curve for non-ruggedized and ruggedized one-inch vidicons.

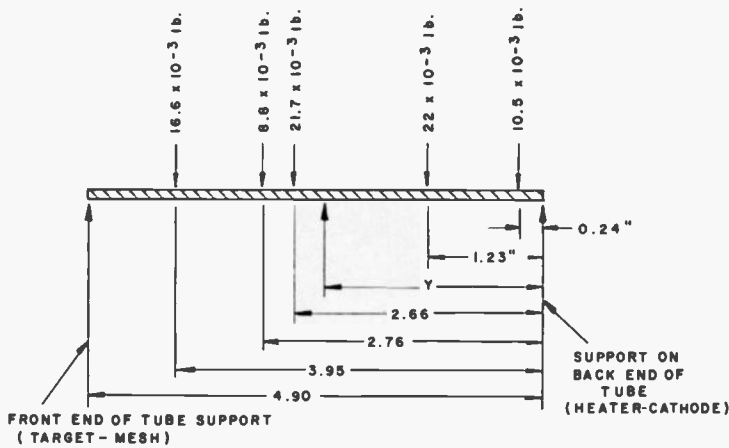


Fig. 6—Equivalent diagram of the electrode assembly.

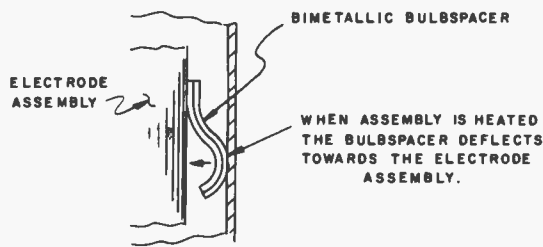


Fig. 7—Sectional drawing of vidicon tube with bimetallic bulbspacer.

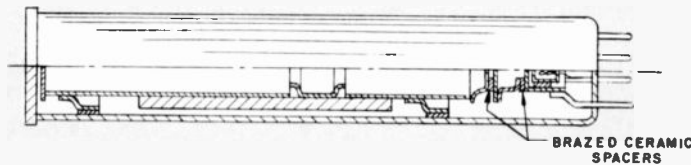


Fig. 8—RCA ruggedized hybrid one-inch vidicon, 8567.

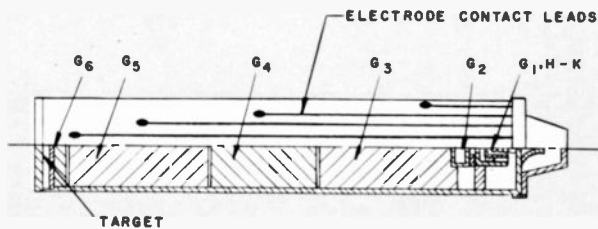


Fig. 9—All-ceramic one-inch vidicon.

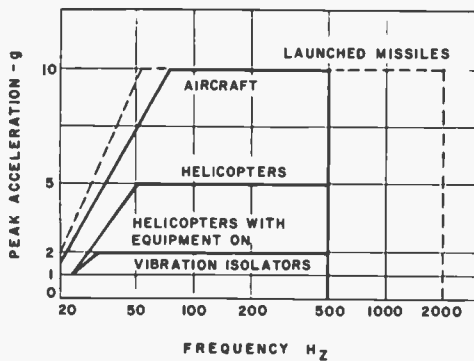


Fig. 10—Sinusoidal vibration test levels per MIL-STD-810.

considerably distorted are shown in Fig. 4.

The electrode weight distribution curve is shown in Fig. 5. This curve is used to determine the required stiffness of the bulbspacers and to assure that the electrode supports resonate well above the required vibration frequency range. This diagram was obtained by carefully weighing each electrode, by measuring its length, and then comparing the weight-to-length ratio to the tube length. For the non-ruggedized tube, the data indicate a non-uniform electrode mass distribution.

With the assumption that the damping within the metal bulbspacers is negligible, the required bulbspacer stiffness  $K_T$  may be obtained as follows:

$$K_T = \omega^2 M \quad (1)$$

If the desired electrode assembly resonance is 3000 Hz, the required bulbspacer stiffness is  $73.1 \times 10^{-3}$  lb./in. This magnitude suggests a very stiff bulbspacer assembly. The total stiffness, of each of the selected bulbspacers is

$$K_T = K_1 + K_2 + K_3 + \dots \quad (2)$$

According to Fig. 5, another set of bulbspacers is needed. The location of the new set of bulbspacers is calculated with the use of Fig. 6 as a reference and the following static equilibrium equations:

$$\sum F = 0 \quad (3)$$

$$\sum M_o = 0 \quad (4)$$

From these equations, the location of the third set of bulbspacers was calculated to be 1.92 inches from the back end of the assembly.

#### Symbols

F	static force	lb
$K_T$	total electrode support spring stiffness	lb/in
M	mass (W/g)	lb-sec <sup>2</sup> /in
$M_o$	moment for static conditions	lb/in
$\omega$	angular frequency ( $2\pi f$ )	rad/sec
f	vibration frequency	Hz

Several new design concepts were developed to overcome the existing manufacturing and assembling difficulties concerning bulbspacers. For example, the stiffness of a bulbspacer is generally controlled by its material configuration, thickness, and length. With stiff bulbspacers, the electrode-assembly insertion problem in the glass

cylinder could be simplified with the use of bimetallic materials for the bulb-spacers. The bimetallic material is used in such a way that when the gun-mount is preheated prior to its insertion in the glass envelope, the bulbspacers deflect towards the electrodes and insertion becomes easy, as shown in Fig. 7. As a result, the glass walls are not scraped and no particles are generated. During the stem-sealing process, the glass softens near the gun-mount and the plain, stiff bulbspacers push the glass out and deform the glass walls; however, stiff bimetallic bulbspacers do not cause deformation.

Another type of bulbspacer that was developed and is widely used in vidicon tubes for military and space projects is the cylindrical bulbspacer that compresses thin sheets of tetrafluoroethylene (Teflon—a trade name of Du Pont de Nemours, Inc.) between the glass and the bulbspacer, as shown in Fig. 3. Teflon prevents the metal from scraping the glass during the electrode assembly insertion in the glass cylinder. The complete electrode and bulbspacer assembly withstands the tube-processing temperatures.

A combination of all the above design features considerably improved the performance of the hybrid vidicon tube (Fig. 4).

This type of design improvement was incorporated in other vidicon tube types, such as the all-magnetic, all-electrostatic, reverse-hybrid. As an example, Fig. 8 shows a ruggedized one-inch hybrid vidicon.

Image-orthicon tubes are facing similar environmental requirements, but the solutions to the design improvements are more difficult. All components are proportionally larger and heavier, and the tube processing is more severe. The choice of available materials that could be used in these tubes is reduced because of the higher vacuum and the sodium, potassium, cesium, and anti-mony elements used for making photocathodes. These tubes are also more sensitive to particles which, from previous observations, have torn both glass and magnesium oxide targets.

With the glass-envelope type of tubes, it is impossible to have all the internal tube components rigidly mounted. Therefore, a new design technique was developed in which electrodes are

evaporated on the inside walls of the ceramic tube envelope. The ceramic cylinder itself resonates at 5000 Hz. This design technique eliminates the need for metal cylinders and bulb-spacers. Fig. 9 shows the all-ceramic one-inch hybrid vidicon built for the Jet Propulsion Labs, Pasadena, Cal.<sup>1</sup>

### Requirements and capabilities

With the growth of military and space exploration programs, the environmental requirements for the components have been increasing. Figs. 10 and 11 show vibration specifications for components such as vidicons and image orthicons, as required by the military contracts. These environmental requirements may not seem too severe, but, unfortunately, several major resonances exist in the systems using these electron tubes. These resonances subject the tubes to vibrations levels which exceed the design specifications and, thus, cause failures. With complete evaluation of the system, these failures can be prevented. Figs. 12 and 13 summarize the capabilities of one-inch vidicon tubes that have been ruggedized in the last four years. The image-orthicon tubes, being more complicated, have not reached as high environmental capabilities as some of the vidicon tubes. Figs. 14 and 15 show the presently available image-orthicon tubes that have reasonable environmental capabilities.

### Conclusions

During the ruggedization of camera tubes, not all the electrode resonances have been eliminated. However, the major and most damaging electrode structures have been eliminated, as shown in Fig. 8. With the ruggedization of camera tubes, the number of particles in the tubes was considerably reduced, the weak electrode structure was removed, the operational tube performance during severe environments was considerably improved, and higher reliability was achieved.

### References

- Ochs, S. A., *Development of a Sterilizable Ruggedized Vidicon for Lunar and Planetary Photography*. Final Report for Jet Propulsion Laboratories, Pasadena, California, Contract No. 950985.
- Ochs, S. A., and Marschka, F. D., "A Sterilizable and Ruggedized Vidicon," *this issue*.
- Harris and Crede, *Shock and Vibration Handbook*, Vols. I and II (McGraw-Hill Book Co.)
- Hartog, *Mechanical Vibration* (McGraw-Hill Book Co.)
- Ziedonis, J. G., "Ruggedization Techniques for Electron Tubes," private correspondence.

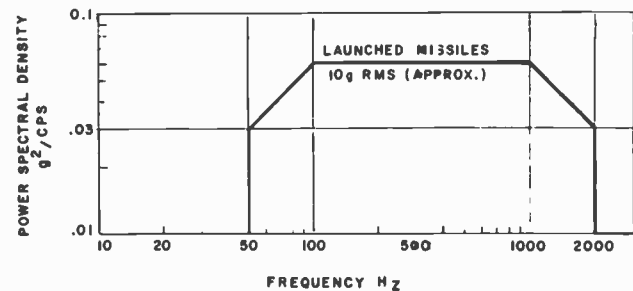


Fig. 11—Random vibration test levels per MIL-STD-810.

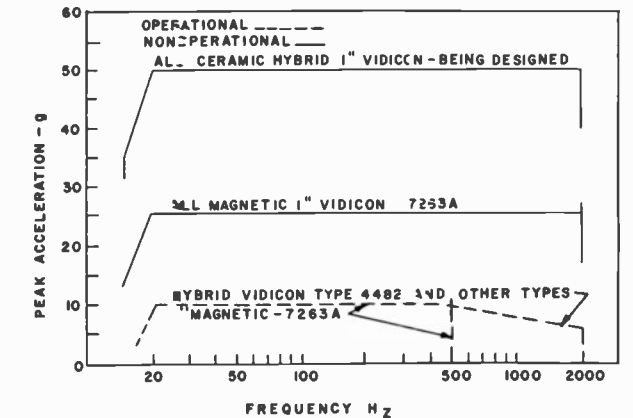


Fig. 12—RCA vidicon tube capabilities—sinewave vibration.

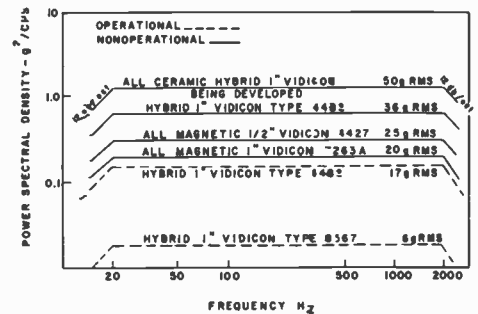


Fig. 13—RCA vidicon capabilities during random vibration tests.

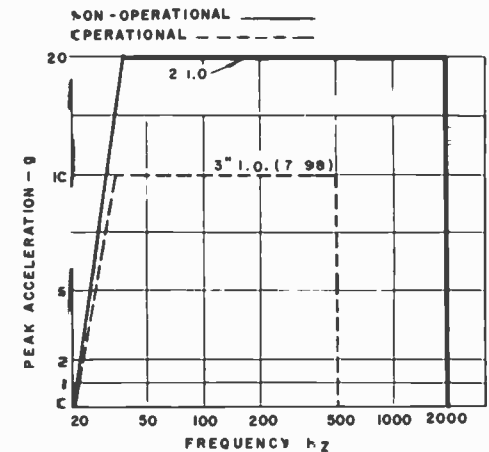


Fig. 14—RCA image orthicon capabilities during sinewave vibration.

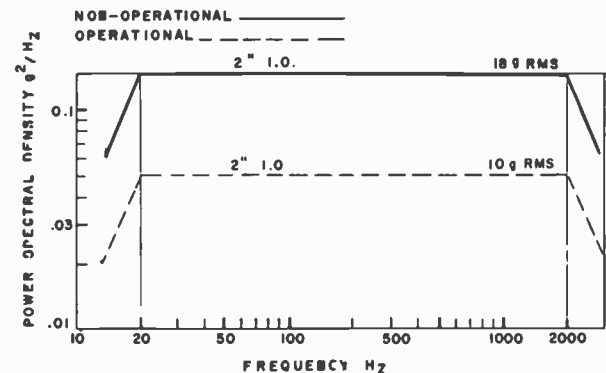


Fig. 15—RCA image orthicon capabilities during random vibration test.

# The coaxitron

J. A. Eshleman | B. B. Adams

The Coaxitron integrates the complete RF input and output circuits and the electron-interaction circuits within a common vacuum envelope. This design eliminates the need of ceramic-window exposure to extremely high RF voltages and ceramic-to-metal seal to extremely large RF currents. It eliminates external spring-contact fingers, blockers, and tuning. By integration of RF circuit elements into the tube envelope, the high-RF-voltage portions of the resonant circuits are insulated by a vacuum dielectric which has a high dielectric strength and excellent self-healing characteristics. Stored energy in the resonant circuits and in the lead inductances is reduced, and the dielectric dissipation and the propensity to arc over are minimized. Because of these advantages, the Coaxitron RF circuit components can be designed for maximum amplifier performance. Instantaneous bandwidths in excess of 10% at the megawatt RF power output levels are readily feasible. These integral packaged amplifier tubes resulted from an extensive developmental effort in the Super Power Devices Group at Lancaster. This paper describes the design features of the RCA Dev. No. A15193B Coaxitron.

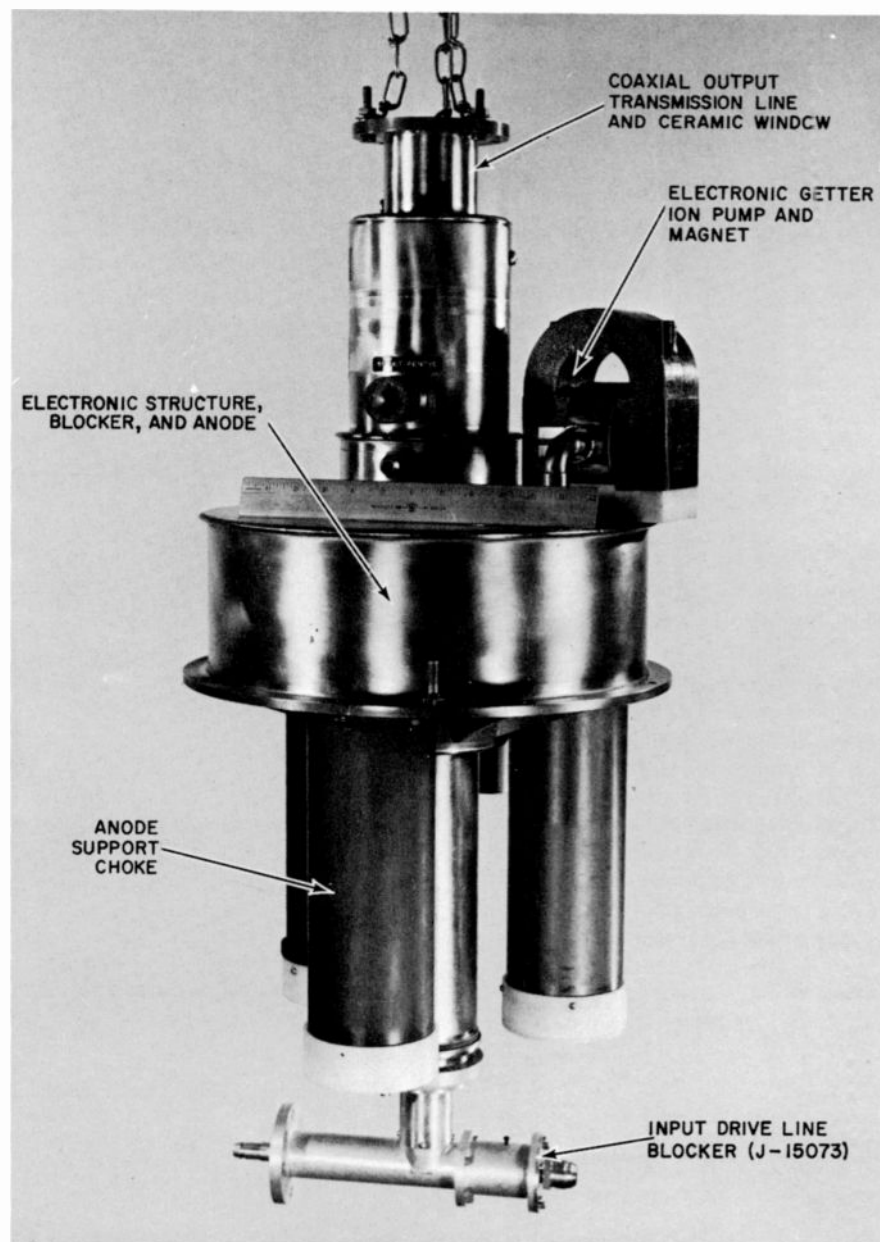


Fig. 1—RCA Dev. No. A15193B Coaxitron.

THE COAXITRON CONCEPT, as developed in the RCA Dev. No. A15193 (Fig. 1), meets the requirements of chirp signals and state-of-the-art, multi-channel, megawatt-level, radar systems. The design requirements are listed in Table I and a simplified longitudinal cross-section is shown in Fig. 2. For ease of discussion, it can be considered as consisting of three basic areas: the triode electron-interaction structure, the output circuit, and the input circuit.

## Triode electron-interaction

Fig. 3 shows the electron-interaction structure of the Coaxitron. It is comprised of a cylindrical array of 48, essentially independent, grounded-grid unit triodes. Each unit triode has a directly-heated, matrix-oxide filament, a double-wound grid, and a high-dissipation anode. A total active cathode area of 150 square centimeters was provided so that the required emission could be obtained with only modest grid-filament RF voltages.

The active filament emitting surface is spaced approximately 0.015 in. from the inner layer of grid wires. For maintenance of this spacing under hot and cold filament conditions, each filament is suspended at one end with a unique pantograph system. These systems take up the expansion of the filament when it is heated to its operating temperature and thus maintain the grid-filament spacing.

The filament cross section is reduced near the support ends. This section is



Authors B. B. Adams (left) and J. A. Eshleman stand alongside a Coaxitron being readied for shipment.

**J. A. Eshleman**  
Product Development  
Industrial Tube Division  
Electronic Components  
Lancaster, Pa.

received the AB in Physics from Franklin & Marshall College in 1961 and is presently pursuing the MS in Physics at the same school. Mr. Eshleman joined the Super Power Tube Design and Development group at RCA, Lancaster in 1957. From 1958 to 1961 he was responsible for the testing of developmental super power tubes and for test equipment maintenance on BMEWS, BTL, and TRADEX. From July 1961 to 1963, as a Product Development Engineer, he established a computer program for the output circuit and RF bypass capacitor design for RCA Dev. No. A-2696A. He also was responsible for the cold probe adjustments on the output circuits and for the evaluation tests. From 1963 to 1966, he was responsible for computer design calculations on the output circuits of RCA developmental coaxitrons. He also made cold probe measurements and computer calculations on coaxitron input circuits. From 1966 to 1967, he was the Project Engineer for the RCA Dev. No. A-15\*91B coaxitron and was responsible for the design calculations and configuration. Mr. Eshleman is presently working on a computer program to calculate electron trajectories in beam type tubes. He is also designing directional couplers

and step transitions for the ORSAY Klystron Application and is doing cavity design work for the RCA Dev. No. A 1401 Klystron. Mr. Eshleman is a member of the Sigma Pi Sigma.

**B. B. Adams**  
Super Power Tube Design Engineering  
Industrial Tube Division  
Electronic Components  
Lancaster, Pa.

received the BSME from Pennsylvania State University and is currently pursuing a course of graduate studies leading to the MS in Engineering. Mr. Adams joined the RCA Electron Tube Division at Lancaster in 1957 as a design and development engineer. He has been instrumental in the mechanical design of RF circuitry, cold probe test gear and special devices utilized in the development of a variety of super power tubes and circuits. He has also provided consultation and engineering support for various Government research and development projects. As Project Engineer, Mr. Adams was responsible for the mechanical design of the RCA Dev. No. A-2696 and A-15193 coaxitrons. He has also been responsible for the design of a variety of high power cavities. He is a licensed professional engineer in the Commonwealth of Pennsylvania, a member of Tau Beta Pi, Pi Tau Sigma and the ASME.

Fig. 4—Broadband output circuit.

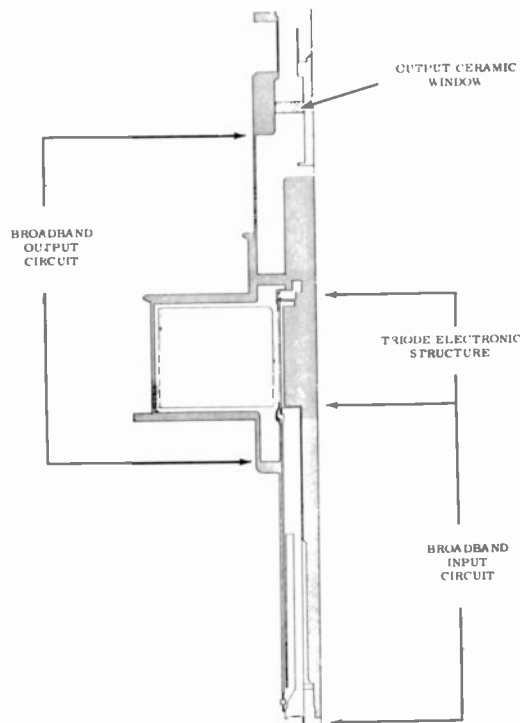


Fig. 2—Simplified longitudinal cross-section of the Coaxitron.

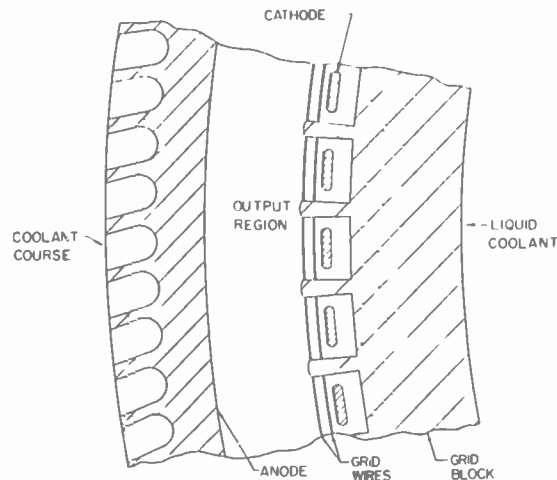
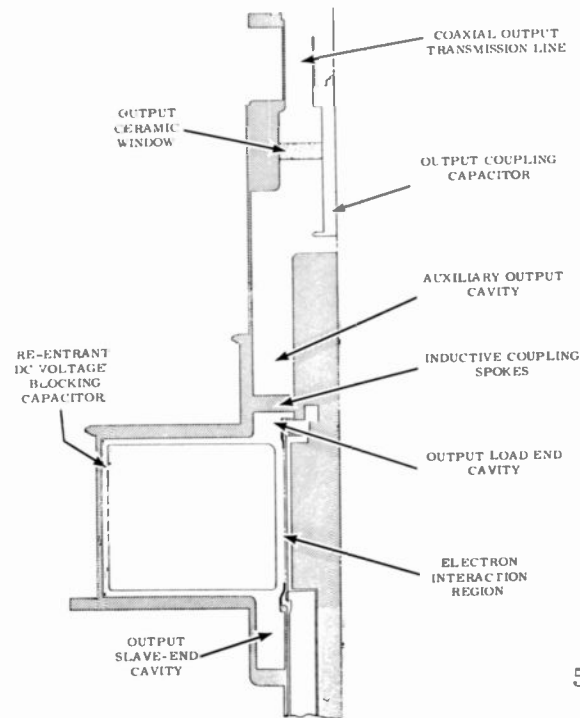


Fig. 3—Triode electronic structure.



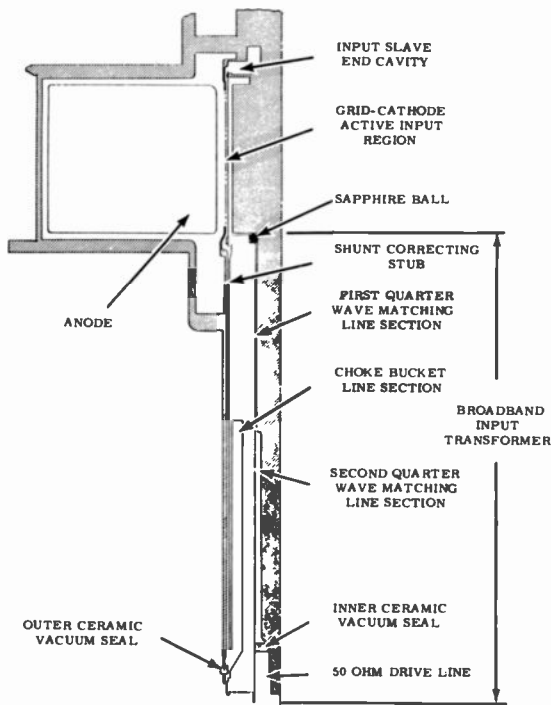


Fig. 5—Broadband input circuit.

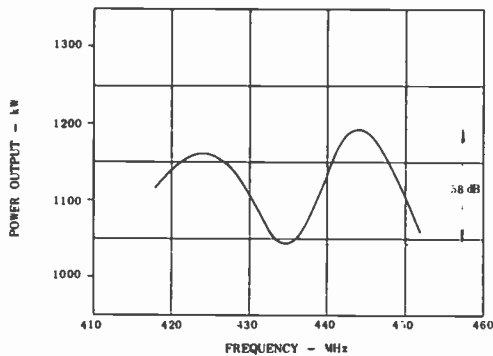


Fig. 6—Power output versus frequency.

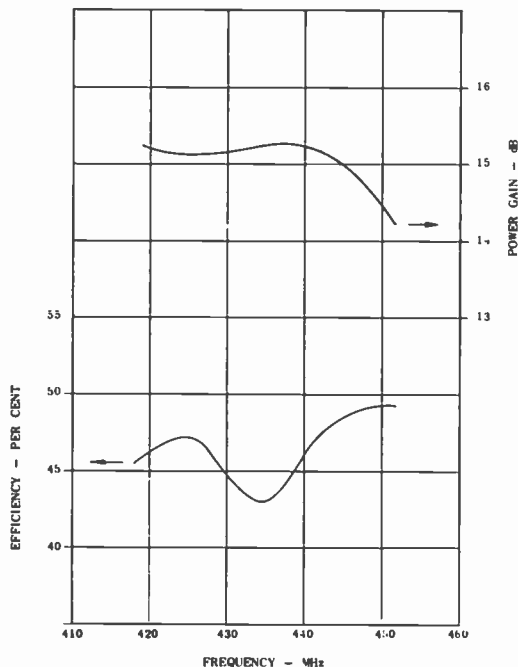


Fig. 7—Efficiency and power gain versus frequency.

called the "filament lead correction"; its purpose is to minimize heat loss to the filament supports and to provide a constant temperature in the active emitting region. The filament temperature in the Coaxitron is maintained within  $\pm 7.5^\circ\text{C}$  over the active 4-in. length.

A double-wound grid of 0.0033-in.-diameter tungsten wire is used in each triode unit for electrostatic isolation of the filament and anode and for class-B tube operation with zero grid bias. This design eliminates the need for neutralization and the need for DC isolation between the grid and cathode.

The tungsten grid wires for each triode unit are supported on OFHC copper lands which extend radially outward from a central cylinder called the "grid cylinder." The grid wires are fastened to these lands by a special notching and peening technique which permits the outer grid wire to be hidden from direct cathode emission by the inner grid wire. Because the grid spans are short and the copper lands form an excellent heat sink for heat generated by grid interception, the design exhibits excellent mechanical stability.

The output of the unit triodes is partially formed by a doughnut-shaped anode. The anode is supported only on one end by three metallic support columns spaced 120 degrees apart. Two of the support columns conduct anode liquid coolant. The flow of coolant through these courses feeds the fluted heat exchanger on the back of the bombarded anode surface. The DC voltage for the anode can be applied by any one of the three support columns.

Because the support columns are metallic, they form coaxial lines which may leak RF energy through the tube envelope. Such leakage is undesirable because it represents wasted energy, presents a potentially dangerous RF environment to operating personnel and increases the potential of RF interference to nearby equipment. Therefore, the RF leakage from each support column is attenuated to acceptable and safe levels by special RF chokes external to the tube envelope (Fig. 1).

#### Output circuit

The output circuit for the RCA Dev. No. A15193B was designed to deliver

an RF power output in excess of 1 megawatt (MW) with a ripple of less than 1 dB over a bandwidth of 34 MHz centered on approximately 435 MHz. Because of the many variants associated with the design, the first prototype design was developed with the use of computer techniques. In this manner, the effect of slight changes in any of the variables was studied very economically. As a result of this approach, a design closely approximating the final tube was derived in a relatively short time.

Fig. 4 shows the basic output circuit used in the Coaxitron. This design has two resonant circuits which are over-coupled through the "inductive coupling spokes." The first resonant circuit comprises the "output slave-end cavity," the "electron-interaction region," the "output load-end cavity," and the "re-entrant DC voltage-blocking capacitor." The second cavity comprises the "auxiliary output cavity" and the area below the large diameter step just below the "output ceramic window." Output coupling to the over-coupled circuits is made through the "output coupling capacitor" into a 50-ohm, 3 $\frac{1}{8}$ -in.-diameter coaxial transmission line. The output ceramic window, like the input seal, is located outside the resonant circuitry; therefore, it is subjected only to the relatively low RF voltage on the output transmission line. This arrangement minimizes arcing and dielectric losses in the window area.

The "re-entrant DC voltage blocking capacitor" is used only as a means of DC isolation of the anode from the tube envelope. With this isolation, a DC anode voltage of 20 kV can be applied without arc-over. Ideally, the RF impedance between the tube envelope and anode is negligible at the output slave-end and load-end cavity. Therefore, the circuit is readily recognized when an RF short is envisioned between the anode and tube envelope at these points.

#### Input circuit

The input circuit of the RCA Dev. No. A15193B transforms the impedance of the 50-ohm, 1 $\frac{5}{8}$ -in. coaxial input transmission line down to the impedance of 0.5 ohm at the driven end of the electron-interaction structure. Despite impedance transformation require-

ments of approximately 100:1 and various complicating factors such as the DC isolation of one end of the filament structure, an input circuit design was derived for the initial RCA Dev. No. A15193B tubes which gave an input vswr of less than 2.5:1 over the 34-MHz band. Computer techniques were again utilized to develop the input circuit design for the first prototype.

Fig. 5 is a simplified drawing of the Coaxitron input circuit. Two quarter-wave coaxial sections are utilized for transformation of the 50-ohm input impedance to the approximate 0.5-ohm impedance at the electron-interaction region. Because of the extremely close spacings required in the first quarter-wave matching line section, small sapphire balls, used as dielectric spacers, maintain the coaxial spacing and alignment.

Since the A15193B was designed for zero-bias class-B operation, it was feasible to connect one end of the filament DC-wise to the grid structure via the "input slave-end cavity." The "input slave-end cavity" was used in this arrangement to provide grid-cathode RF isolation and to insure that an RF voltage antinode would occur approximately in the center of the active input electron interaction region.

Because one end of the filament was connected DC-wise to the grid structure, it was necessary to both DC and RF isolate the opposite end. This function is accomplished with the quarter-wave "choke bucket line section" and the "inner ceramic vacuum seal." The "choke bucket line section" not only inhibits RF leakage at the "outer ceramic vacuum seal" but through a 1:1 transformation via half-wave coaxial section, termed the "shunt correcting stub," it provides a high grid-cathode impedance at the base of the "grid-cathode active input region." The "inner ceramic vacuum seal" serves a dual role as a coaxial input window and as a DC insulator for the "hot" filament terminal.

### Mechanical design

Although an oil dielectric had been used in anode chokes of prior Coaxitron tubes, oil could not be used on the A15193B because of its temperature expansion characteristics and its tendency to develop leaks at the choke

seal. After a series of experimental tests, vacuum-potted Dow Corning Sylgard was selected as a substitute because it featured a high dielectric strength, eliminated trapped air, was semi-flexible, and provided excellent metal bonding characteristics. The chokes so fabricated exhibited excellent reliability.

The massive doughnut-shaped anode with its associated support structure was required to withstand 18, 15-g, 11-ms shock pulses without arc-over, loss of vacuum integrity, or permanent distortion. A support arrangement of three stainless steel pipes, connected as parallel cantilever beams, was selected for the anode after analyses indicated that the structure would withstand the specified environment. The results of these analyses indicated that a maximum anode displacement of 0.016-in. would occur during the shock pulse and that this displacement would not cause arc-over nor a permanent offset in the anode structure. For assurance of vacuum integrity, the support pipes were connected to their respective high-voltage DC ceramic insulators through short OFHC copper strain-isolation rings which provided a resilient, but strong connection.

The weight of an 18-pound ion pump magnet connected externally to the tube presented severe mounting and support problems. Any large relative displacement of the magnet with respect to the associated ion pump during the shock pulse could destroy the ion pump, the pump tubing, and the Coaxitron vacuum integrity. Various magnet support designs were investigated and many proved bulky and impractical. A simple solution was ultimately obtained by use of a magnet bolted directly to the Coaxitron housing through a Delrin plastic pad. This system reduced the relative motion of the pump and magnet to negligible values and thus protected the tube from being damaged by the magnet.

### Test results

The performance of RCA Dev. No. A15193B met or exceeded all the design requirements listed in Table I. Typical operating conditions are listed in Table II. Fig. 6 shows the variation of power output across the frequency band with constant plate voltage; the uniformity of response is approxi-

mately 0.58 dB. Fig. 6 also displays the typical band-pass characteristics of the A15193B.

Fig. 7 shows the efficiency and power gain as a function of frequency. The fall-off of power gain near the upper edge of the operating band is caused by a greater increase in the vswr of the input circuit at the upper band edge than at the lower band edge.

Table I—Design requirements for RCA Dev. No. A15193B.

<i>Electrical</i>	
Frequency	418 to 452 MHz
Pulse width	15 $\mu$ s
Bandwidth	34 MHz
Uniformity of response	1 dB (max)
Power output	1,000 kW (min)
Efficiency	40% (min)
Power gain	13 dB
Input vswr	2.5:1 (max)
Plate voltage	20 kV
<i>Mechanical</i>	
Weight	175 lb. (max)
Length	39 in. (max)
Diameter	17 in. (max)
<i>Environmental</i>	
Temperature	-54 to +55°C
Altitude	15,000 ft.
Shock	15 g at 11 ms (half sine wave)
<i>Vibration</i>	
Frequency	5 to 500 Hz
Amplitude	0.100 in. from 5 to 65 Hz
Acceleration	2 g from 65 to 500 Hz

Table II—Typical operating conditions of RCA Dev. No. 15193B.

Pulse plate voltage	16 kV
Pulse plate current	157 A
Pulse drive power	45 kW
Pulse Power Output	1,070 kW
Efficiency	42.5%
Power gain	13.8 dB
Filament current	800 A (steady state)
Filament voltage	1.38 V (steady state)

### Summary

The RCA Dev. No. A15193B Coaxitron was successfully designed, fabricated, and evaluated for wide-band, high-power operation. This Coaxitron is designed for grounded-grid zero-bias class-B operation and provides a typical power output of 1 MW, a power gain of 13.8 dB, and a conversion efficiency of 42.5%, with a 1-dB instantaneous bandwidth of 34 MHz centered on approximately 435 MHz.

The elimination of moving circuit components and the placement of ceramic windows in low-voltage fields combine with the use of welded and brazed joints to reduce the tube-circuit weight, improve tube capability for withstanding relatively severe environmental conditions, substantially reduce maintenance problems, and increase tube reliability.

# Noble-gas-ion lasers

R. J. Buzzard | J. A. Powell | J. T. Mark | H. E. Medsger

RCA has been manufacturing noble-gas-ion lasers as a commercial product since early in 1967 when a 100-mW argon-ion laser was first designed by K. G. Hernqvist.<sup>1</sup> Since then, the line of commercially available ion lasers has expanded to seven types ranging in rated output power from 10mW to 10W and utilizing such inert gases as argon, krypton, and neon. The product line includes both pulsed and continuous-wave types and covers the visible, ultra-violet and infrared portions of the spectrum. This paper describes the major design features and performance of noble-gas-ion lasers.

## J. A. Powell

Heat Transfer Engineering  
Industrial Tube Division

Electronic Components, Lancaster, Pa.

received the BS in Ceramic Engineering from N.Y.S. College of Ceramics, Alfred University. He joined RCA Lancaster in 1955 as a Product Development Engineer in the Small Power Tube Design section where he worked on the development of small ceramic vacuum tubes. In 1957, he was assigned to a special project team developing bakeable ceramics, sapphire, and glass-to-metal seals for use in a large, ultra-high vacuum chamber designed specifically for the military. From 1961 to 1965, Mr. Powell was assigned to the Vacuum Engineering Group and engaged in the design and development of ceramic-to-metal and glass-to-metal feedthroughs including a complete product line of bakeable sapphire and fused-silica windows for ultra-high vacuum applications. Since 1967, Mr. Powell has been responsible for laser-tube design at Lancaster. Before joining RCA, Mr. Powell was with the General Electric Company and with the Star Porcelain Company for two years each and the Frenchtown Porcelain Company for five years as a Research and Development Engineer working in the field of ceramics engineering. Mr. Powell has been granted one patent in the field of ceramics and has authored several papers on the subject. He is a member of the American Ceramic Society and the American Society of Metals.

## H. E. Medsger, Supt.

Manufacturing Dept. 953  
Industrial Tube Division

Electronic Components, Lancaster, Pa.

joined RCA in 1958 as an associate design and development engineer with twenty-two years of diversified product design and manufacturing engineering experience. He had been associated with the Glenn L. Martin Co., as manufacturing engineer; IBM as assistant project engineer on computer mechanisms; General Electric TV Division as a manufacturing engineering leader; and P. G. Spaulding and Associates as executive engineer. Since joining RCA he has been engaged in the design development and fabrication of Super Power Tube evaluation equipment, manufacturing

equipment, and product design. He was responsible for the design of several large space chambers. He was also responsible for the mechanical design of a 5-MW peak, 300-kW average power cavity for the RCA 2054 family of Super Power Tube and complex air and high purity water systems. As engineering leader of the Super Power Tube Vacuum Group, he was responsible for the mechanical design and development and the initial production of the LD2100, 100-mW argon gas laser and the LD2101 1-W argon gas laser. Prior to his present position, he was Manager of Production Engineering, Super Power Tube ITD. Mr. Medsger has completed mechanical engineering courses at Syracuse University and Penn State University and industrial design at Maryland Institute and Johns Hopkins University. He is a member of ASTME and is past chairman of the Lancaster Chapter #89 ASTME.

## J. T. Mark, Mgr.

Regular Power Tube Engineering  
Industrial Tube Division

Electronic Components, Lancaster, Pa.

received the BS in Radio Engineering from Valparaiso Technical Institute in 1950 and joined RCA Lancaster the same year. Since 1950, he has done graduate work in physics and has had extensive experience in the design, fabrication, and testing of ultra-high vacuum equipment and systems, megawatt electro-mechanical devices, megawatt vacuum tubes and gas lasers. Mr. Mark was assigned initially to the design and development of black and white and color kinescope tubes. Upon transfer to the Super-Power Tube Engineering Department, he became responsible for the design and fabrication of one of the first multimewatt test equipments at the Lancaster plant. He also designed and developed new electron guns for super-power microwave tubes. Assigned as Project Engineer on the Matterhorn Project in 1958, Mr. Mark was responsible for the overall direction and control of the design and development of the ultra-high ( $10^{-10}$  Torr) vacuum system for the C-Stellarator research facility. Later, he directed the design of several large vacuum systems. Promoted to Engineering Leader in 1961, Mr. Mark was responsible for the conception, design, and development of sophisticated components and systems

for use in ultra-high vacuum applications and laser applications. He has been granted eight patents and has two additional patents pending in electron tube design, lasers, and vacuum technology. He has presented and published numerous papers. He is a member of the AVS committee on standards, IEEE, IVOST, ASLE, IES, and the ASTM Committee E-21 for standards in the aerospace industry.

## R. J. Buzzard, Ldr.

Heat Transfer Devices Engineering  
Industrial Tube Division

Electronic Components, Lancaster, Pa.

received the AB in physics from Franklin and Marshall College in 1962. He joined RCA in 1953 in the Large Power and Gas Tube Laboratory. Upon completing his undergraduate work, Mr. Buzzard was reassigned as an engineer in the Thermionic Converter Engineering Group where he participated in the successful development of RCA's initial nuclear-fueled converter. In a continuation of this effort, he developed the basic computer programs required to solve the thermal and electrical design problems for high power converters and their associated components. Since 1963, he has extended this computer approach to a comprehensive equation which analyzes the design for all the various parameters. Mr. Buzzard was engaged in RCA's original investigations in power conditioning associated with thermionic converters. He participated in the development of tunnel diode inverters and their evaluation in circuits employing thermionic converters. Mr. Buzzard was promoted to Engineering Leader in 1965. During 1965 and 1966, he provided the technical direction for the NASA Isotope-Thermionic Development Program. Currently, Mr. Buzzard is directing the development of a number of special power devices; these include heat pipes, alkali metal vapor arc lamps, and high-power gas lasers. Mr. Buzzard has co-authored several technical papers on Thermionic Conversion Devices.



In the photo (left to right) Powell, Mark, Medsger, and Buzzard are seated behind some of the Lancaster-produced lasers.

THE BASIC COMPONENTS of a DC-excited gas laser are the discharge tube, a stable optical resonator, and the DC power supply. Fig. 1 shows a cross-sectional diagram of a typical gas laser. The discharge tube contains a cathode, an anode, and a long plasma-confining bore structure. The plasma bore is the region in which the coherent light is generated. The bore can be formed from either a uniform insulator tubing, or a series of short tubing sections uniformly spaced and insulated from one another. The discharge tube is filled with the noble gas at the proper pres-

sure (typical in the order of 0.1 torr). Energy is supplied to the plasma by a discharge current between the cathode and anode. The optical resonator consists of two mirrors, one totally reflective and the other partially reflective, placed at opposite ends of the discharge tube. When this optical cavity is properly adjusted with respect to the discharge tube, "lasing" takes place as the emitted light energy is coupled out through the partially reflective mirror. A magnetic field is usually provided around the discharge tube to improve the power output.

### Design considerations

The five major components that affect the performance of noble gas ion lasers are: the bore structure, the optical cavity, the envelope, the electrode structure, and the power supply.

#### Graphite bore structure

RCA continuous-wave ion lasers utilize a segmented graphic bore structure<sup>2</sup>, of the type shown in Fig. 2. This bore structure was chosen because it exhibits a minimum of sputtering and bore erosion. Fig. 3 is a photograph of an individual bore disc which is composed of high-purity, isostatically pressed graphite. The material was chosen after extensive testing and comparison with other possible bore materials. The outer diameter of the graphite discs is determined by the input power level of the laser. The center bore hole in each disc is between 1 and 4 mm in diameter. The exact bore diameter is determined by optical considerations. The length of the bore determines the total gain of the laser and the total light output.

#### Optical cavity

The optical cavity consists of two dielectric-coated mirrors mounted in a stabilized tuning mechanism. The orientation, reflectivity, and geometry of the mirror all affect the performance of the laser. The mirrors are, in most cases, curved and arranged as shown in Fig. 4. The condition for resonant stability of a laser is  $0 < g_1 g_2 < 1$  for  $g_1 = (1 - d/R_1)$  and  $g_2 = (1 - d/R_2)$  where  $d$  the distance between the mirrors, and  $R_1$  and  $R_2$  are the radii of the respective mirrors.

Many laser applications require the output beam of the laser to have a

Gaussian distribution of intensity across the beam diameter. A Gaussian distribution requires that the laser operate in the fundamental transverse mode ( $TEM_{00}$ ). Mode selection is accomplished by the proper choice of mirror radii and the bore diameter or aperture in the optical resonator. Figs. 5 and 6 show the diffraction losses for the two lowest-order ( $TEM_{00}$ ,  $TEM_{01}$ ) modes of a stable resonator using a pair of identical mirrors.<sup>3</sup> The correct combination of mirrors and bore diameter at these low-order modes will result in substantial losses in light output when the laser is operated at higher-order modes; i.e., the higher-order modes are attenuated and do not appear in the laser output.

#### Discharge-tube envelope

The discharge-tube envelope is made of fused silica (quartz), which has many desirable properties for this application. The material is capable of containing the graphite bore segments at temperatures as high as 1000°C. In addition, the infrared-transmission properties of fused silica allow the heat from the graphite segments to be radiated to an external heat acceptor with a minimum of absorption. The continuous-wave lasers generally have quartz windows fused permanently to the tube structure to provide a completely vacuum-tight, bakeable structure. The windows are placed at Brewster's angle with respect to the incident light beam to minimize losses caused by reflections at the window surfaces.

#### Electrodes

The cathode material is also very important because it must have good electrically emissive properties, withstand high ion bombardment, and be resistant to gas impurities that may be evolved from other tube components during discharge operation. In the high-power-laser discharge tubes, a barium-impregnated tungsten-matrix cathode is used. Emission life in excess of 10,000 hrs can generally be expected from this type of cathode when used in the laser environment.

Because the anode material has little effect on laser performance, it is generally made of the same material as the bore segments and made simply an extension of the graphite structure.

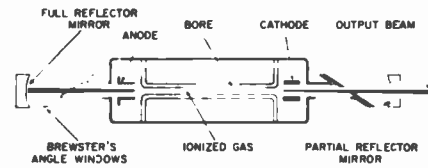


Fig. 1—Typical gas laser.

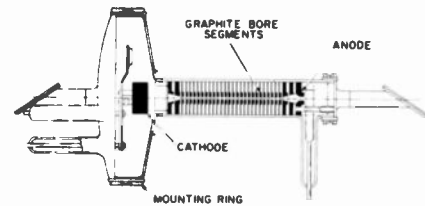


Fig. 2—The RCA-LD2110 10-mW Argon laser tube.

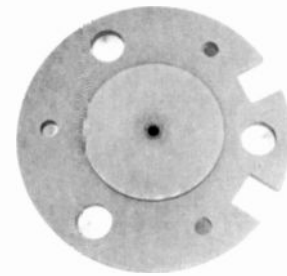


Fig. 3—Graphite bore segment.

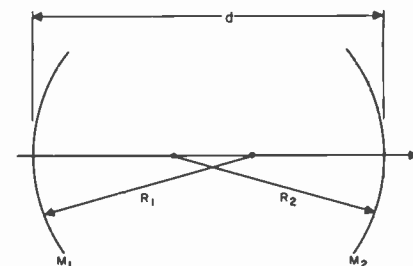


Fig. 4—Spherical mirror resonator.

#### Ballast tank

During the operation of the discharge tube, small amounts of gas are gradually lost as a result of sputter pumping. The phenomenon is referred to as "gas clean-up" and results when atoms sputtered from the bore confinement structure "bury" gas atoms on cooler surfaces. Although the sputtering and the resulting gas clean-up are minimal in a well-processed graphite-bore discharge tube, provisions must be made for extra gas storage. Consequently, a gas ballast tank is provided in one of the configurations shown in

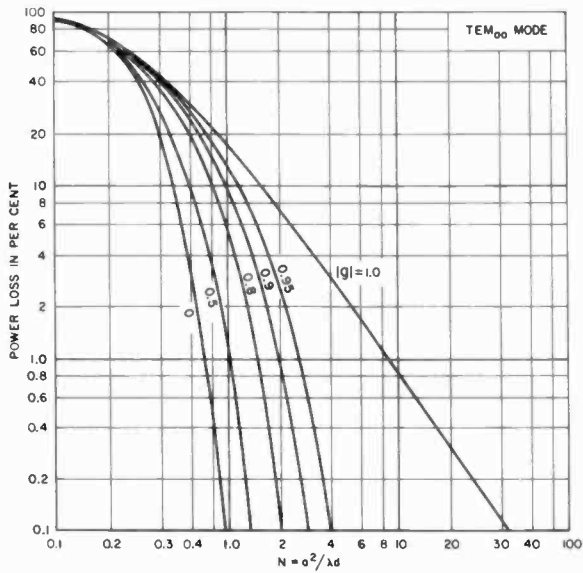


Fig. 5—Power loss per transit of the fundamental (TEM<sub>00</sub>) mode for circular mirrors.

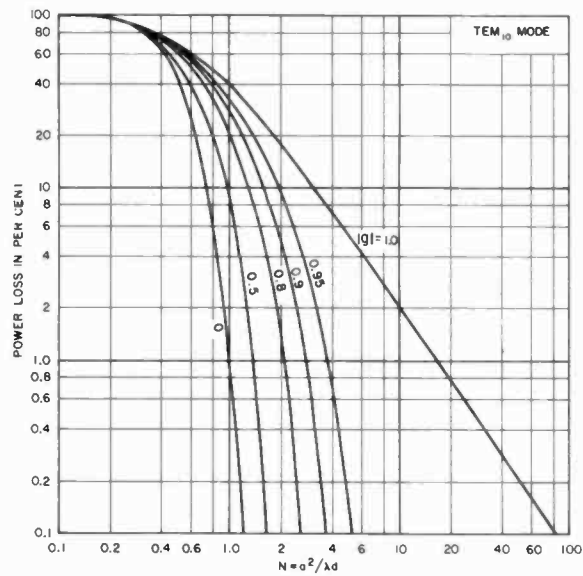


Fig. 6—Power loss per transit of the TEM<sub>10</sub> mode for circular mirrors.

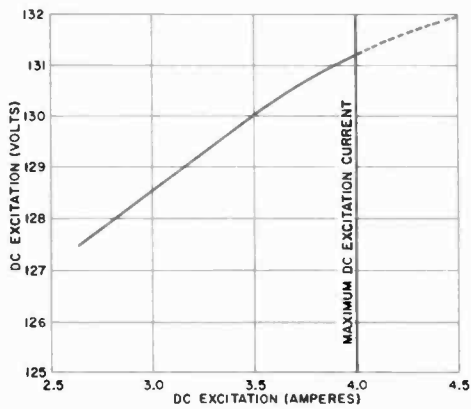


Fig. 8—Typical excitation characteristics.

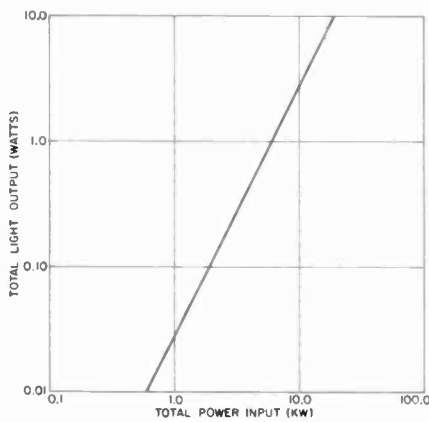


Fig. 9—Light output versus power input for Argon-ion lasers.

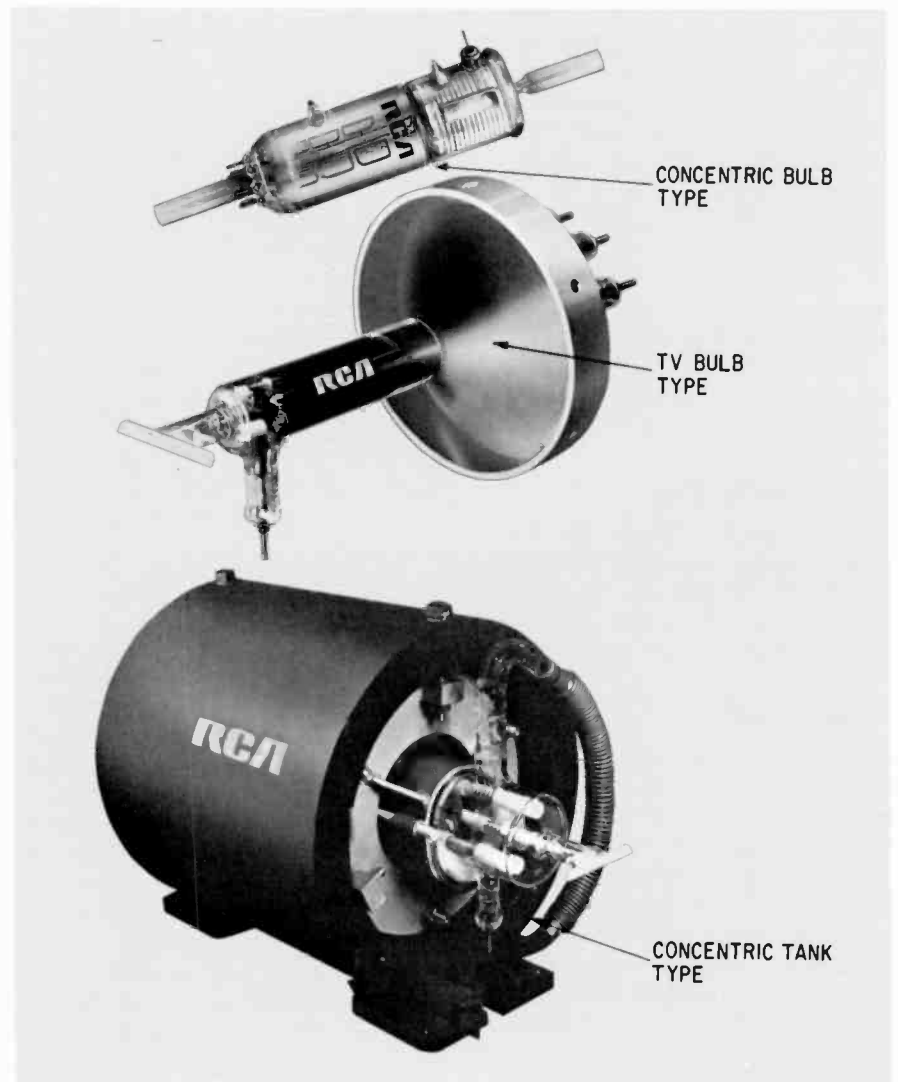


Fig. 7—Ballast tank configuration.



Fig. 10—Mirror mount.



Fig. 11—Some of the Argon-ion lasers produced at Lancaster (the size relationships are not accurate).

Fig. 7. The type of ballast tank employed depends upon the magnitude of the discharge current and the intended duration of operation. Most tubes with gas reservoirs have an operating life of up to 10,000 hrs.

#### Power supply

The noble-gas ion lasers typically operate at current levels between 3 and 30 A and with tube voltage drops of 100 to 300 volts. Fig. 8 shows the voltage-current relationship for a typical optimized laser. Because the stability and noise on the laser beam varies greatly with slight fluctuations in the discharge current, the power supplies must be designed to have current regulation to within 0.1%.

At the higher power and discharge current levels, a significant improvement in power output and efficiency

can be achieved through the use of an axial magnetic field, which helps to confine the plasma within the bore structure and also reduces sputtering and bore erosion. The field is supplied either by an array of periodic permanent magnets or by an electrically powered solenoid. The requirements for the field range from a few hundred gauss for argon lasers of moderate power operating in the visible portion of the spectrum to more than 1000 gauss for ultra-violet output from krypton or neon.

#### Heat dissipation

Most of the electrical energy supplied to the laser discharge tube is transformed into heat which must be removed from the system. Fig. 9 shows a plot of the output power as a function of total input power for several argon-ion lasers. The difference in power in the form of heat is distributed along the bore structure, causing incandescence of the graphite segments. This heat is removed by radiation through the quartz envelope of the discharge tube to a heat acceptor. Two forms of heat acceptors are currently in use. When the input power to the laser is less than 2000 watts an air-cooled heat acceptor is used. When greater input power levels are required, a water-cooling jacket is used.

#### Mechanical stability

Because precise alignment is important for proper operation of the laser, the entire laser structure, including the discharge tube and the mirrors forming the resonant cavity must be held rigidly in place. This stability requires the use of rugged cast aluminum mounting structures. The mirror mounts must be particularly stable and yet be capable of precise adjustment to tune the cavity. A typical mirror mounts is shown in Fig. 10.

#### Commercially available lasers

RCA is currently manufacturing noble gas ion laser types. Table I lists the important performance characteristics of each type. Photographs of some units are shown in Fig. 11.

#### References

- Hernqvist, K. G., "Argon Lasers." RCA Reprint RE-15-1-17
- Hernqvist, K. G. & Fendley, J. R. Jr., "Construction of Long Life Argon Lasers," *J. of Quantum Electronics*, Vol. QE-3, No. 2 (Feb 1967).
- Kozelnik, H., and Li, T., "Laser Beams and Resonators" *J. of Applied Optics*, Vol. 5 (Oct '66) p. 50.

Table I—Performance characteristics of RCA lasers

Type No.	Gas	Typical power	Major wavelengths (angstroms)
LD2108	Argon	10 mW	4880 blue-green 5145 green
LD2111	Neon	50 mW	3224 Ultra-violet
LD2100	Argon	200 mW	4765 blue 4880 blue-green 5145 green
LD2127	Krypton	400 mW	3507 Ultra-violet 4762 blue 5208 green 5682 yellow 6471 red
LD2101	Argon	2 W	4765 blue 4880 blue-green 5145 green
LD2122	Argon	10 W	4880 blue-green 5145 green
LD2125	Argon	50 mW (pulsed)	4880 blue-green 5145 green

# Design of Cermolox tubes for single-sideband

A. Bazarian

Since the conception and design of Cermolox tubes by the design engineering group led by M. B. Shrader at Lancaster in 1956, a large family of tubes has been developed. These tubes cover the frequency spectrum from audio through UHF, and have useful power outputs ranging from a few tens of watts to greater than 15,000 watts. In general, the Cermolox design has provided the flexibility needed for design modifications for many and diverse requirements. This paper investigates some basic problems in the linear tube development and discusses the methods used in the design of these tubes.

CERMOLOX TUBES have performed in a wide variety of applications from communications to radar and counter-measures equipment. In addition, they have been used in applications which required stringent mechanical stability such as vehicular, aircraft, and shipboard equipment. The demands upon the available RF spectrum, particularly by the military, have necessitated greater use of single-sideband (SSB) transmission. The high order of frequency stability (stressed by I. P. Magasiny in Ref. 1) and the reduced spectrum requirements of SSB permit the assignment of a large number of channels to the same radio spectrum. Cermolox construction in a ribbon beam formation, without side-rod and lateral wire obstructions by the control grid and screen grid, provides the essential features for the linear tubes with the lowest intermodulation distortion (IMD). Present work is concentrated on tubes having 500 W (8791) and 1200 W (8792) of useful power at HF and UHF bands.

The single-sideband amplifier must not generate distortion levels above a specified maximum. With nonlinear distortion in the final amplifier, 3rd, 5th, 7th and possibly higher orders of intermodulation distortion (IMD) products will fall within or near the desired sideband. Spectrum crowding requires IMD products to be reduced to  $-45\text{dB}$  for 3rd, and  $-50\text{dB}$  for 5th corresponding to 0.5 and 0.3 percent, respectively, of a fundamental tone of a two-tone test.<sup>2</sup>

## Theoretical transfer curves

A completely linear tetrode may be characterized as having constant plate-

current curves which are parallel and equidistant for equal increments of grid bias. An operating line, as shown in Fig. 1a, would be established on these curves by the specification of  $E_c$ ,  $E_{c1}$ ,  $I_p$ ,  $P_o$ , and  $R_p$ . The resulting transfer characteristic would be the straight line as shown in Fig. 1b. Furthermore, for a high power-output efficiency, the "knee voltage" would be a small fraction of the screen voltage. It will be shown that if this tube is operated with the bias at cutoff (Class B), the resulting IMD will be negligible. Class A operation will also provide negligible distortion. Class AB operation, contrary to normal expectation, does result in considerable levels of IMD.

Other idealized transfer curves have been studied. These curves include quadratic,  $3/2$  power, and combinations of curves consisting of a linear upper part and various curvatures of the lower part. Results from these curves provide some insight as to how an actual tube should be designed and how it should be operated to yield the minimum distortion level.

## Computer analysis of the transfer characteristic

When a signal with varying amplitude such as that generated by a two-tone test in the RF spectrum is amplified by a nonlinear tube, many new frequencies are generated. The frequency and amplitude of the IMD components which lie within the fundamental bandpass region of the tuned circuits may be determined mathematically with representation of the transfer curve by a finite series of Tchebycheff polynomials, expanded about a zero signal operating point:

$$I_b = C_0 + C_1 T_1 + C_2 T_2(e) + \dots + C_n T_n(e) \quad (1)$$



Albert Bazarian  
Power Tube Development  
Industrial Tube Division  
Electronic Components

received the BA in Physics from New York University and the MS in Physics from the University of Pennsylvania in 1951. He has completed 30 credits of post-graduate studies majoring in gaseous electronics. His early experience was in mass-spectrometer tubes and infrared devices at the Franklin Institute Laboratories. From 1952 to 1957 he was at Chatham Electronics working on basic studies in gaseous discharge and development of gas discharge tubes. In 1957, he joined the Red Bank Division of the Bendix Corporation as a design engineer. In 1960, he was promoted to Senior Engineer in charge of gas and receiving tube development engineering. His experience at Bendix included development of gas-discharge microwave noise standards, spark gaps, gas lasers, high-energy xenon flash tubes, and special-purpose receiving tubes. He has received six technical patents in counting tubes, storage tubes, microwave noise standards, and high-energy transfer spark gaps. In 1965, he joined the RCA power tube design group in Lancaster as a product development engineer. He is responsible for power tube development programs. Mr. Bazarian is a member of IEEE and Sigma Pi Sigma.

where  $I_b$  is the peak plate current and  $T_n(e)$  is an  $n^{\text{th}}$  order Tchebycheff polynomial.

If a two-tone signal such as:

$$E = A(\cos \alpha + \cos \beta) \quad (2)$$

is applied to the grid, it may be shown with evaluation of Tchebycheff polynomials that the resulting plate current  $I_b$  is given by

### Nomenclature

$E_{bb}$	DC plate supply voltage
$E_b$	DC plate voltage
$E_{c1}$	control-grid bias voltage
$E_c$	control-grid bias voltage referenced to cut-off
$I_p$	peak fundamental component of the plate swing
$P_o$	output power
$R_p$	effective plate load resistance
$E_{c2}$	DC screen-grid voltage
$E_d$	peak control-grid drive signal
$E_{c0}$	cut-off voltage
$I_{b0}$	zero signal plate current
$I_b$	average plate current
$E_p$	peak AC component of plate swing

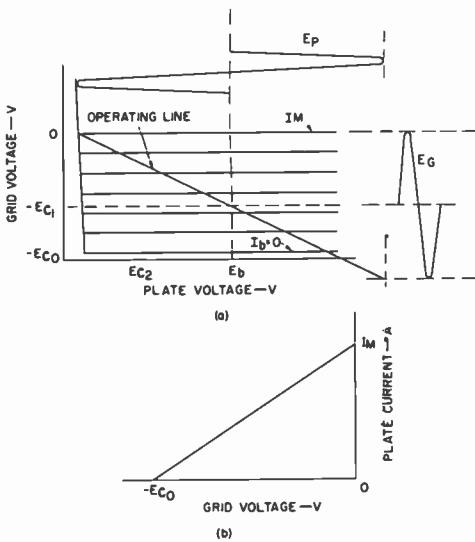


Fig. 1—Characteristics of an ideal linear tetrode: a) plate current curves; b) dynamic transfer curve obtained from the operating line for class AB<sub>1</sub>.

$$I_b = I_0 + I_1(\cos \alpha + \cos \beta) + \dots + I_2(\cos 2\alpha + \cos 2\beta) + \dots + I_{12}[\cos(2\alpha - \beta) + \cos(2\beta - \alpha)] + \dots + I_{23}[\cos(3\alpha - 2\beta) + \cos(3\beta - 2\alpha)] + \dots + I_{31}[\cos(4\alpha - 3\beta) + \cos(4\beta - 3\alpha)] + \dots + \dots \quad (3)$$

where the coefficients  $I_n, I_1, I_{12}, \dots$  are polynomials with coefficients  $C_n, C_1, C_2, \dots$  of Eq. 1. The various orders of distortion products are defined as follows:

$$\begin{aligned} 3rd \text{ order: } dB &= 20 \log (I_1/I_{12}) \\ 5th \text{ order: } dB &= 20 \log (I_1/I_{23}) \\ 7th \text{ order: } dB &= 20 \log (I_1/I_{31}) \\ nth \text{ order: } dB &= 20 \log (I_1/I_{jk}) \end{aligned} \quad (4)$$

where  $n$  is an odd integer and  $jk$  is a two digit integer with  $j = (n - 1)/2$  and  $k = (n + 1)/2$ . This analytical method<sup>3</sup> provides the basis for a distortion analysis of theoretical as well as actual transfer curves. In addition, with the study of the distortion of various transfer curves, a technique is obtained for predicting the design of actual tube transfer curves and for locating the grid bias on the curve for minimum distortion. This method is programmed to allow a rapid determination of IMD. For a given set of input data, coefficients of the Tchebysheff expansion are computed (the  $C$ 's of Eq. 1), and then various coefficients of intermodulation frequencies of Eq. 3 are evaluated. IMD products are calculated from Eq. 4 by using these coefficients.

In general, when actual tubes are analyzed, measurements of  $I_b$  are made at points along the operating line at equal intervals of  $E_c$  and  $E_b$ . These readings are supplied as input data to the com-

puter and a least-square fit method is used to calculate a polynomial approximation of the transfer curve from the coordinates. The polynomial is then used to obtain the expansion points for the Tchebysheff analysis. Tubes have been analyzed in this manner and it was found that, generally, distortion will increase with drive signal and will decrease as grid bias moves toward Class A.

The 3<sup>rd</sup> and 5<sup>th</sup> IMD for a typical tube are shown in Fig. 2. The bias is  $-36.5$  volts and the signal amplitude ranges from 18.3 volts to 36.5 volts peak. The tube output power is also computed and is plotted for the corresponding amplitudes of drive signal.

### Analysis of ideal transfer curves

Linear, quadratic, and three-halves power idealized transfer curves have been computed as shown in Fig. 3. In addition, a family of idealized transfer curves consisting of an upper linear portion and a lower curved portion which ranges in curvature from a 3.0 power (cubic) to 1.2 power have been studied. These curves range from remote cutoff to rather sharp cutoff tubes, as shown in Fig. 4.

The results of the linear transfer curve of Fig. 3 are shown in Fig. 5. The very low distortion at  $-31.3$  volts and  $-62.6$  volts bias is representative of Class-A and Class-B operation, respectively. At bias levels of  $-40.7$  volts and  $-50.1$  volts (Class AB<sub>1</sub>), the distortion amplitude increases rapidly as the signal amplitude exceeds the cutoff voltage. The computer was programmed to scan the bias from cutoff to one-half the bias voltage and, for each bias voltage, to scan the grid-drive signal from the full bias amplitude to one-half amplitude.

The quadratic transfer curve of Fig. 3 was analyzed and the results are shown in Fig. 6. The slope of the quadratic was continuous at the point of intersection with the grid bias axis. It is noted that at Class-B operation, the distortion is high for all levels of grid signal. As the operation moves toward Class A, the distortion decreases and is less for low amplitude signals.

The third and fifth-order distortion products for the 3/2-power curve of Fig. 3 are shown in Fig. 7. It was found that for the higher ratios ( $E_o/E_c > 4$

to 5) the data points of  $E_o/E_c$  for various  $E_o$  did overlay each other very closely. For lower values of  $E_o/E_c$ , however, the location of the cusps shifted for a scan of  $E_o$  at various bias levels. The minimum distortion level and the number of cusps, however, always remained the same.

For the 3/2-power curve, Class-A operation ( $E_o/E_c$  approximately equal to 1) would yield low distortion. Otherwise the cusps for the 3<sup>rd</sup> and 5<sup>th</sup> orders do not provide any other convenient low distortion operating point. In addition, 5<sup>th</sup>-order distortion for this curve, as for all others, is generally lower than the 3<sup>rd</sup> except in the regions of the cusps where a reversal does occur.

The distortion curves for the 1.2, 1.6, and 3.0-power curves of Fig. 4 are shown in Figs. 8, 9, and 10. Although these transfer curves consist of a curved and linear portion, the resulting distortion curves are similar to the 3/2 distortion results. The 3.0-power curve does not exhibit any cusps for  $E_o/E_c \leq 10$ . For this curve, the most linear operation would occur for Class A where  $E_o/E_c$  is less than 0.6.

For low-distortion operation, the results of the 2.0-power linear curve of Fig. 11 are promising. For a particular bias in Fig. 11, the cusps for the 3<sup>rd</sup> and 5<sup>th</sup> do occur at the same ratio for  $E_o/E_c$ . It may be inferred from curve symmetry that the cusps for 7<sup>th</sup>, 9<sup>th</sup> and higher orders will likewise occur at the same value for  $E_o/E_c$ . This curve is discussed by Pappenfuss<sup>1</sup>, and, as pointed out in this reference, if the bias point is chosen to be at or near the projected intercept of the linear segment on the

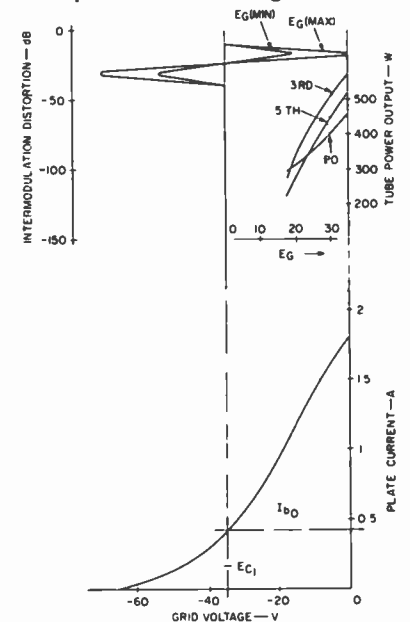


Fig. 2—Typical tube transfer curve analyzed by the Cleary 12-point system.

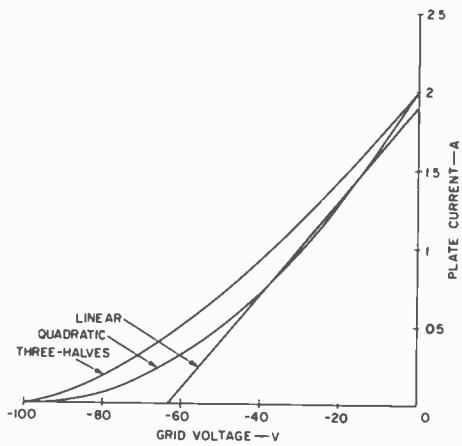


Fig. 3—Linear, quadratic, and three-halves power theoretical transfer curves.

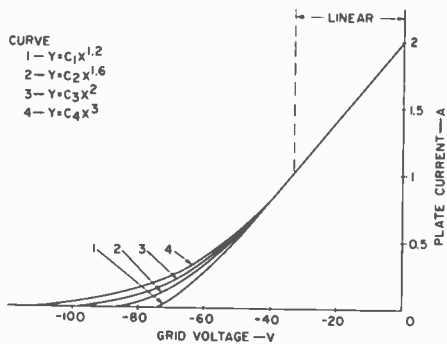


Fig. 4—Theoretical transfer curves consisting of upper linear portion and various lower curved portions, including curvatures of 1.2, 1.6, 2.0, and 3.0 powers.

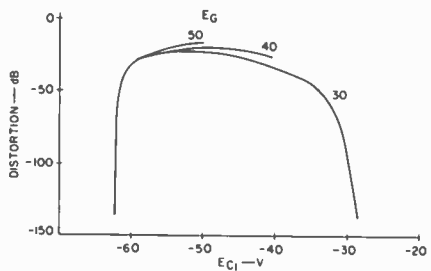
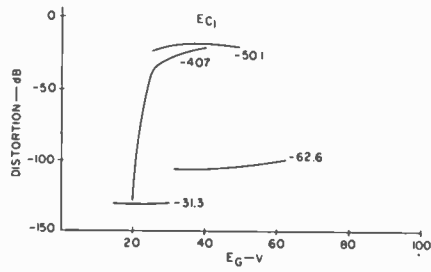


Fig. 5—Third-order distortion for the linear transfer curve of Fig. 3: a) distortion as a function of grid drive; b) distortion as a function of grid bias.

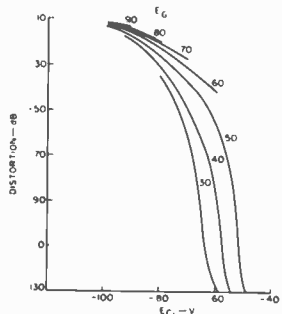


Fig. 6—Third-order distortion for the quadratic transfer curve of Fig. 3.

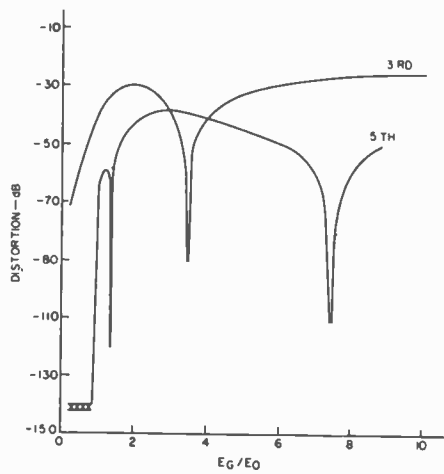


Fig. 7—Third and fifth-order distortion products for the three-halves power curve of Fig. 3.

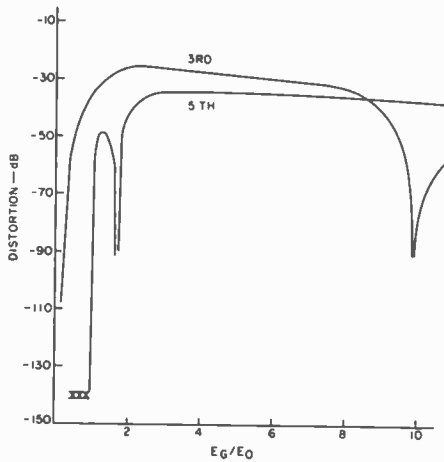


Fig. 8—Third and fifth-order distortion products for the 1.2 power curve of Fig. 4.

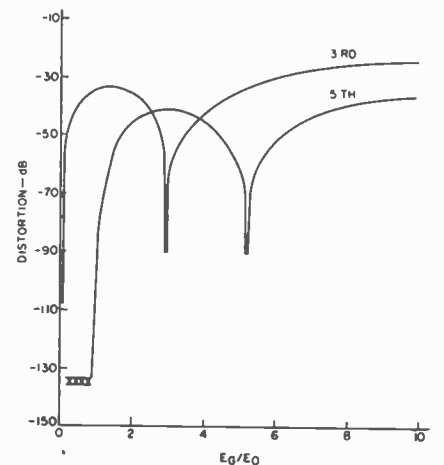


Fig. 9—Third and fifth-order distortion products for the 1.6 power curve of Fig. 4.

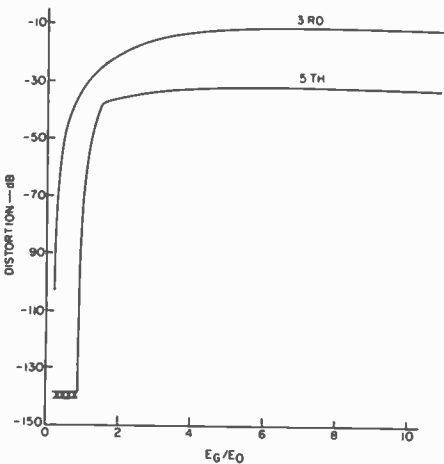


Fig. 10—Third and fifth-order distortion products for the 3.0 power curve of Fig. 4.

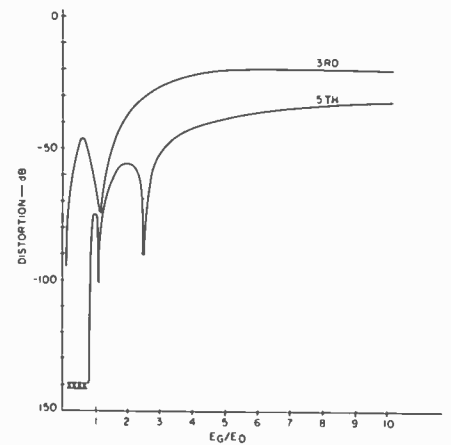


Fig. 11—Third and fifth-order distortion products for the 2.0 power curve of Fig. 4.

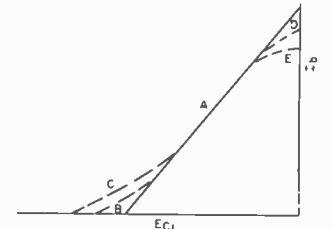


Fig. 12—Causes of curvature of the transfer curve: a) ideal case; b) velocity distribution of emitted electrons; c) non-uniform electric field at the cathode; d) space charge; e) current division between anode and screen grid.

grid-bias axis, then the resulting IMD products will be very low. In terms of an ideal tube, the most desirable transfer curve would consist of a linear segment with a sharp slope for high  $g_m$  and with a zero bias current of sufficient magnitude to provide the required output power. The lower quadratic portion would comprise only a fraction of the total curve length, thereby insuring a low idling current and high tube output efficiency.

### Correlation

Separate computer programs have been written such that upon specification of the  $E_b$ ,  $E_{c1}$ ,  $E_g$ ,  $P_o$ , and  $R_p$ , for a particular tube, the  $E_c$  and  $E_b$  values for the dynamic operating curve for the Tchebycheff expansion points are printed out. The transfer curve corresponding to these points is obtained by measurement, and the curve is analyzed for distortion. For a 12-point analysis, the random errors in measurement of the current may cause a large variation in the computed value of distortion products. If the transfer curve is well defined by a large number of readings and by utilization of the least-square-fit technique, the correlation between measured and computed results is considerably improved. The reading error for both  $I_b$  and  $E_{c1}$  have been reduced by use of electronically regulated power supplies. With the use of Tektronix Type -Z amplifier

for recording  $E_r$  and with a 1% precision current transformer for  $I_b$ , agreement between measured and computed values for both 3<sup>rd</sup> and 5<sup>th</sup> IMD has been found to be within 2 to 3 dB,

### Tube design

The design of a tube having low distortion products is based on understanding of the causes of nonlinearity of the transfer characteristics. Whenever curvatures of the transfer characteristic occur, the input power is distorted in the output circuit. The characteristic features<sup>8,9</sup> of actual tubes which preclude the construction of an idealized tube are as follows:

- 1) Electrons are emitted from the cathode with velocity and angular distributions which lead to a distortion curvature of the transfer curve as shown in Fig. 12, curve b.
- 2) The field at the cathode is generally not uniform. Because of the direct alignment of control-grid and screen-grid wires, the effective emitting area at the cathode changes as the electric field is varied with the grid signal. The resulting distortion curvature is shown in curve c.
- 3) Space-charge formation at relatively high plate currents reduces the effective electric field at the cathode and may cause distortion as shown in curve d.
- 4) A change in the ratio of screen-grid to anode current with a change in anode current produces distortion curvature similar to curve e. The change in this ratio may be due to the following causes:
  - a) When the anode potential swings below the screen-grid voltage, many of the electrons deflected by the control-grid wires cannot reach the anode and therefore return to the screen grid.
  - b) Tubes with aligned control-grid and screen-grid wires may show a variation in the number of electrons intercepted by the screen grid as a result of changes in focusing with changes in plate current.<sup>7</sup>
  - c) The effect of secondary emission at the screen grid is appreciable and may contribute currents greater than the intercepted portion of the primary beam.

An experimental procedure devised to study the parameters interfering with the tube design has provided some progress toward the desired tube linearity. This procedure includes systematic investigation of the anode design, focusing cathodes, and design of the control-grid structure. The experimentation technique utilizes an analysis of variance of several parameters at more than one level of each parameter. In this way, the effect of each para-

meter upon the static characteristics, as well as the IMD products, is tested. In addition, the effect of any interactions is detected. Follow-up single-parameter tests are used after the effectiveness of a specific parameter has been detected.

Improvements in the anode design have included reduction of secondary emission by surface preparation such as glassblasting and special surface-configurations to entrap secondary electrons for improved "knee" characteristics. Interactions of the anode configuration with optimized screen-grid-to-anode spacing have been studied to establish a minimum level for the "knee" potential.

Focusing cathodes<sup>8</sup> have been studied primarily for reduction of screen-grid current. Contoured emitting surfaces are designed to confine the origin of the beam to a more limited area. With the elimination of emitting surfaces directly behind the control-grid wires, the number of stray electrons is reduced, the effective field at the cathode is more homogenous, and the effect of secondary electrons from the screen grid is greatly reduced.

The control-grid structure of the tube has been improved to attain the most linear segment of the transfer curve coincident, with a curved portion which yields the lowest IMD level.

### Experimental data

Type 8791 has been designed to meet specific linearity requirements. Typical test data for two different plate voltages with corresponding optimized screen-grid voltages are shown in Table I. For comparison, the effects of feedback with a 10-ohm cathode resistor are also included.

Fig. 13 shows the distortion as a function of peak envelope power output of the 8791 in a two-tone, 30-MHz, linear amplifier with no feedback and with a 10-ohm resistor inserted in the cathode circuit. To summarize the tube performance: the third-order intermodulation distortion decreases as the zero-signal plate current increases; the effect of the 10-ohm cathode resistor is to reduce both 3<sup>rd</sup> and 5<sup>th</sup>-order distortion by approximately five to seven dB; and the 5<sup>th</sup>-order distortion curves are generally 5 to 10 dB less than the 3<sup>rd</sup>, and distortion decreases with lower output powers.

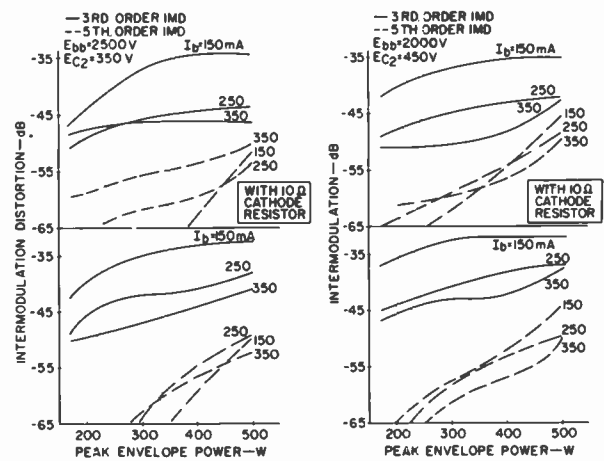


Fig. 13—Intermodulation distortion as a function of power output for RCA 8791 Cermion tube.

### Acknowledgments

The writer thanks Mr. D. Mentzer for programming contributions during the conduct of this work.

1. Magasly, I., "Airborne military transceiver finds room in crowded spectrum," *Electronics* (Apr 15, 1968) pp. 113-138.
2. Pappenfuss, E. W., Bruene, W. B., and Schoenike, E. O., *Single Sideband Principles and Circuits* (McGraw Hill 1964) pp. 179-187.
3. Cleary, R. E., *Approximate Intermodulation Distortion Analysis*, Collins Radio Company, Collins Radio Technical Report No. 173 (Oct 5, 1956).
4. Pappenfuss, E. W., et al, op. cit., pp. 188-189.
5. Rodda, S., "Space Charge and Electron Deflection in Beam Tetrode Theory," *Electronic Engineering*, Vol. 17, (Jul 1945) pp. 589-592.
6. Diemer, G., and Jonker, J. L., "Low Distortion Power Valves," *Wireless Engineering*, Vol. 26 (Dec 1949) pp. 385-389.
7. Shade, O. H. Jr., "Beam Power Tube Design Considerations," *Electron Tube Design*, Electron Tube Division, RCA, Harrison, New Jersey, (1962) pp. 656-658.
8. Harris, L. A., Beggs, J. E., and Andrews, C. I., "Bipotential Cathodes for Reduction of Grid Current," *IEEE Trans. on Electron Devices*, Vol. ED-11, No. 9, (Sep 1964) p. 428.

Table I—Two-tone modulation test for a linear RF power amplifier, class AB<sub>1</sub> for SSB suppressed carrier service

	No feedback	With 10-ohm cathode res.
DC plate voltage (v)	2000 2500	2000 2500
DC grid-No. 2 voltage (V)	450 350	450 350
DC grid-No. 1 voltage (V)	-32 -22	-38 -21
Zero signal plate current (mA)	300 300	300 300
Effective RF load resistance (Ω)	1850 2750	1850 2750
plate current (mA) at peak envelope (two tone)	550 480	555 485
Average plate current (mA—single tone)	430 390	430 395
grid-No. 2 current (mA) at peak of envelope (two tone)	-3.0 -4.0	-3.5 -3.5
Average grid-No. 2 current (mA)	-1.8 -2.5	0.4 -4.0
Average grid-No. 1 current (mA—single tone)	40 50	45 50
Peak envelope driver/power (W—approx)	1 1	1 1
Output-circuit efficiency (%—approx)	90 90	90 90
Distortion product level:		
3rd order (dB)	-38 -40	-43 -44
5th order (dB)	-44 -53	-50 -51
Useful power output (approx):		
Average (W)	250 250	250 250
Peak envelope (W)	500 500	500 500

# A sterilizable and ruggedized vidicon

Dr. S. A. Ochs | F. D. Marschka

To qualify for a berth on a spacecraft destined to land on one of our sister planets, a device has to be capable of withstanding pre-flight sterilization as well as the rigors of launch and touchdown. The camera tube described in this paper is intended for such an application. It is a one-inch ceramic vidicon with a slow-scan photoconductor and employs electrostatic focusing and magnetic deflection. The tube is designed to produce a high-quality picture after undergoing rigorous test procedures. The sterilization requirements presented a potential problem in tube development because of the possible adverse affect of high temperatures on the photoconductor and the material used for potting the tube within the magnetic shield. The remaining tests concerned the whole vidicon.



**Dr. S. A. Ochs**  
Vidicon Advanced Development  
Industrial Tube Division  
Electronic Components  
Lancaster, Pa.

received the BSME in 1943 from Columbia University. In 1949 he received the AM and in 1953 the PhD in physics from Columbia. Dr. Ochs was an instructor in physics from 1947 to 1951, during the course of his graduate studies. Also, while pursuing his doctorate, he was the recipient of an Atomic Energy Commission pre-doctoral fellowship (1951-52). His thesis research involved the use of the atomic and molecular beams technique for the study of the hyperfine structures of rubidium and potassium isotopes and of sodium chloride. Dr. Ochs became associated with RCA in 1952, working first on television camera tubes. This included work on a tri-color vidicon, on structure-type vidicon targets, and developmental work on new image orthicon targets. He later worked on electrostatic signal storage, on tunneling current in insulators, and on injection-luminescent lasers. Presently, he is engaged in the development of a ruggedized, sterilizable vidicon. Dr. Ochs is the holder of five patents, is represented in the *Reinhold Encyclopedia of Electronics* with an article on image orthicons, and has received two RCA Achievement Awards (1954 and 1957). He is a member of the American Physical Society, Sigma Xi, and a Senior Member of IEEE.

Final manuscript received October 15, 1968.

The work described in this paper was performed for the Jet Propulsion Laboratory under contract NAS7-100.



**F. D. Marschka, Ldr.**  
Vidicon Advanced Development  
Industrial Tube Division  
Electronic Components  
Lancaster, Pa.

received the BS in physics and mathematics from Juniata College in 1948, and continued with graduate work at the University of Maryland. He has also pursued graduate studies at Franklin and Marshall College. Joining RCA in 1949, he has been concerned with production engineering and product design engineering of television camera tubes, oscilloscopes, and storage tubes. An Engineering Leader since 1958, he has made significant contributions in advanced development work on the aforementioned families of tubes. He was instrumental in the development work associated with the vidicons used in the TIROS weather satellite. Mr. Marschka is a member of Sigma Pi Sigma.

**A** ONE-INCH VIDICON capable of withstanding sterilization treatments and severe environmental testing has been developed for space applications. The ceramic vidicon, which represents a significant advance in rugged camera-tube design, uses electrostatic focusing and magnetic deflection provided by photo-etched deflection coils to produce an image comparable to that of commercial one-inch vidicons using the same photoconductor. The sterilization tests, con-

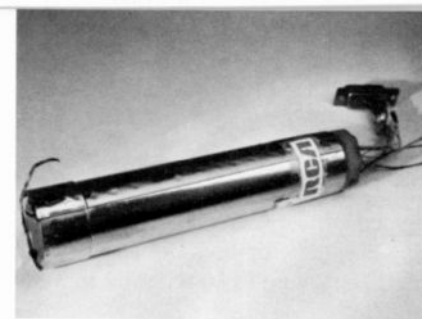


Fig. 1—Experimental ceramic vidicon.

sisting of ethylene-oxide exposure and a prolonged 135°C dry-nitrogen bake, caused some increase in dark current and a small gain in sensitivity of the slow-scan photoconductor. The tube operates satisfactorily after undergoing high-amplitude vibration tests, and several half-sine shock pulses of 3000-g amplitude.

The tube, shown in Fig. 1, consists of a ceramic body with a quartz faceplate and copper pinch-off; the faceplate is attached to the tube with an indium seal. The filament is potted within the cathode sleeve of the ruggedized electron gun. The wall electrodes consist of metal coatings on the inside wall of the tube envelope, while the mesh decelerating screen is mounted on a support that is brazed to the tube body. Metal pins, brazed into the tube wall, provide electrical connections to the various electrodes. The complete tube is potted within a magnetic shield. The ruggedized ceramic vidicon produces as good a picture as the more conventional one-inch non-ceramic tubes.

## Tube construction

The tube design was guided by the following considerations:

- 1) All components had to be capable of withstanding the required environmental tests.
- 2) The cathode surface and photoconductor could not be exposed to brazing temperatures.
- 3) No magnetic material could be used in the middle and front sections of the tube because of the possibility that such materials might impair picture quality.
- 4) Weight and power requirements were to be minimized.

Fig. 2 is a cross-sectional sketch of the final tube design. To avoid the weakest features of the standard vacuum tube, the construction method chosen for the ruggedized vidicon consists of a brazed metal-and-ceramic structure. The glass envelope of the ordinary vacuum tube was eliminated, as well as the internal glass beads, thin-walled electrodes, wire leads, and bulb spacers. The main section of the tube

body consists of an alumina-ceramic cylinder with internal shoulders for supporting the mesh and the electron gun. A Kovar section brazed to the rear of this cylinder carries the copper exhaust tubulation.

The gun used in the tube is similar in geometry to the low-heater-power type used in several commercial vidicons except that its components are brazed together instead of being supported by glass beads. As indicated in Fig. 3, the control and accelerating grids are brazed to a ceramic spacer which insures accurate and stable positioning of the accelerating-grid cup relative to the control-grid cup. The control-grid cup is brazed to a ceramic support ring; the ring is brazed to the tube envelope.

The cathode heater in the gun consists of a double helix of rhenium-tungsten wire just under 0.001 in in diameter; the wire is coated with aluminum oxide. The cathode structure is mounted on the control-grid cup conventionally. The ends of the heater consist of two straight leads which protrude from the long, thin cathode sleeve that contains the filament. The straight leads are welded to two 0.030-in Kovar rods whose ends are brazed to the tube wall. The helical section of the filament is potted within the cathode sleeve by means of loose alumina powder capped with a high-temperature cement.

The filament potting causes relatively good thermal coupling between heater and cathode sleeve. This coupling results in a slightly greater heat loss than found in commercial tubes, but permits the filament to operate at a temperature somewhat lower than normal. The increase in heater power is less than 5%.

The electrostatic unipotential lens consists of three cylindrical sections formed by nickel-plated molybdenum coatings on the inside tube wall. The lens was designed with a magnification near unity with minimum spherical aberration. Typical operating voltages are about 400 V for the outside electrodes and 65 V for the central electrode.

The decelerating screen consists of an electroplated 1000-line/in nickel mesh. It is stretched over a flat nichrome ring under high tension (close to the yield

point); the tension keeps the ring flat without the need of the usual firing operation. As a result, the mesh has a relatively high internal damping coefficient that makes it highly resistant to damage from severe shock pulses and that minimizes microphonics. The resonant frequency of the mesh ranges from 2300 to 4500 Hz, with most samples resonating near 3600 Hz; the typical decay time is 0.2 s. The nichrome ring that supports the mesh is screwed to a molybdenum support ring. The support ring is brazed to the ceramic tube envelope.

The quartz faceplate supports the rhodium signal electrode and slow-scan photoconductor and is attached to the front surface of the ceramic tube body by a thin layer of indium metal. The indium seal is strong and reliable provided that the ceramic end surface of the tube is polished flat and free of scratches. The electrical connection to the target is made by a nichrome ribbon welded to a stainless-steel ring that encircles the indium seal.

All other electrical contacts are made through the ceramic envelope by molybdenum or Kovar pins brazed to the tube wall. These pins are connected to metalized strips on the outside surface of the envelope. Copper wires are soldered to the strips near the rear of the tube. The external connections can be seen in Fig. 4 which shows a tube, without deflection yoke, before being potted in the magnetic shield.

The vidicon is evacuated through the copper tubulation at the rear end. After completion of the standard vacuum-bake, cathode-activation, and getter-flash procedures, the copper tube is pinched off to form a vacuum-tight seal.

The scanning beam is deflected by the action of a lightweight yoke which fits snugly over the tube; the yoke design was borrowed from the unit used in the RCA Dev. No. C23080 vidicon. The spiral coils that produce the magnetic deflection fields consist of photoetched copper patterns deposited on a thin dielectric sheet; each coil contains forty turns. Fig. 5 is a close-up of two coils; the copper pattern shown is about 0.002 in thick and is deposited on 0.005-in fiberglass. Two deflection yokes are shown in Fig. 6; one has not yet been rolled into the required cylindrical shape, while the other is

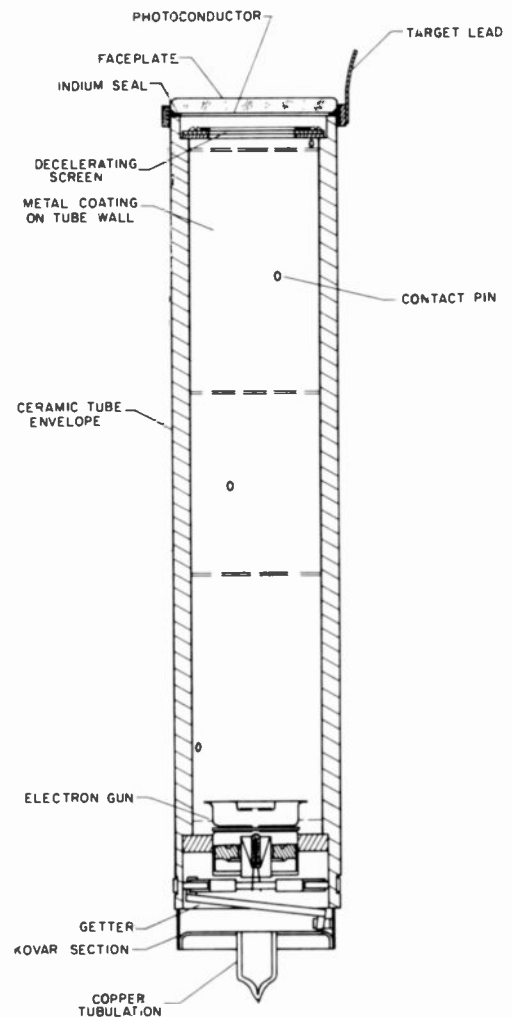


Fig. 2—Cross section of the new ceramic vidicon.

ready to be slipped onto a tube. A yoke consumes about 2 W but could be redesigned to require less than 1 W.

The vidicon, with deflection yoke in place, is potted in a polyurethane compound within a magnetic shield of 0.025-in Moly Permalloy. The mass of the total unit is 200 grams. About half of this mass is contributed by the ceramic tube; the other half is contributed by the potting, magnetic shield, and external wire leads.

### Environmental testing

The environmental tests outlined in Table I were performed by RCA environmental engineering activity in Lancaster. Fig. 7 shows the two high-acceleration shock machines designed for this project. The eight-pound magnesium drop table of the larger machine slides on Teflon bearings and is capable of providing impact shocks of 3700-g at a drop height of 60 inches. The 0.45-ms pulse profile for the larger machine is obtained by using fiberglass material as the impact spring.

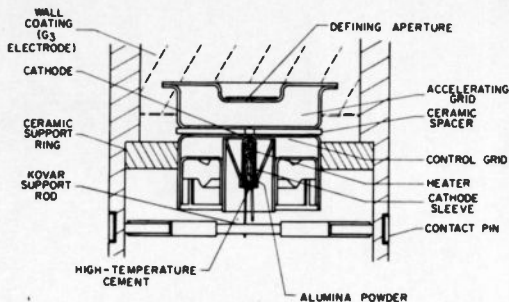


Fig. 3—Cross section of the gun.

The smaller machine was built to provide a 3000-g pulse with a risetime of 0.10 ms; it uses a steel block as the impact spring.

Separate tests were made on all portions of the tube considered to be potentially prone to failure; the separate tests were followed by several made on assembled vidicons.

Static loads were applied to the faceplate of the tube to establish the strength of the quartz disk and of the indium seal. An axial force applied to the faceplate so as to push it away from the tube caused failure equally often from separation of the indium seal and from cracking of the faceplate. Failure occurred with an average applied force of 181 lbs. A lateral force of 60 lbs caused faceplate slippage. Because the weight of the quartz faceplate is 0.0075 lb., a pulse of 3000-g causes a peak inertial force of  $3000 \times 0.0075$  or 22.5 lbs. This force is well within the limits acceptable to the faceplate and indium seal and both therefore are judged to be sufficiently rugged for the intended application.

### Photoconductor

The slow-scan ASOS (antimony sulfide-oxysulfide) photoconductor, developed by RCA for earlier space applications, was chosen for this tube because preliminary tests had shown it to be relatively resistant to high temperatures. The photosurface is deposited on the faceplate; a substrate of vitreous quartz of very high surface quality. To avoid coherent noise caused by imperfections on or in the photoconductor, the faceplate is subjected to a very thorough cleaning process. The signal electrode and the photoconductor are evaporated in an oil-free system evacuated by absorption and ion pumps. All depositions are made in a single pump-down—i.e., without breaking vacuum between the evaporation of different materials. The continuous vacuum assures a sensitive and spot-free photosurface. As expected, the prolonged exposure

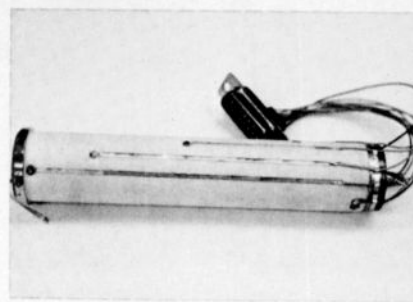


Fig. 4—Ceramic vidicon before potting.

to the elevated temperatures required during the sterilization treatments described in Table I causes an increase in dark current. However, the increase is not excessive and is accompanied by an improvement in signal current. In general, the dark current grows by 50 to 100% while the sensitivity rises between 15 and 25%. Fig. 8 shows typical tube performance both before and after complete sterilization. Dark current and signal current are plotted for a faceplate illumination of one footcandle; the temperature of the front end of the tube was held at 25°C during the measurements.

Sterilization causes a decrease of less than 10% in resolution and an almost imperceptible shift in the spectral response toward longer wavelengths. No systematic changes are observed in the slope of the transfer characteristic, gray-scale rendition, or lag characteristics of the photosurfaces. These results indicate that the ASOS slow-scan photoconductor can withstand the sterilization procedure without significant impairment of performance.

The tightly stretched nickel decelerating screen was tested under axial shock in a test arrangement designed to simulate the mounting used in the vidicon. A considerable number of samples was exposed to shocks of 3000-g's for 0.45 ms; no permanent damage or wrinkling occurred.

A major part of the design effort was spent on the brazed gun structure to assure satisfaction of the two principal gun requirements: precise alignment and strength. The final gun design shown in Fig. 3 provides the necessary accuracy and has been shown to be capable of withstanding shock pulses of 3000-g's.

Several potted heaters were mounted in special test units and exposed to the complete set of 3000-g shock pulses described in Table I; all of the samples survived. An accelerated life test run on the samples following the shock

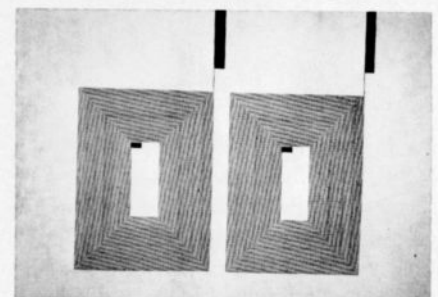


Fig. 5—Close-up of two photo-etched deflection coils.

test showed the life expectancy of the heaters to be at least 2000 hours. In spite of these results, the two complete tubes which were given shock tests of 3000-g's at the end of the program developed open heater connections before all sixty shocks had been applied. In both cases, failure resulted from a break in one of the straight heater sections at or near the Kovar support rods. In the complete tubes, the heaters were connected to Kovar rods of greater length and flexibility than those used in the test units. An unexpectedly large deflection of these rods is likely to have overstressed the straight sections of the heaters and caused them to break.

Static or shock tests were made on several other components of the tube including the brazed-in feedthrough pins, ceramic-to-Kovar joint, deflection yoke, and magnetic shield. These were all found to have a considerable immunity to damage when exposed to 3000-g shock pulses.

The three complete tubes which were exposed to environmental testing were capable of good performance prior to the shock tests. One tube was passed through the entire ethylene-oxide decontamination and heat sterilization procedures, as well as the static acceleration, sinusoidal vibration, and wide-band noise tests, without deterioration in tube performance. However, the filament opened after one 7500-g shock test. The other two tubes were exposed to shock tests in which the amplitudes were held to slightly above 3000-g. One tube was in good condition after the first set of five shocks, but devel-

Table I—Environmental tests performed on the vidicon

*Ethylene-oxide decontamination:* six 28-hr cycles at 50°C.

*Dry-heat sterilization:* six 92-hr cycles at 135°C.

*Static acceleration:* six tests at  $\pm 190$  g for 20 min along three orthogonal axes.

*Sinusoidal vibration:* tests of each type along three orthogonal axes with vibration swept at  $\frac{1}{2}$  octave/minute, up and down in frequency.

$\pm 0.5$  in displacement, 5 to 16 Hz.

5 g RMS, 17 to 50 Hz.

15 g RMS, 50 to 100 Hz.

35 g RMS, 100 to 2000 Hz.

*Wideband noise:* three tests at 25 g RMS, 9 min duration, 15 to 2000 Hz along each axis.

*Shock:* sixty tests with designated shocks applied 5 times in each of 6 directions.

$\pm 3000$  g half-sine pulse, 225  $\mu$ s risetime.

$\pm 3000$  g half-sine pulse, 100  $\mu$ s risetime.

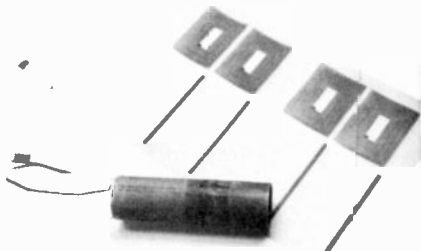


Fig. 6—Two photo-etched deflection yokes.

oped an open heater connection during the second set. The second tube went through twenty-five shocks with no damage but lost heater continuity during the following five shocks. The failure of each of the three tubes was caused by breaks in the straight section of the heater wire.

### Tube performance

The performance characteristics of the ceramic vidicon are described in Figs. 9, 10 and 11. In slow-scan operation, a typical cycle consists of three steps: exposure, readout, and erase. In exposure, the lens shutter is opened for a specified time. The photosurface then carries a charge pattern corresponding to the scene whose image appears on the tube. In readout, the electron beam scans the photosurface and generates the video signal in accordance with the charge stored on the photosurface. During the erase step, the electron beam scans the photosurface a second time and removes most of the remaining stored charge. The erase scan is desirable because the beam ordinarily removes only part of the stored charge in any single scan. In a typical experiment, the beam erased slightly less than half of the remaining stored charge with each scan. Therefore, after the readout and erase scans, about two-thirds of the originally stored charge had been removed. More com-

Fig. 7—Tube performance before and after sterilization (standard frame rate).

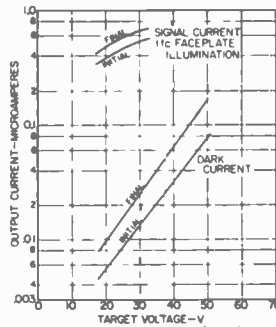
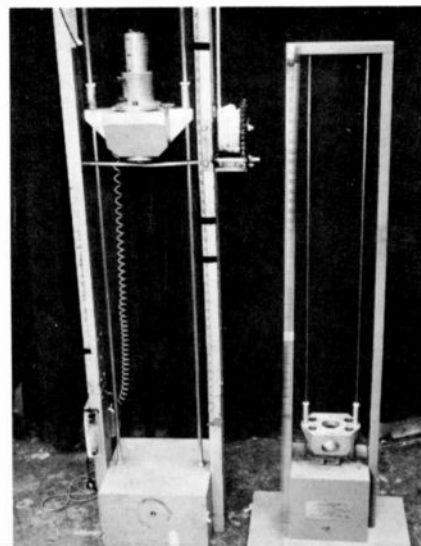


Fig. 8—High-acceleration shock machines.

plete erasure can be obtained by scanning the photosurface several times, possibly at a fast rate, during the time allotted to the erase step.

The transfer characteristic shown in Fig. 9 describes the sensitivity of the tube in terms of the signal current generated for various faceplate exposures. The tube was operated in a two-second cycle with one second used for the readout. A reciprocal relationship was found to exist between shutter time and illumination (at least within the shutter-time range of 1/100 to 1 second). Therefore, for a given exposure value (the product of illumination and shutter time) the signal remains the same if, for example, the illumination is doubled and the shutter time is halved. The transfer characteristic, in logarithmic form, is essentially a straight line with a slope  $\gamma$  of 0.71. This transfer characteristic is typical of vidicons and permits operation over a relatively wide range of exposure times.

The resolution capability of the tube is shown in Fig. 10. The uncompensated horizontal peak-to-peak response at the center of the raster is shown for a square-wave test pattern with the tube operated at the standard television rate of 30 frames/second. The performance is essentially the same as that of an RCA-8134 vidicon, a commercial one-inch tube with electrostatic focusing and magnetic deflection.

Fig. 11 shows the spectral response of the ruggedized tube in the visible-light range; power input at all wavelengths is the same. As indicated in the figure, the photoconductor has a maximum sensitivity at some wavelength between 500 and 600 nanometers.

### Acknowledgements

The authors acknowledge contributions to this work by J. Ziedonis in environmental engineering, L. Rhoads in ceramic engineering, and D. Neuer in tube construction.

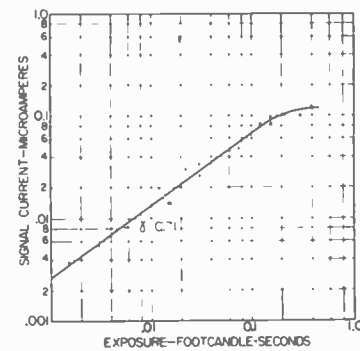


Fig. 9—Transfer characteristic.

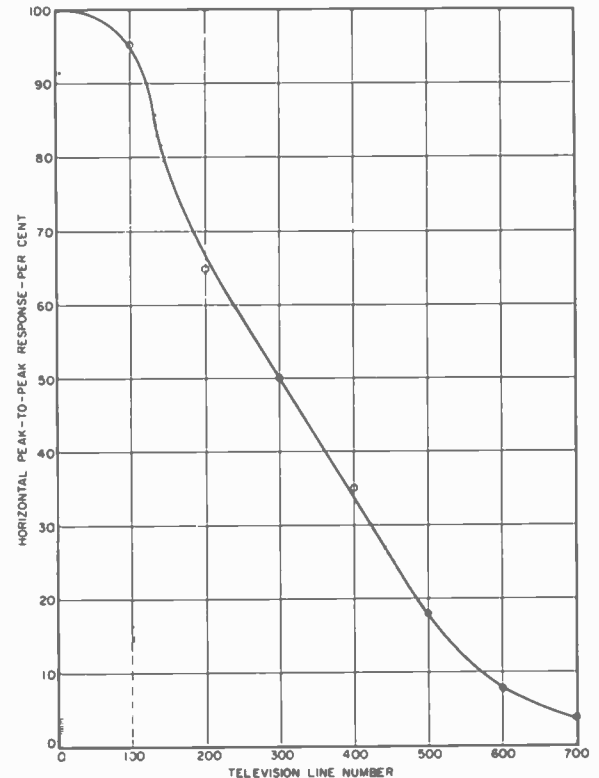


Fig. 10—Resolution capability.

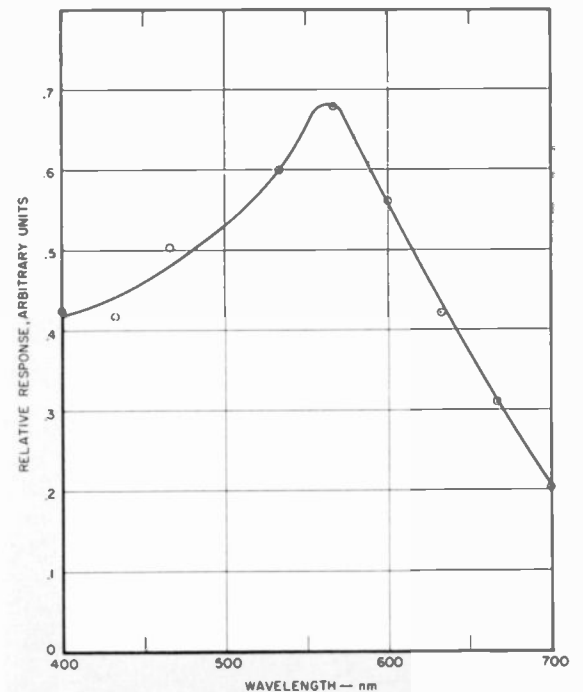


Fig. 11—Spectral response.

# Broadband, high-gain, L-band, power amplifier module

R. L. Bailey | J. R. Jasinski

Increasingly sophisticated radar systems, such as phased arrays, have created a need for RF power amplifiers that have wide bandwidths together with excellent phase stability and uniformity of characteristics. This paper describes the unique design and fabrication of the RCA Dev. No. Y1043\*, a six-stage, L-band amplifier module that has performance characteristics which fulfill these requirements.

AMPLIFIERS utilizing grid-controlled tubes have been operated successfully in narrow-band phased-array radars for a number of years; only recently, however, have their full capabilities in broadband, high-gain applications been demonstrated. The development of the Y1043 amplifier module has substantially advanced the state-of-the-art in this area. The compact, wide-band, pulsed amplifier module uses gridded electron tubes, and is designed for operation at a center frequency of 1300 MHz with an instantaneous electronic bandwidth of 10% measured at the 1-dB points.<sup>1</sup> Performance objectives included a peak power output of 5 kW and an overall gain of 45 dB utilizing a minimum number of stages. The amplifier module was limited to 24 inches in length and 4½ by 4½ inches in cross section. In this particular phased-array application, each amplifier module was to drive an individual radiating element. For proper antenna spacing, this modular approach required that the amplifier not exceed one half wavelength in cross section.

The degree of phase variation from input to output as a function of drive level, frequency, and supply-voltage variation was required to be small to minimize the cost of auxiliary operating equipment.

## Conventional amplifiers

Analysis of the specifications described above indicated that conventional cascading techniques would not yield the desired results, particularly if the overall size and gain-bandwidth requirements were to be achieved. Conventional L-band (390-to-1550-MHz) gridded power-tube amplifiers typically

consist of tuned input and output cavity or stripline resonators in conjunction with the appropriate bypass circuits required for operation. A typical 5-kW unit may be 5 to 7 inches on each side in cross section and 12 to 15 inches in length. These amplifiers are normally single-tuned, and yield characteristic gains of 10 to 15 dB. Gain is increased when two or more independent stages are cascaded with interconnecting coaxial cables. An impedance-matching transformer at the load end of each interconnecting cable permits transmission of interstage

**J. R. Jasinski**  
Regular Power Devices Engineering  
Industrial Tube Division  
Lancaster, Pa.

was an honor graduate of the T-3 Engineering curriculum, RCA Institutes in 1958. He joined RCA in 1958 as an electronics technician at the Lancaster plant, where he was engaged in the evaluation of RCA's new line of Cermolox tetrodes to establish their capability in pulsed RF service at L-band frequencies. In 1962, Mr. Jasinski was assigned to evaluation of the S-band coaxitron being developed for the Air Force. Compilation and organization of data from this evaluation led directly to the successful development of external broadband circuits for Cermolox tubes designed to operate at L-band frequencies. In 1964, Mr. Jasinski was assigned to the developmental L-band module program. He was upgraded to Engineer in 1967 and is presently responsible for the prototype development of all new module variants and the manufacture and testing of existing module types.

power at the cable surge impedance (usually 50 ohms) and thus makes interstage performance independent of cable length. Interstage loading and tuning adjustments are made with an impedance transformer at the generator end of each cable. The overall gain of the amplifier chain increases with the addition of each new single-tuned stage, while system bandwidth continually decreases; desired gain-bandwidth characteristics may be achieved by changes in the degree of coupling between stages and/or by the use of stagger-tuning.

Fig. 1 shows a single-tuned, single-stage amplifier, RCA Dev. No. Y1015. This amplifier uses an RCA-7651 tube, delivers a minimum peak power output of 6 kW, and can be mechanically tuned across the 950-to-1225-MHz band with an average instantaneous bandwidth of 3%. The RCA-7651 is capable of a peak power output of 39 kW at 1200 MHz when operated at its maximum ratings in a narrow-band circuit (less than 1% instantaneous bandwidth). The threaded coaxial fittings

**R. L. Bailey**  
Advanced Development, Power Devices  
Industrial Tube Division  
Lancaster, Pa.

received the BSEE in 1958 from Washington State University, and the MS in Physics in 1968 from Franklin and Marshall College. He joined RCA in 1958 as a design engineer in the Power Tube department, where he worked until 1963 on the design and development of UHF circuits. In 1963 he joined the Power Tube Advanced Development group, where he was engaged until 1965 in the design of a broadband, high-gain L-band amplifier. Since 1965 he has been engaged in developing techniques for producing high power from RF transistors. Mr. Bailey is a member of IEEE and Sigma Pi Sigma.

The development of the gridded-tube L-band, power-amplifier module was supported by U.S.A.E.L., Evans Laboratories, under Contract DA36-039-AMC-03203(E).



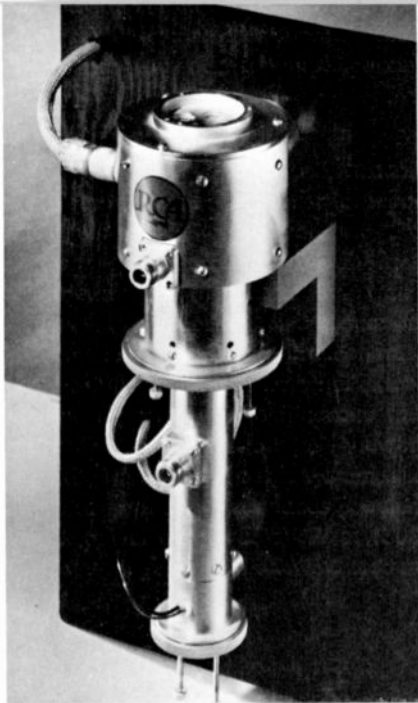


Fig. 1—Conventional Y1015 single-tuned, single-stage amplifier.

shown in Fig. 1 permit connection of standard 50-ohm RF drive and RF output cables to the cavity; however, because the cables join the coaxial resonators at right angles to the main cavity axis, they add considerably to the cross-sectional dimension. This cavity measures about 6 inches at its major cross section. When the cavity is tuned to its lowest operating frequency of 950 MHz, the input tuning rods extend 2 inches below the cavity and produce an overall length of 14½ inches.

This type of amplifier is generally not satisfactory for use in multistage *broadband* chains. Because the unnecessary impedance transformations to the 50-ohm interconnecting cable surge impedance severely limits gain-bandwidth product, double- or triple-tuned circuits cannot be utilized to best advantage, and the resulting size of the cascaded amplifier chain exceeds the requirements of many applications.

#### New cascading technique

Fig. 2 shows the RCA Y1043 "totem-pole" amplifier. This amplifier incorporates techniques which enhance the inherent gain-bandwidth capabilities of gridded tubes and, at the same time, achieves a considerable size reduction over classical cascaded amplifier chains. The amplifier is shown with the external housing removed to illustrate the end-to-end configuration as viewed from the input end. In this system, six stages of gridded power tubes provide a peak power output of 5 kW at 1300 MHz with a gain of 53 dB. The system

uses two commercial 7768 planar triodes (small tubes) and four cermolox tetrodes (two each 8226 and 7651 generic types), samples of which are shown adjacent to the module. The cermolox tetrodes used in this amplifier differ from other tubes of the same generic type in that they use integral conduction-cooling aluminum jackets instead of air-cooled radiators. The RF drive, liquid coolant (high purity at ½ GPM), and all operating voltages are applied through the five connectors at the input bulkhead. Output power of the amplifier is extracted through a coaxial connector at the opposite end. A 3-kV DC power supply, the highest voltage required for operation, provides plate voltage for the four tetrodes. The tetrodes are modulated by a 1-kV pulse which is applied to the screen grids. The plate voltage for the 7768 triodes is provided by a 300-volt DC supply; the grids are modulated by a small 6-volt bias pulser. All voltages are applied through bus lines which are located in the corners of the module. A few of these bus lines are visible in Fig. 2. The module is packaged in an aluminum container which measures 4¾ x 4¾ x 23 inches. This size satisfies the required dimensions for use in a 1300-MHz phased-array radar.

Fig. 3 shows the instantaneous bandwidth characteristic of the module for an applied peak drive power of 25 mW. The module measured produced a nominal peak power output of 5.75 kW at 2% duty, with a ripple factor of less than 1 dB and an instantaneous bandwidth of 10.5%.

Fig. 4 shows the final amplifier package. The absence of connectors on the large surfaces allows many such modules to be inserted side-by-side, "honeycomb" fashion, into an array panel to form a multi-megawatt phase-steerable beam. Fig. 5 shows a cross-sectional view. No conventional, lengthy interstage circuits are used in the amplifier chain; instead, the stages are stacked in a "totem-pole" fashion, and each of the stages is directly interconnected by a full-electrical-wavelength circuit. Minimum system dimensions are produced with this coaxial, in-line configuration. A considerable portion of each interstage circuit, especially in the tetrode stages, is contained within the internal output and succeeding

input sections of the tubes; as a result, the amplifier stages have an average length of only 4 inches. Two overcoupling elements are contained in the interstage circuit external to the tube (about one-half wavelength) to provide optimum gain-bandwidth in a minimum amount of space. In each stage, these elements consist of shunt inductance and series of capacitance. The inductor is composed of several ¼ inch-diameter spokes shunted across the cavity. In each tetrode stage, two of the spokes are hollow to allow anode coolant to flow into and through the anode seat, which is a portion of the coaxial center conductor. The series overcoupling capacitor is formed by a break in the center conductor of the interstage coaxial line. This capacitor also isolates the plate voltage of a particular stage from the cathode potential of a driven stage. The module contains mica RF radial bypass capacitors which provide DC isolation for the various tube elements.

#### Basic design techniques

##### Overcoupled RF circuits

The RF circuits used throughout the module are overcoupled resonant coaxial cavities which are aligned to produce triple-tuned, maximally flat responses. Each stage in the chain has the same response. This approach provided full freedom to change the number of stages at any time during the development of the module. The alternative approach, stagger tuning of individual stages, would have restricted this freedom.

The overcoupled circuits have an inherently greater gain-bandwidth product than the simple single-tuned circuit; the improvement is a function of the number of circuits coupled together. A useful figure of merit for broadband circuits is the resistance-times-bandwidth ( $R \times BW$ ) product which the circuit presents to the fundamental component of the tube beam current. A circuit can be evaluated on the basis of the ratio of the *actual*  $R \times BW$  product to the *maximum*  $R \times BW$  product for a simple parallel resonant circuit having the same amplifier output capacitance. A valid comparison, however, must include a specification of the shape of the actual response. For this discussion, it is assumed that the response is maximally flat and, further, that the  $R \times BW$  value

is the product of the resistance and bandwidth both referred to the points 1/6 dB down from the peak value of  $R$ . (Because the module has six stages, this reference provides the overall  $R \times BW$  product at the -1-dB points.) For the single-tuned circuit, the  $R \times BW$  product is the half-power resistance times the half-power bandwidth.

On this basis, an optimized double-tuned circuit can provide an  $R \times BW$  product as great as 1.22 times that of a single-tuned circuit. A triple-tuned circuit can provide up to 1.66 times as much  $R \times BW$  product. The limit approaches  $\pi$  as the number of tuned circuits is increased. (These numbers were calculated from tabulated data for ladder networks given by Weinberg<sup>2</sup>; verification of the extension to high-frequency bandpass circuits was made by Green.<sup>3</sup>) Because the circuit complexity increases directly with the number of coupled circuits, a triple-tuned circuit provides a good compromise between  $R \times BW$  improvement and circuit complexity.

The triple-tuned coaxial circuits employed in the Y1043 L-band module are very similar conceptually to the double-tuned circuits employed in RCA super-power coaxitrons.<sup>4,5,6,7</sup>

**Tube selection and computer calculations**

Because the  $R \times BW$  product for the simple parallel resonant circuit can be easily calculated for a hypothetical lumped-constant circuit, it is possible to estimate the performance of any tube used with triple-tuned circuits. Tubes for use in the amplifier module were selected on this basis. For inter-stage analysis, the dynamic drive-point impedance was measured at the input terminals of each tube at the required drive power. A modified version of the

7651 cermolox tetrode was chosen for the final stage; an equivalent circuit for this stage is shown at the top of Fig. 6. The impedance and admittance plots for such a circuit can be obtained from straightforward but tedious calculations. A program was written for the RCA-301 digital computer to greatly improve the calculation time. The program included provision for 15 different sections of transmission line, and made allowances for lumped reactive elements at various line junctions. The output data provided the impedance as a function of frequency at key line junctions.

The impedance and resistance plots in Fig. 6 are comprehensive presentations of data obtained from computer analysis of the conceptual design of the final output stage. The particular values listed for the circuit parameters produced the Smith plot variation in impedance  $Z_T/Z_0$  as a function of frequency shown at the lower right. Within the passband, the impedance response follows a constant  $R$  locus, indicating a maximally flat condition. The resistive component of  $Z_T$  is plotted at the lower left. Obviously, the first set of parameters used in the computer calculation did not produce this optimized response, because the values of the parameters were chosen primarily by educated guesses. However, with the Smith plots used as guides, successive computed sets of data converged rapidly.

During the series of computer calculations to determine the specific set of parameter values for the optimum response, much valuable insight was gained on quantitative effects of varying each parameter. This information was later found to be very useful for circuit alignment. The computer re-

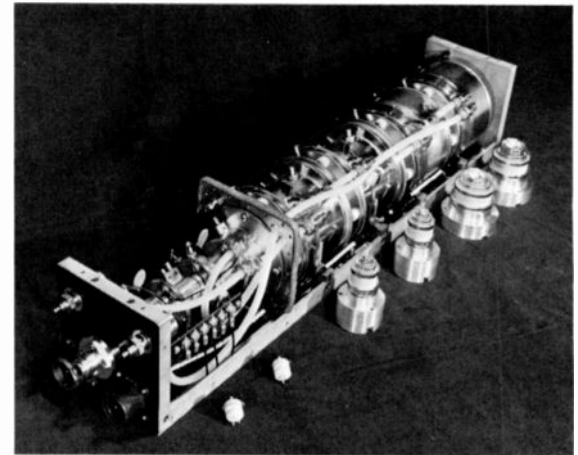


Fig. 2—Y1043 amplifier module with cover removed to show the end-to-end configuration.

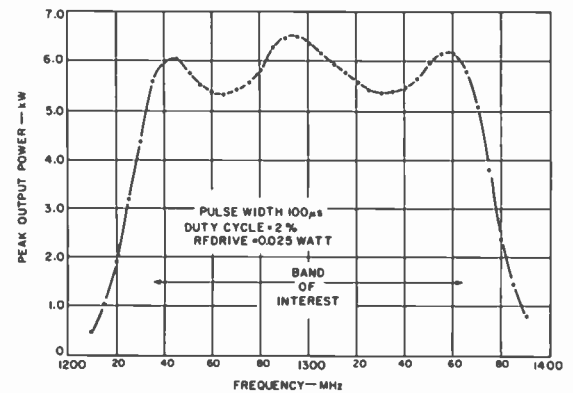


Fig. 3—Y1043 typical output response.

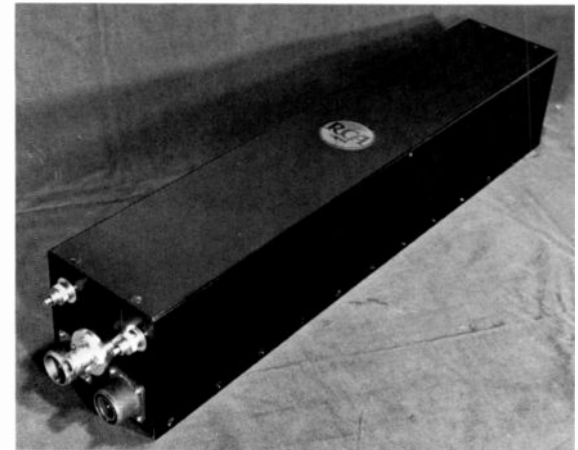
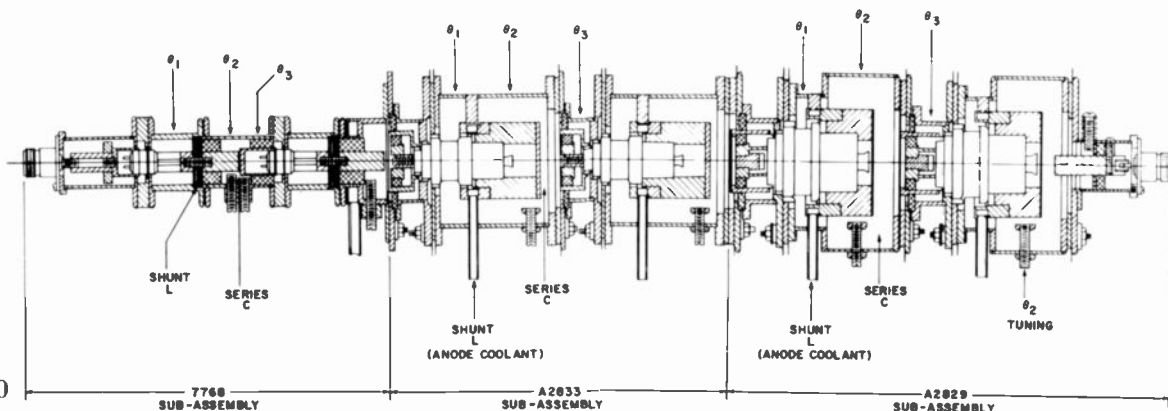


Fig. 4—Y1043 shown fully housed to illustrate its modular concept.

Fig. 5—Tube cross section.



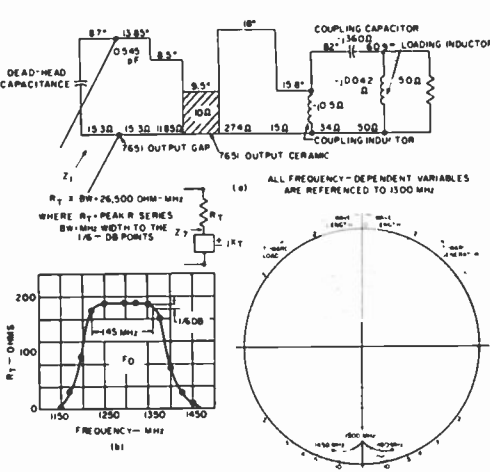


Fig. 6—Smith-chart plot of impedance versus frequency.

sults were used to calculate projected operating conditions for each stage. In practice, it is necessary to derate the computed value of  $R_T$  by approximately a factor of 30% to compensate for the practical limits on circuit efficiency and for the smearing of the RF current pulse because of transit-time effects.

#### Cold-probe verification of amplifier design

After paper designs of circuits were available, cold-probe models were fabricated and analyzed to verify predictions based on computer calculations. These models consisted of cavities that included provisions for variation of every parameter external to the tube; they used dummy tubes consisting of only screen-grid-and-anode assemblies.

The output gap of the dummy tube was energized with approximately 1 watt of frequency-swept power, and a crystal detector was used to monitor the transmission response of the cavity into a 50-ohm load. The output of the crystal detector was then displayed as an oscillogram. Variation of parameters while the instantaneous display was monitored allowed swift attainment of a flat response with the desired center frequency and bandwidth. Results obtained with models of the final output and the interstage circuits verified that the computer program accurately simulated the RF circuitry.

#### Amplifier assembly and alignment

The final design and fabrication of all the amplifier stages were based completely on computer and cold-probe results. As shown in Fig. 5, the module consists of three basic subassemblies.

Each subassembly contains two stages of amplification, and each was extensively tested as a single-stage and then a two-stage broadband amplifier to confirm successful operation of each tube at the required power level. The input to the first stage was not triple-tuned, but used a shunt capacitive "matching slug" that produced a single-tuned transformation to 50 ohms. Because the transformation ratio was relatively low, the input VSWR is better than 1.5:1 (4% reflected power) across the 1200-to-1400-MHz band.

Final assembly and alignment proceeded progressively, one stage at a time, starting with the low-power stages. With this method, two stages were operated into a passive load, then three stages and finally up to six stages so that alignment of the most recently added stage could be accomplished at the correct drive level. The DC grid-current response of the driven stage served as an excellent indicator of interstage performance. The use of swept-frequency drive at all times provided comparative ease of circuit adjustment.

#### Phase measurements

The phase characteristics of the module are of major interest for use in phased-array systems. Two independent measurements of these characteristics were made with nearly identical results, one at MIT Lincoln Laboratories and the other at RCA Lancaster. These measurements were made with a differential phase bridge which had a resolution capability of better than three degrees. The measured phase-sensitivity data are presented in Fig. 7. As expected of any device that utilizes gridded power tubes, phase sensitivity of the module is extremely low. The most sensitive operating parameter, the tetrode screen-grid voltage, produced an approximate shift of only one degree per 1% change in voltage. As a result of this high degree of phase stability, power-supply costs are reduced because voltage-regulation requirements are minimized. As a direct comparison, a velocity-modulated device, such as a traveling-wave tube typically exhibits a twenty-degree phase change for a 1% change in anode voltage<sup>8</sup>; these results show that much better voltage regulation is required for the same degree of phase stability. Variations of DC volt-

ages, the filament voltage, and drive power produced negligible phase changes through the module.

The phase characteristics as a function of frequency, shown in Fig. 8, indicate that extreme linearity ( $\pm 2^\circ$ ) exists over 75% of the pass band with no significant irregularities appearing in the curve.

#### Extended applications

Since the successful prototype development of the Y1043 module, customer interest has warranted the establishment of a manufacturing facility for fabrication of such modules on a continuing basis. Although the module was primarily designed for phased-array applications, present interest includes other areas where small size and high gain-bandwidth requirements are also of prime concern. The Y1043 module, and variants thereof, have either been proposed for or are presently being used in RF pulse-coded systems for command and guidance, phase-stable broadband drivers for higher-power radar systems, multi-channel airborne navigational beacons, and broadband applications where the major interest is in frequency agility.

As an illustration, the RCA Y1048C amplifier shown in Fig. 9 was designed specifically to operate in one of the above application areas and is an extension of Y1043 techniques. The module consists of 5 cascaded tetrode stages. It is designed to operate at a center frequency of 1375 MHz with an instantaneous 1-dB bandwidth of 5%. The peak power output is 10 kW with a gain of 47 dB. Because this module was not to be used in a phased array, the cross-sectional dimensions were allowed to increase to 5x6 inches; the length is 22 inches. The increased cross-sectional area was required for secure mounting of the module and its auxiliary components within the aluminum container to meet shock and vibration specifications.

RCA Dev. Nos. Y1057 and Y1049 modules (not shown) are the one- and two-kilowatt versions of the Y1043. The Y1057 delivers 1 kW of peak power at a center frequency of 1270 MHz with an instantaneous 1-dB bandwidth of 70 MHz and a gain of 37 dB. The Y1049 delivers 2 kW of peak power at a center frequency of 1088

Parameter varied	1235 MHz	1265 MHz	1300 MHz	1335 MHz	1365 MHz
I. 3,000-V supply (tetrode plate) Lowered 10% Lowered 16.7%	+ .3 - .45				- 4.25
II. 1,000-V supply (tetrode screen) Lowered 10% Lowered 20%	+ 6.7 +16.9	+ 5.5 +13.5	+ 7.2 +15.6	+ 9.75 +24.8	+11.1 +23.6
III. 300-V supply (triode plate) Lowered 10%					+ 3.76
IV. Filament supply (all stages) Lowered 8.75%			- 4.38		
V. Drive power Lowered 2dB Lowered 4dB					- 2.8 - 7.2
VI. Drive Lowered 1dB 3,000-V, 1,000-V, and 300-V supplies Lowered 10%	14.		12.7		4.9

Fig. 7—Phase sensitivity data

MHz with an instantaneous 1-dB bandwidth of 70 MHz and a gain of 37 dB. Both modules are capable of operating at 5% duty and each contains a single tube type, the RCA Dev. No. A2833; the Y1057 has four stages and the Y1049 only three. Proposals have recently been written for design and fabrication of 50k W and 100k W modules to cover the 750-to850 MHz and the 405-to-450 MHz bands, respectively.

All of the above circuits use the same triple-tuned, coaxial, "totem-pole" circuit concepts described for the Y1043 module. For a particular tube type, the high-frequency limit is determined by the internal screen-grid-to-anode "strap resonance" of the tube, i.e., the frequency at which the shunt-over-coupling inductor appears just at the tube terminals. Attempts at circuiting at frequencies above "strap resonance" would produce a loss of this shunt-inductor "tuning handle". For a given frequency, the ideal circuit has the shunt overcoupling inductors very close to the output terminals of the tube. This condition produces inter-stage circuits of the shortest possible length and optimizes the dimensions of the module. The upper frequency limits of the tetrodes used in the Y1043 are approximately 1410 MHz and 1600

MHz, respectively. Thus, the 1235-to-1365-MHz operating spectrum for the Y1043 permits use of the ideal circuit configuration. The larger tube types, because of their greater power capability, have inherently lower strap resonant frequencies. The upper frequency limit is approximately 600 MHz for the 100kW module and about 90 MHz for the 50kW module.

Cross-sectional size and total length primarily determine the lowest practical operating frequency. Lower frequencies require an increase in cross section for maintenance of effective RF radial bypassing of the mica DC blockers. A typical 800-MHz module would have to be increased to 8x8 inches in cross section to prevent blocker radiation. Another consideration for lower-frequency operation is water-cooling requirements. As the operational frequency is decreased, the shunt inductors move further from the tube and anode seat; hence, a more complex mechanical configuration is required for cooling.

### Conclusions

High-gain, broadband amplifiers using triple-tuned coaxial resonators in combination with gridded power tubes can

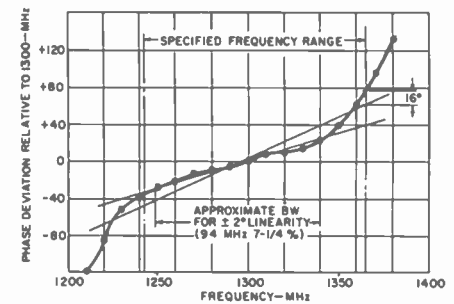


Fig. 8—Measured shift in phase with frequency for the module.

be arranged in a very compact circuit. The design and analysis of these complex circuits are facilitated by the use of a digital computer. Several stages of power tubes with maximally flat responses can be cascaded or stacked "totem-pole" fashion to form a compact, high-gain amplifier module. Recent circuit refinements have produced overall gains of 60 dB, corresponding to 2.6 dB per linear inch of module.

Measurements on a six-stage module have proven that the excellent phase stability of gridded power tubes is preserved through as many as six stages of amplification. The phase-versus-frequency characteristics of the module are such that phase-linearity compensation can be accomplished easily.

### Acknowledgments

The authors thank W. P. Bennett, F. W. Peterson, M. V. Hoover, and L. F. Heckman for their important contributions to the design and testing of the module described; H. Kaunzinger and G. Fincke of USAEL, the technical monitors of the contract work, for their many helpful suggestions; and L. Cartledge and others of MIT Lincoln Laboratories for measurements of the phase characteristics of the module.

### References

1. Bailey, R. L., "A Broadband, High-Gain Power Amplifier for Phased Arrays Using Phase-Stable Gridded Tubes," IEEE International Convention, New York, N.Y. (Mar. 26 1965).
2. Weinberg, L., "Optimum Ladder Networks" *Journal of Franklin Institute* (July 1957).
3. Green, E., "Amplitude-Frequency Characteristics of Ladder Networks," Marconi's Wireless Telegraph Co., Ltd.
4. Parker, W. N., "The Coaxitron Tube," *RCA Pioneer* (Feb 1961).
5. "The Development of an Experimental Model of a High-Power, Broadband Coaxitron Amplifier," RADC-TR-60-94 (June 1960).
6. "The Continuation of the Development of an Experimental Model of a High Power Broadband Coaxitron Amplifier," RADC-TDR-61-315 (Nov 1961).
7. Keith, F. S., Parker, W. N., Rintz, C. L., "The Coaxitron—A High-Power, Broadband, Integral-Cavity UHF Amplifier," AIEE General Meeting in New York (Jan 31 1962).
8. Molz, K. F., "Selecting Tubes and Receivers for Large Phased-Arrays" *Microwaves* (Mar 1964) p. 18.

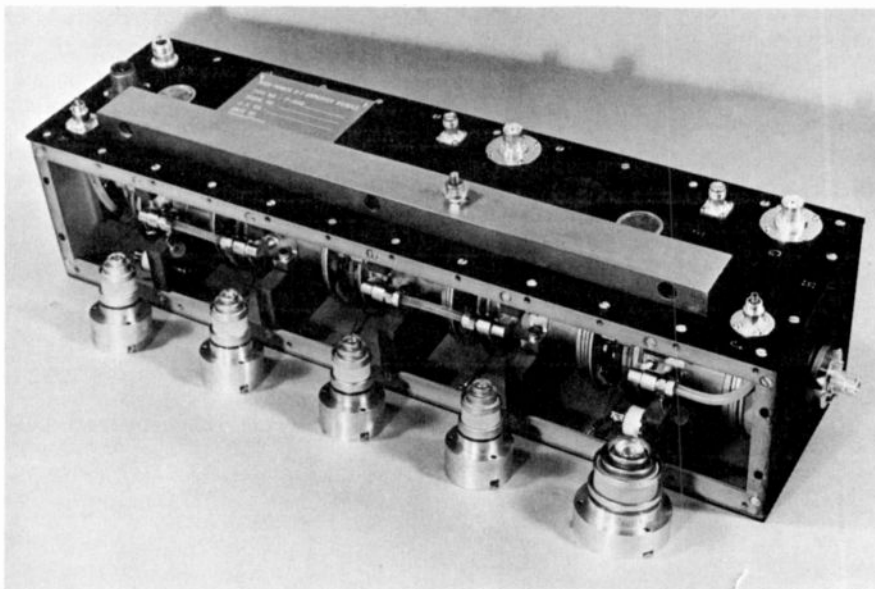


Fig. 9—Y1048C five-stage ruggedized module with side cover removed.

